

## Multinuclear Olefin Polymerization Catalysts

Massimiliano Delferro and Tobin J. Marks\*

Department of Chemistry, Northwestern University, Evanston, Illinois 60208-3113, United States

## CONTENTS

1. Introduction	2450
1.1. Inspired by Nature	2450
1.2. Olefin Polymerization Catalysis Background	2450
1.3. Scope of This Review	2453
2. Group 4 Bimetallic Catalysts	2454
2.1. Linked Metallocene Catalysts	2454
2.1.1. Phenylene-Bridged Catalysts	2454
2.1.2. Silane- and Siloxane-Bridged Catalysts	2456
2.1.3. Polymethylene-Bridged Catalysts	2457
2.1.4. Flexible/Rigid Bridged Catalysts	2457
2.2. Linked Constrained Geometry Catalysts	2458
2.2.1. Ethylene Polymerization Properties	2460
2.2.2. Ethylene + $\alpha$ -Olefin and Ethylene + Encumbered Isoalkene Copolymerizations	2462
2.2.3. Styrene Polymerization and Ethylene + Styrene Copolymerizations	2463
2.2.4. Alkenylsilane Chain Transfer	2464
2.3. Linked Phenoxyiminato Catalysts	2465
3. Group 10 Bimetallic Catalysts	2468
3.1. Nickel Catalysts	2469
3.1.1. $\alpha$ -Diimine Catalysts	2469
3.1.2. Phenoxyiminato Catalysts	2469
3.1.3. Other Ligations	2471
3.2. Palladium Catalysts	2473
4. Bimetallic Catalysts with Other Metals	2474
4.1. Iron and Cobalt Catalysts	2474
4.2. Rare Earth Metal Catalysts	2474
5. Heterobimetallic Catalysts	2475
6. Multimetallic Catalysts	2477
7. Conclusions and Outlook	2480
Author Information	2481
Biographies	2481
Acknowledgment	2481
Glossary	2481
References	2481

## 1. INTRODUCTION

## 1.1. Inspired by Nature

In many enzymes, such as ureases (Figure 1), two or more metal centers are poised in close proximity to activate both electrophilic and nucleophilic reactants,<sup>1</sup> thereby achieving superior activity and selectivity.<sup>2</sup> These enhanced catalytic properties versus

nonproximate catalytic centers are due to the creation of high local reagent concentrations, conformationally advantageous active-site—substrate proximities, as well as multicenter directed covalent and noncovalent interactions. Cooperative multimetallic substrate activation and conversion has been established mechanistically in a sizable number of metalloenzyme-catalyzed processes and illustrates one way in which nature achieves the activation and conversion of otherwise challenging substrates.<sup>1–3</sup> For these reasons, recent abiotic homogeneous catalytic research has also focused on mimicking the structures and organizational capabilities of enzymes to discover unique/more efficient catalytic processes. For example, the cooperation in a single catalytic system of Lewis base and Lewis acid centers has been applied to a variety of transformations, including Diels–Alder reactions,<sup>4</sup> asymmetric Strecker reactions,<sup>5</sup> asymmetric transformations using metallocene catalysts,<sup>6</sup> enantioselective cycloaddition reactions between ketene enolates and various electrophiles,<sup>7</sup> Corey–Chaykovsky epoxidations,<sup>8</sup> and many other reactions catalyzed by multinuclear assemblies (e.g., Chart 1).<sup>9,10</sup>

## 1.2. Olefin Polymerization Catalysis Background

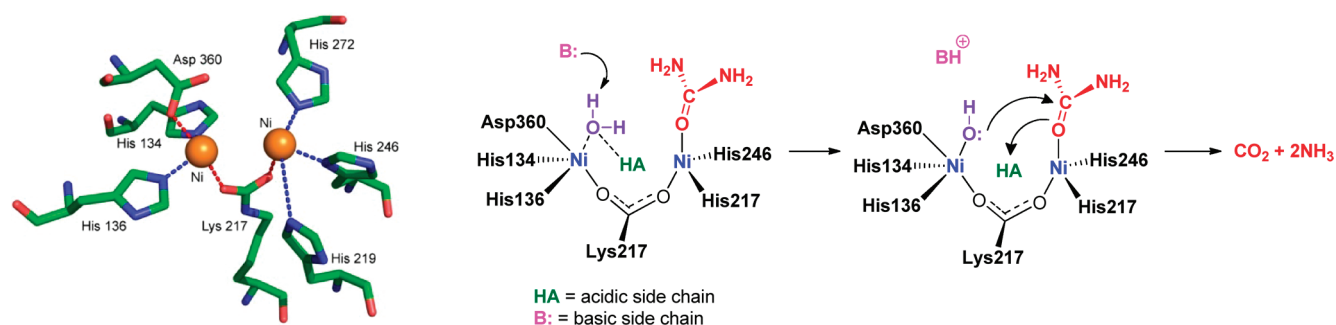
In 1963 Ziegler and Natta were awarded the Nobel Prize in Chemistry “for their discoveries in the field of the chemistry and technology of high polymers.”<sup>11</sup> Heterogeneous Ziegler–Natta catalysts are binary combinations of supported  $\text{TiCl}_4$  and  $\text{AlR}_3$  ( $\text{R} = \text{alkyl, aryl, hydride}$ ) components<sup>12</sup> and are today employed on a huge scale to produce HDPE (high-density polyethylene) and iPP (isotactic polypropylene). In 1980, Kaminsky and co-workers<sup>13</sup> reported an efficient activator for homogeneous group 4 metallocene catalysts (Chart 2), a partially hydrolyzed trimethyl aluminum reagent, methylaluminoxane (MAO). With these highly active new homogeneous systems, it is possible to fine-tune the product polymer polydispersity and microstructure, solely by modifying the organic ligands around the group 4 metal.<sup>14</sup> This breakthrough was followed by the development of isolable, structurally well-defined cocatalysts and catalytically active 1:1 ion pairs which are the actual catalysts (e.g., Figure 2).<sup>15</sup> Here the strength and steric hindrance of the ion pairing<sup>16</sup> can strongly influence catalytic activity, catalyst stability, chain-transfer processes, and product tacticity.<sup>15</sup>

What followed was a detailed, atomistic-level understanding of olefin enchainment, polymerization, and chain-transfer processes in such catalysts.<sup>17</sup> Quantum chemical calculations reveal different basic reaction pathways between ethylene and catalyst–cocatalyst ion pairs depending on the cocatalyst, solvent, temperature, and ethylene concentration.<sup>15,18</sup> For example, early studies of  $\text{B}(\text{C}_6\text{F}_5)_3$ -cocatalyzed polymerization mediated by constrained geometry titanium complex (CGCTi, vide infra)

**Special Issue:** 2011 Frontiers in Transition Metal Catalyzed Reactions

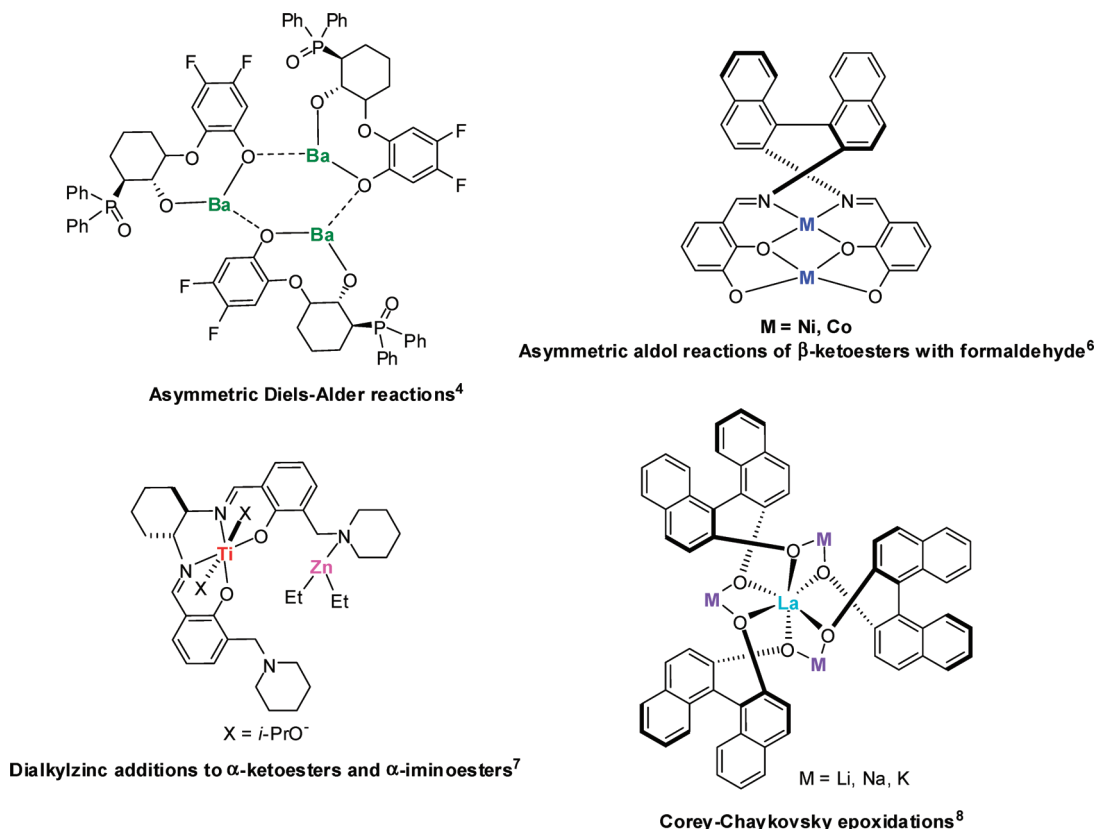
**Received:** October 27, 2010

**Published:** February 17, 2011



**Figure 1.** Left:  $\text{Ni}_2$  core in urease;  $\text{Ni} \cdots \text{Ni}$  distance = 3.5 Å. Right: proposed mechanism of urea hydrolysis into carbon dioxide and ammonia mediated by the urease enzyme.

**Chart 1.** Selected Examples of Cooperative Centers in a Single Structure for the Indicated Catalytic Transformations

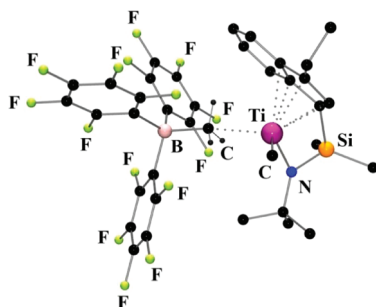
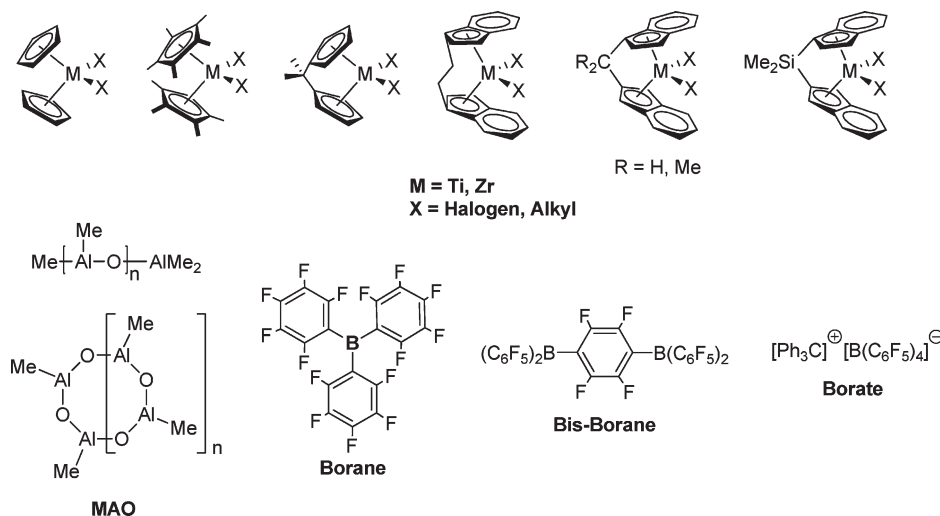


indicated that ethylene approach from the side opposite (A) the  $\text{H}_3\text{CB}(\text{C}_6\text{F}_5)_3^-$  counteranion is energetically more favorable versus other reaction channels involving olefin approach on the same side (B and C) of the counteranion (Figure 3).<sup>15k</sup> However, this scenario may be unfavorable for subsequent enchainments requiring a “chain-swinging” step before each ethylene insertion. Later work has argued that olefin approach on the same side of the counteranion is generally more favorable since it does not require site epimerization of the growing polymer chain.<sup>15a</sup> Nevertheless, each pathway occurs via two discrete steps (Scheme 1): (1) anion displacement with formation of an intermediate  $\pi$ -ethylene complex; (2) ethylene insertion into the  $M\text{--}C$  bond, which is the turnover-limiting step of the propagation process. After the first insertion, two different

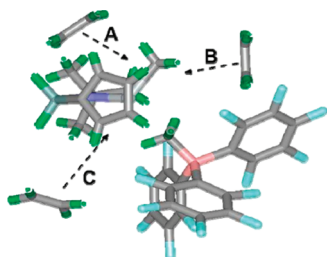
structures may be present: (i) a structure with short  $M^+ \cdots \text{H}_3\text{CB}(\text{C}_6\text{F}_5)_3^-$  contacts involving metal coordinative saturation by the  $\text{CH}_3^-$  group; (ii) a structure with a longer  $M^+ \cdots \text{H}_3\text{CB}(\text{C}_6\text{F}_5)_3^-$  contact, and the counteranion remaining out of the metal coordination sphere with an agostic interaction involving the  $n$ -propyl chain and the metal center.

Detailed thermodynamic/thermochemical and molecular dynamics studies of single-site ion-paired catalytic systems have also emphasized the importance of the counteranion in olefin polymerization catalysis.<sup>15,18</sup> The energetics and kinetics of ion-pair formation and structural reorganization of  $L_nM\text{--}R^+\text{MeB}(\text{C}_6\text{F}_5)_3^-$  systems are a sensitive function of borane acidity, metal ancillary ligation, R substituent, and solvent polarity. These trends can be interpreted in terms of the electron-withdrawing

Chart 2. Selected Examples of Metallocene Precatalysts (Upper Row) and Activating Cocatalysts (Lower Row)



**Figure 2.** Molecular structure of the mononuclear ion-pair polymerization catalyst  $[1\text{-Me}_2\text{Si}(3\text{-ethylindenyl})(t\text{BuN})]\text{TiMe}^+\text{MeB}(\text{C}_6\text{F}_5)_3^-$ . Adapted from ref 15i. Copyright 2003 American Chemical Society.



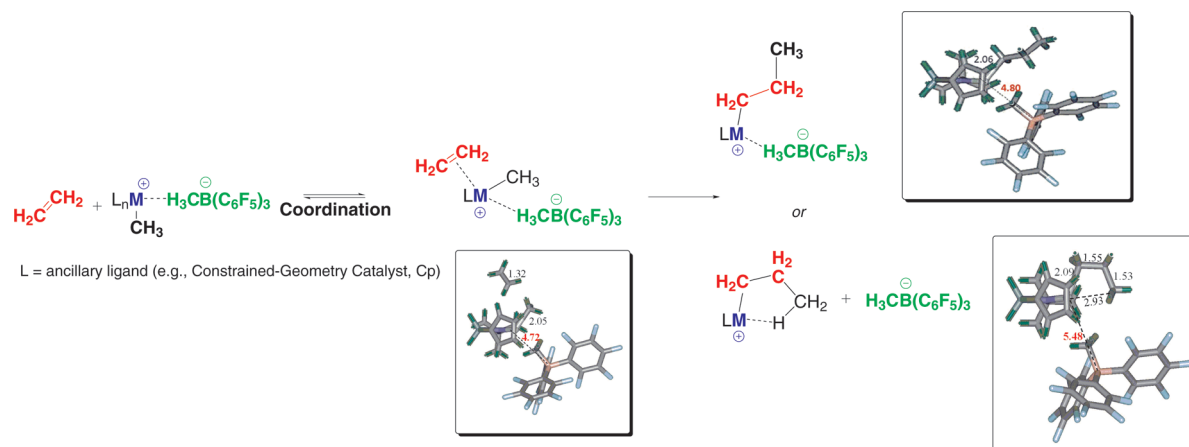
**Figure 3.** Schematic view of possible ethylene approach directions preceding enchainment in the  $\text{CGCTiCH}_3^+\text{H}_3\text{CB}(\text{C}_6\text{F}_5)_3^-$  contact ion pair. Reprinted from ref 15j. Copyright 2003 American Chemical Society.

power and steric characteristics of the borane substituents, the ability of the metallocene ancillary ligands to stabilize the cationic charge and prevent overly tight ion pairing, and the homolytic  $\text{M}-\text{CH}_3$  bond dissociation enthalpies. In addition, sterically encumbered R groups strongly stabilize ion-pair formation by stabilizing the metal cationic charge and by release of steric strain from the neutral metallocene dialkyl precursor, indicating that the ion-pair reorganization barriers generally decrease as the alkyl substituent increases in size. It was also found that the counterion plays an important role in syndiospecific polypropylene formation.<sup>15c,15h,15o</sup> For example, using  $\text{C}_s$ -symmetric precatalysts activated with boranes, borates, and aluminates the ion-pairing

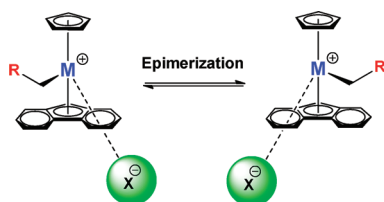
strength is of central importance in determining the relative rates of individual insertion, reorganization (epimerization, Scheme 2), stereodeflect production, and chain-release processes operating during metallocene-mediated propylene polymerization (Scheme 3).

Another polyolefin revolution began in the 1990s when new generations of “nonmetallocene”<sup>20</sup> catalysts were reported, such as various phenoxyiminato ligands combined with early transition metals, reported by Makio and Fujita (Chart 3),<sup>21</sup> or with late transition metals as reported by Grubbs and co-workers (Chart 3).<sup>22</sup> Regarding late transition metals, in 1995 Brookhart’s group reported the high catalytic activity of bulky  $\alpha$ -diimine Ni and Pd complexes with respect to olefin polymerization and (co)polymerization of ethylene with polar monomers (Chart 3).<sup>23</sup> In the early 1990s, another important family of active homogeneous polymerization catalysts was developed: constrained geometry complexes (CGCs, Chart 3, rightmost structure).<sup>24</sup> The exceptional properties of CGC-based catalysts compared to metallocenes in ethylene polymerization and the copolymerization of ethylene with  $\alpha$ -olefins is generally attributed to (i) a less crowded coordination sphere, (ii) a smaller  $\text{Cp}-\text{M}-\text{N}$  bite angle, (iii) a decreased tendency of the growing polymer chain to undergo competing chain-transfer reactions, and (iv) a more Lewis acidic metal center.

The field of mononuclear single-site olefin polymerization catalysis<sup>25,26</sup> experienced intense research activity over the past 2 decades. Research has focused on the development of new active catalytic species generated by the combination of a transition metal organometallic catalyst precursor and a cocatalyst. The resulting electrophilic/coordinatively unsaturated ion-paired species then undergo rapid olefin enchainment at the metal center. The strength of the catalyst–cocatalyst ion pairing can also be used to bind catalytic centers both structurally and functionally. For example, mononuclear CGCZr-derived catalysts typically exhibit moderate activities and typically yield low molecular weight polymers. In marked contrast, mononuclear CGCTi-derived catalysts exhibit high activity and high selectivity for  $\alpha$ -olefin coenchainment, as well as high molecular weight product polyolefins. Pronounced cooperative effects can be elicited using *electrostatic connectivity* by combining mononuclear catalysts and a binuclear cocatalyst/dianion (**M1B2**), where the CGCZr center serves as an “oligomer

Scheme 1. Proposed Mechanism in Which the Catalyst/ $\text{B}(\text{C}_6\text{F}_5)_3$  Cocatalyst Ion Pair Initiates Ethylene Polymerization<sup>a</sup>

<sup>a</sup> Selected calculated molecular structures for ethylene insertion at the  $\text{CGCTiCH}_3^+ \cdots \text{H}_3\text{CB}(\text{C}_6\text{F}_5)_3^-$  ion pair are also depicted. Reprinted from ref 15j. Copyright 2003 American Chemical Society.

Scheme 2. Proposed “Chain-Swinging” Mechanism in  $\text{C}_s$ -Symmetric Catalyst/Cocatalyst Ion Pair Mediated Syndiotactic Propylene Polymerization

maker” and the CGCTi center as a “polymer maker” (Chart 4).<sup>27</sup> The  $\text{M1B2} + \text{CGCTi} + \text{CGCZr}$  double ion pairing primarily produces a homogeneous, highly branched polyethylene in contrast to that provided by  $\text{M1B1} + \text{M1B1}'$ , which yields a heterogeneous mixture of high and low molecular weight polyolefins. Statistically present  $\text{CGCZr} + \text{CGCZr}$  and  $\text{CGCTi} + \text{CGCTi}$  pairs yield smaller quantities of very soluble oligomers and ultrahigh molecular weight polyethylene, respectively, which are readily separated by washing or by filtration, respectively.<sup>27</sup>

The new catalysts and cocatalyst/activators have achieved remarkable success in the production of technologically advanced polyolefin materials.<sup>28</sup> In this regard, academic and industrial research has focused on the synthesis of new catalysts that are better able to control product molecular weight, polydispersity, comonomer enchainment level and pattern, the tacticity of poly( $\alpha$ -olefin) products,<sup>29</sup> copolymerization of olefins with polar comonomers,<sup>30</sup> and the catalytic synthesis of block copolymers by processes such as chain-shuttling polymerization.<sup>30b,31</sup> As a recent example of the latter, the Dow Chemical Company has recently introduced a postmetallocene chain-shuttling technology [INFUSE Olefin Block Copolymers (OBCs)], in which two different catalysts in a single reactor, via a reversible main group (e.g.,  $\text{ZnR}_2$ ) alkyl-mediated chain-transfer mechanism, produce linear statistical multiblock polymer architectures with alternating “hard” (high-crystallinity

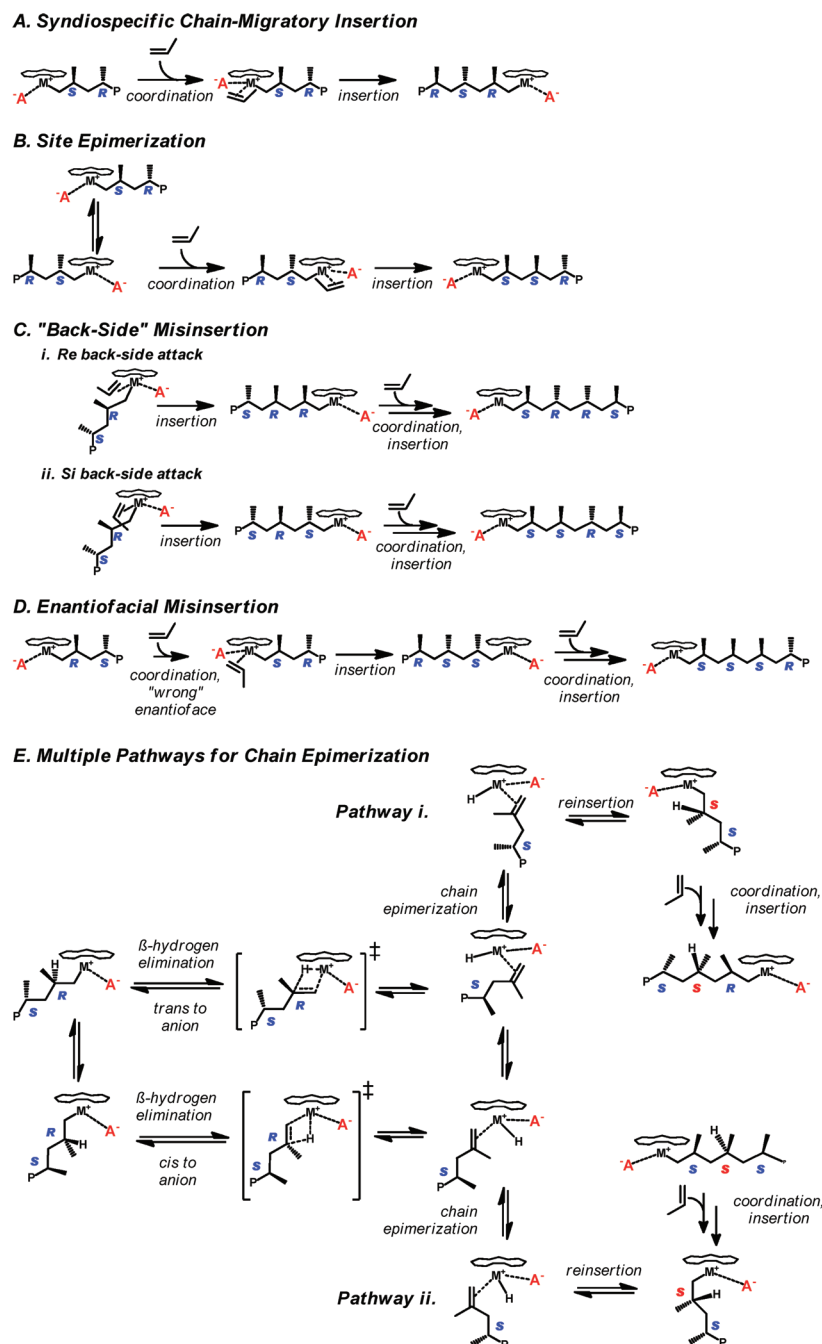
polyethylene) and “soft” (ethylene/octene copolymer) segments having dissimilar physical and mechanical properties (Scheme 4).<sup>32</sup>

### 1.3. Scope of This Review

In 2006, a short overview of nuclearity and cooperativity effects in binuclear catalysts and cocatalysts for olefin polymerization was published from this laboratory.<sup>26a</sup> It focused exclusively on bimetallic group 4 “constrained geometry” catalysts investigated at Northwestern University. The area of bimetallic olefin polymerization catalysis has experienced remarkable activity in the intervening years so that a review of the field now seems opportune. The present review highlights the recent developments in the design and properties of new multimetallic olefin polymerization catalysts, along with polymerization results that have been reported since the early 1990s. In this review, we focus only on multimetallic olefin polymerization catalysts where the active sites are held together by one or more covalent linkages. Included are group 4 metal systems with metallocene and half-metallocene-type ligands, group 10 metals with a wide range of ligands, bimetallic catalysts with other metals, as well as heterobinuclear and multinuclear catalysts. The emphasis here is on nuclearity and cooperativity effects in terms of product polymer chain branching,  $\alpha$ -olefin comonomer enchainment selectivity, molecular weight enhancement, and other characteristics, compared to the mononuclear counterparts. Cooperative effects in olefin polymerization catalysis are particularly pronounced when secondary interactions occur between weakly basic monomer substituents and a second metal center. These can play a key role in modifying enchainment and chain-transfer kinetics. It will be seen here that synergistic reactivity patterns involving two or more metal centers are strongly dependent on the catalyst architecture; if well-designed interactions between the active sites are present, substantial cooperative effects can be observed, whereas if weak or no interactions are present, cooperative effects are frequently weak or negligible (Chart 5). The mechanistic basis of these effects is also discussed where sufficient data are available.

In this review, catalysts are classified according to their transition metal group and the ligand structure. Catalytic activities are converted, where necessary, into units of kg polymer  $[\text{mol cat.}]^{-1} \text{atm}^{-1} \text{h}^{-1}$ . They are classified as very high ( $>1000$ ), high ( $1000-100$ ), moderate ( $100-10$ ), low ( $10-1$ ), and very low ( $<1$ )  $[\text{mol cat.}]^{-1} \text{atm}^{-1} \text{h}^{-1}$ .<sup>33</sup> However, for a given metal–ligand



Scheme 3. Mechanistic Pathway for  $C_s$ -Symmetric Catalyst-Mediated Syndiotactic Propylene Polymerization<sup>a</sup>

<sup>a</sup> Note that the "chain swinging", as modulated by ion pairing in concert with enantiofacially selective propylene enchainment, is key in syndiosselection (ref 19).

center, polymerization activities are often strongly dependent on various factors such as the nature of the cocatalysts and/or scavenger, temperature, pressure, time, solvent, and many other parameters. For these reasons, standardization of catalyst olefin polymerization results is sometimes necessarily approximate.

## 2. GROUP 4 BIMETALLIC CATALYSTS

### 2.1. Linked Metallocene Catalysts

**2.1.1. Phenylene-Bridged Catalysts.** A number of variations on phenylene bridging units in titanocenes and zirconocenes

have been reported. Propylene polymerizations with binuclear zirconocene monophenylene-bridged<sup>34</sup> complex **1** (Chart 6), activated with MAO, do not exhibit a significant difference in activity or deactivation behavior compared to the monometallic analogue  $Cp_2ZrCl_2$ . However, the molecular weight of the polypropylene product decreases in the case of **1**, implying a higher rate constant for chain transfer, e.g., via  $\beta$ -hydride elimination, versus propagation. More crowded Cp diphenylene-bridged binuclear Zr (**2**) and Ti (**3**) complexes exhibit increased molecular weight as well as comparable or even greater catalytic activity in ethylene and styrene polymerization versus their mononuclear counterparts  $Cp_2ZrCl_2$ , and

Chart 3. Examples of Nonmetallocene Olefin Polymerization Catalysts

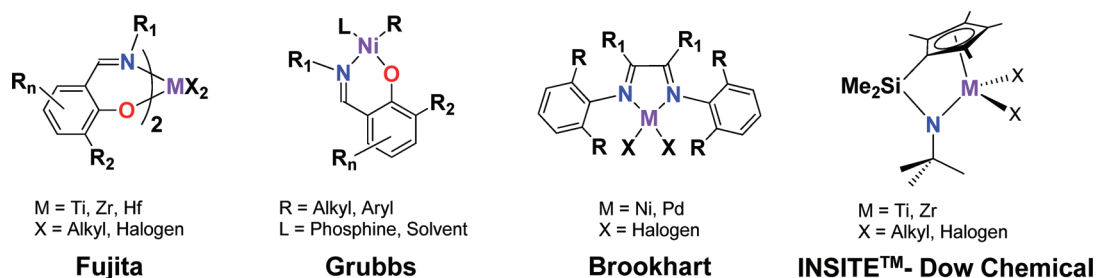
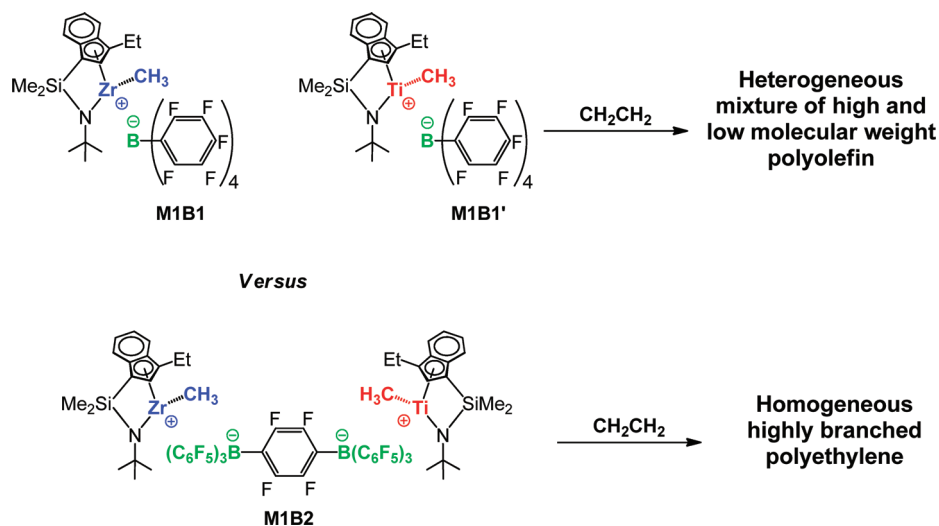
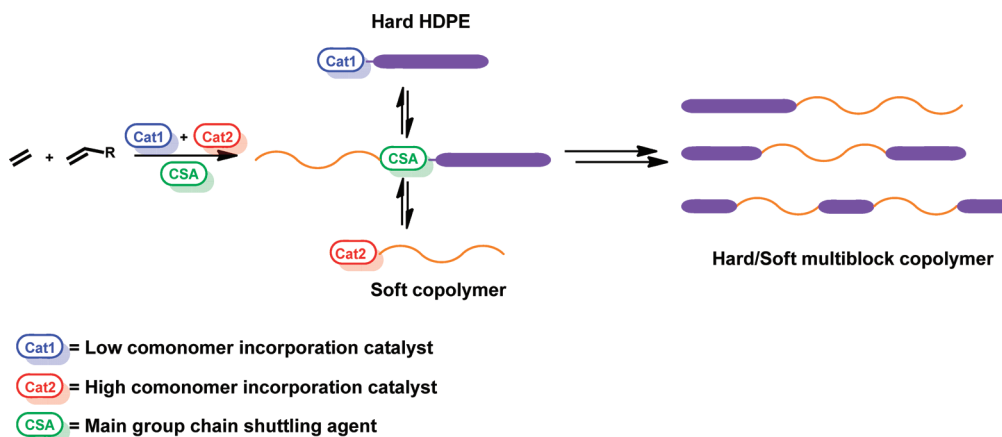


Chart 4. Examples of CGCM-Derived (M = Ti, Zr) Mononuclear and Multinuclear Catalytic Assemblies



Scheme 4. Mechanism of the Chain-Shuttling Multiblock Polymerization Process

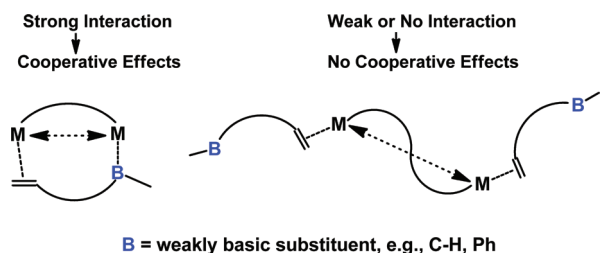


$\text{Cp}_2\text{TiCl}_2$ , respectively (Chart 6).<sup>35</sup> A similar biphenylene-bridged Zr catalyst was reported by Soga et al.<sup>36</sup> where a cyclopentadienyl ligand is replaced with a bis(indenyl)phenylsilane ligand, complex 4 (Chart 6). *ansa*-Zirconocene 4 combined with MAO or  $[\text{Ph}_3\text{C}]^+[\text{B}(\text{C}_6\text{F}_5)_4]^-$  as the cocatalyst in toluene solution at temperatures spanning 40–100 °C yields linear polyethylenes with

a broader molecular mass distribution ( $\text{PDI} = 4.2\text{--}10.8$ ) in much higher yield than does the mononuclear catalyst derived from  $[\text{Ph}_2\text{Si}(\text{Ind})_2]\text{ZrCl}_2$  activated under similar conditions. Considering the rigid geometry imposed by the ligand structures and the large metal-center...metal-center differences, the mechanism of any cooperative effect is not obvious, especially in catalysts 2–4. In

these cases, it might involve some trapping of monomers or oligomers within the ion pairs or intramolecular/aggregation effects. The latter could be investigated by concentration-dependent studies.<sup>26</sup> On the other hand, electronic, steric, and ion-pairing effects present in binuclear catalysts 1–4 could conceivably play a role in achieving high catalytic activities with respect to the mononuclear analogues.

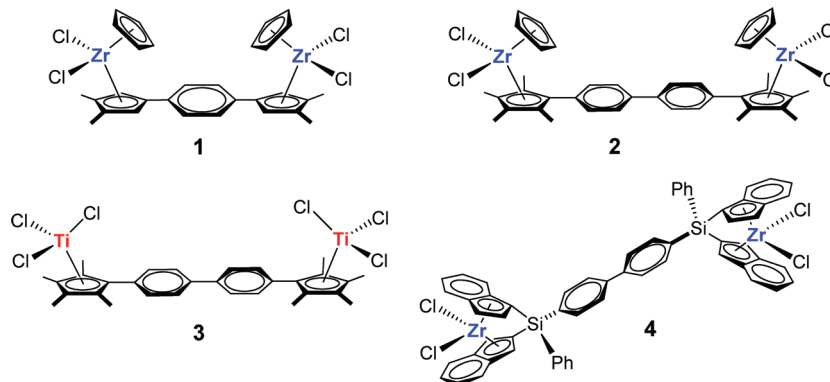
**Chart 5. Proposed Structures for Cooperative Effects between Metal Centers**



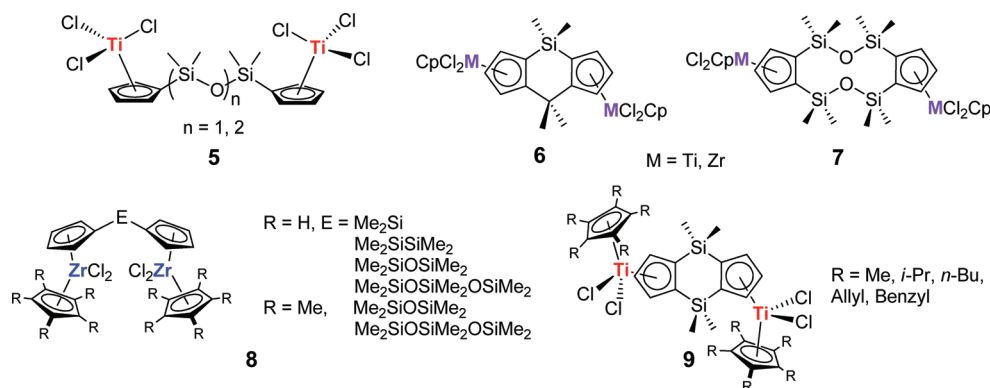
**2.1.2. Silane- and Siloxane-Bridged Catalysts.** Noh and co-workers<sup>37</sup> reported moderately active siloxane-bridged binuclear titanium metallocene catalyst 5 for the polymerization of styrene ( $21 \text{ kg mol} [\text{cat.}]^{-1} \text{ atm}^{-1} \text{ h}^{-1}$ ), comparable in catalytic properties to  $\text{CpTiCl}_3$  (Chart 7). However, the polystyrene syndiotactic index for catalyst 5 is greater (95.6) than that for  $\text{CpTiCl}_3$  (82.2). The higher syndiotacticity value in the case of 5 is believed to reflect the larger steric hindrance around the Ti centers introduced by the siloxane bridge, and not a genuine

cooperative effect between the two metal centers. Further studies by the groups of Xu et al. and Jung et al.<sup>38</sup> showed that monosilane and doubly siloxane-bridged binuclear metallocenes 6 and 7, respectively (Chart 7), in combination with MAO, are very active toward ethylene polymerization. The monosilane-bridged zirconocene 6 exhibits the highest activity at low temperature ( $40^\circ\text{C}$ ), whereas the doubly siloxane-bridged zirconocene 7 exhibits highest activity at higher temperature ( $60^\circ\text{C}$ ). This difference in behavior was attributed to catalyst 7 participating in slower bimolecular deactivation processes<sup>25</sup> than catalyst 6. Mechanistic details concerning possible cooperative enchainment effects between the two active centers were not reported. In 2002 Tian et al.<sup>39</sup> reported a series of silane- and siloxane-bridged binuclear zirconocenes 8 (Chart 7). These metallocenes were studied as catalysts for ethylene polymerization in the presence of MAO. The polymerization results indicate that the catalytic activities increase as the bridging ligand becomes longer for the same type of Cp ligands. The trisiloxane-bridged systems also exhibit greater activity than the mononuclear zirconocene,  $\text{Cp}_2\text{ZrCl}_2$ . It is possible that a Lewis acid–base interaction of the acidic MAO aluminum with the weakly Lewis basic siloxane oxygen is operative and that this electron-withdrawing interaction may reduce the polymerization activities of the disiloxane catalysts; however, the same trend is not observed in the trisiloxane analogues, where steric effects may be more pronounced.<sup>40</sup> Furthermore, the Lewis acid–base interaction may increase the catalyst thermal stability, as suggested by the enhanced activity at higher temperatures ( $>60^\circ\text{C}$ ).

**Chart 6. Phenylene-Bridged Binuclear Metallocene-Type Polymerization Catalysts**

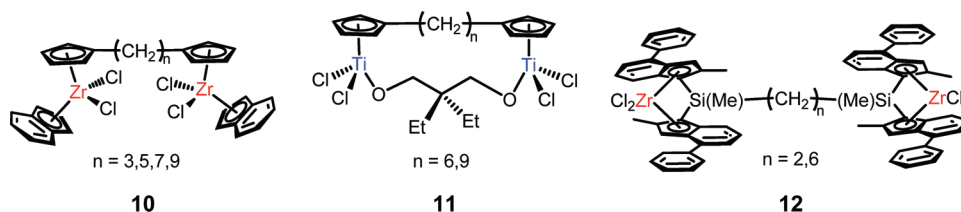


**Chart 7. Silane- and Siloxane-Bridged Binuclear Cyclopentadienyl Group 4 Catalysts<sup>a</sup>**



<sup>a</sup>Note that catalysts 6–9 are produced as mixtures of isomers having syn or anti occupation of the two ring planes.

Chart 8. Polymethylene-Bridged Group 4 Catalysts



The decreased polyethylene molecular weight may reflect reduced electron density at the metal centers, which may enhance the  $\beta$ -hydride elimination versus propagation rate.<sup>41</sup> Other examples of silane-bridged titanium complexes which contain alkyl and potentially coordinating allyl and benzyl groups on the Cp rings include complexes **9**.<sup>42</sup> Catalysts **9** are highly active in ethylene polymerization at low Al/Ti ratios. Compared to  $Cp_2TiCl_2$ , alkyl substituents on the Cp rings enhance ethylene polymerization activity, whereas allyl and benzyl groups depress activity, possibly due to steric crowding and/or metal coordination which would hinder ethylene insertion.<sup>43</sup> In any case, the molecular weight distributions are very broad and bimodal (PDI = 26.75). These results indicate that there is more than one kind of species active during the polymerization but provide no information on possible cooperative enchainment effects.

**2.1.3. Polymethylene-Bridged Catalysts.** Binuclear metallocenes sometimes exhibit distinctive polymerization properties versus the well-defined mononuclear analogues. Moreover, their polymerization properties can have a strong dependence on the length and the nature of the bridging ligands. To enable high bridge flexibility and allow cooperation between the two metal centers, Noh et al.<sup>44</sup> reported a family of polymethylene-bridged zirconocene complexes **10** (Chart 8). The most striking feature of these polymethylene-bridged binuclear zirconocenes is the large increase in ethylene polymerization activities versus that of the corresponding mononuclear metallocene, as well as that of the polysiloxane-bridged binuclear zirconocenes of structure **8** (Chart 7).<sup>44</sup>

These results suggest that the greater electron density and steric screening provided by the polymethylene bridges stabilize the active site and accelerate the rate of ethylene enchainment. On the other hand, for the binuclear zirconocene with a relatively short bridge length of three  $CH_2$  units, steric congestion around the metal centers is likely more pronounced and leads to depressed activity. A  $(CH_2)_5$  linkage corresponds to a distance where bridge electronic effects dominate steric hindrance between the two metal centers and maximize the catalytic properties of **10**. However, higher activity is observed, as well as enhanced product polystyrene tacticity and molecular weight in styrene polymerization, if doubly bridged ligands connect the two metal centers (**11**, Chart 8) and constrain them to close proximity,<sup>45</sup> as opposed to binuclear  $CpTi$  catalysts with a single bridge. The second bridge clearly plays an important role in producing high levels of syndiotacticity in styrene homopolymerization. It is proposed that the second bridge prevents rotation around the polymethylene bridge and holds the two metal centers in a favorable conformation for stereospecific styrene enchainment. Another example of single polymethylene-bridged complexes effective for propylene polymerization is the  $C_2$ -symmetric indenyl zirconocene **12** described by Spaleck et al.

(Chart 8).<sup>46</sup> Catalyst **12** (activity =  $93\,000\text{ kg mol}^{-1}\text{ h}^{-1}\text{ atm}^{-1}$ ) is less active than the mononuclear analogue [dimethylsilanediy(2-methyl-1-indenyl)(2-methyl-4-phenyl-1-indenyl)zirconium dichloride ( $LZrCl_2$  =  $446\,000\text{ kg mol}^{-1}\text{ h}^{-1}\text{ atm}^{-1}$ )] but yields increased polypropylene molecular weight (**12** =  $780 \times 10^3\text{ g/mol}$ ;  $LZrCl_2$  =  $530 \times 10^3\text{ g/mol}$ ) with an increased atacticity index (6.1 wt % versus <0.2 wt % for  $LZrCl_2$ ). Additional mechanistic details supporting possible cooperation between the active centers were not reported.

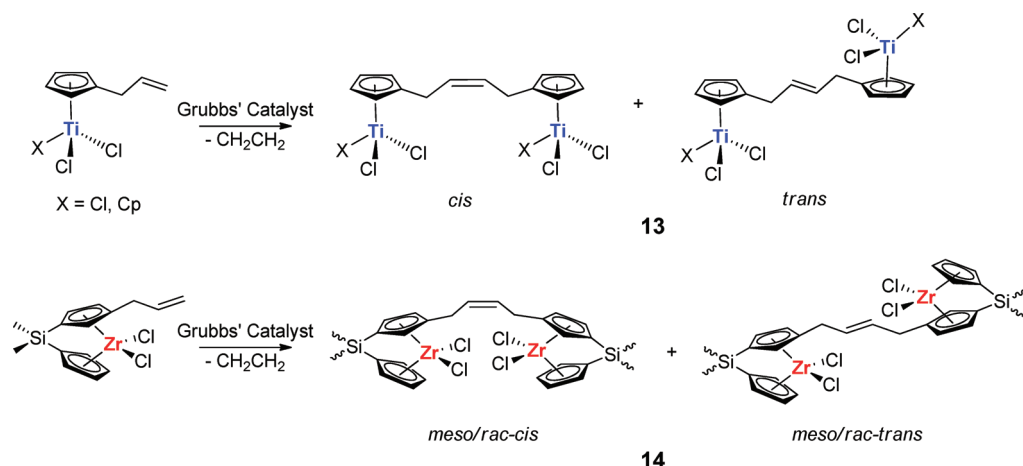
**2.1.4. Flexible/Rigid Bridged Catalysts.** To enhance the cooperative effects between the catalytic centers via high local reagent concentrations and/or conformationally selective active-site–substrate binding, several binuclear metallocene series having flexible/rigid bridges were reported by several research groups. Sierra et al.<sup>47</sup> described the synthesis of binuclear titanium (**13**) and zirconium (**14**) complexes, prepared by olefin metathesis as depicted in Scheme 5. In both cases, a mixture of isomers was detected (cis and trans for complex **13** and rac-cis, meso-cis, rac-trans, and meso-trans for **14**). Only complexes **14** were preliminarily tested as ethylene and propylene polymerization catalysts, and both exhibited lower activity than their mononuclear analogues.

Using a similar synthetic approach, Kuwabara et al.<sup>48</sup> reported a binuclear zirconium complex with flexible bridging ligands (**15**; Scheme 6). The mononuclear Cp-allyl Zr complex undergoes intermolecular metathesis of the vinyl functionality by a second-generation Grubbs' catalyst<sup>49</sup> to yield the cis-only vinylene-bridged binuclear complex. Hydrogenation of the product on Pd/C affords **15** with a flexible polymethylene chain bridging the two metal centers (Scheme 6). Binuclear complex **15** catalyzes the homopolymerizations of ethylene and propylene in the presence of MAO. In the case of ethylene polymerization, **15** shows greater activity ( $3840\text{ kg mol}^{-1}\text{ h}^{-1}\text{ atm}^{-1}$ ) than does the mononuclear precursor ( $2350\text{ kg mol}^{-1}\text{ h}^{-1}\text{ atm}^{-1}$ ). The major active species in a polymerization catalyzed by the binuclear complexes are the dicationic complexes, and bulky counteranions formed from MAO may have mutual steric or electrostatic repulsions that weaken the ion pairing with the cationic dizirconium complex. The higher catalytic activity of the binuclear complexes may be due to this greater effective separation of the cationic centers from the anions (vide infra, section 2.2.1).

To constrain the metal catalytic centers in closer proximity, Noh and co-workers,<sup>50</sup> and Liu et al.<sup>51</sup> reported xylene-bridged binuclear titanocenes **16** for styrene and ethylene homopolymerizations (Chart 9). Different xylene linkage patterns (ortho, meta, para) and catalytic center spatial relationships were proposed to be a principal factor leading to the different polymerization characteristics of these binuclear catalysts. In styrene homopolymerization, catalysts **16** activated with MAO at  $40\text{ }^\circ\text{C}$  exhibit a greater syndiotacticity index (SI) versus the mononuclear



Scheme 5. Synthesis of Binuclear Group 4 Polymerization Catalysts 13 and 14



Scheme 6. Synthesis of Binuclear Zirconocene 15

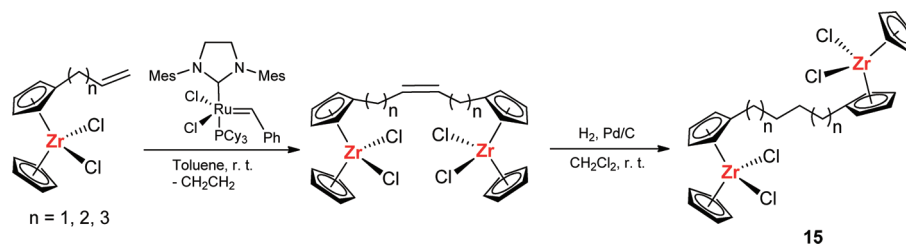
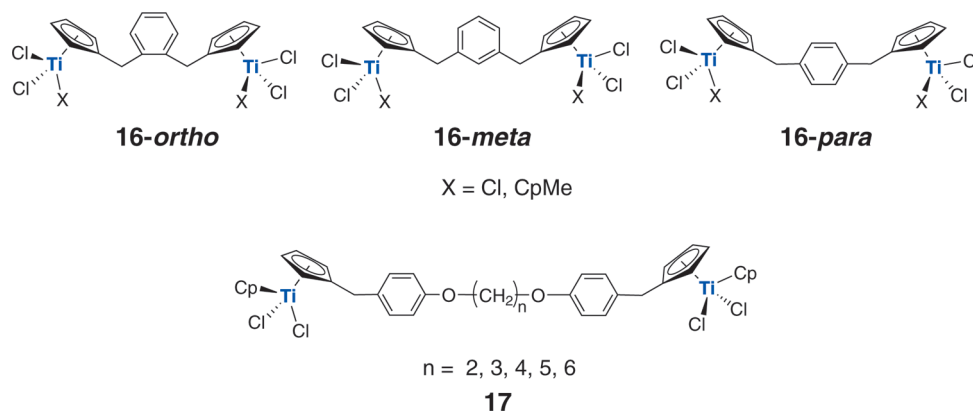


Chart 9. Xylene-Bridged and Related Binuclear Half-Sandwich Organotitanium Catalyst Precursors



analogue, and interestingly, the SI value increases in the order meta > ortho > para, whereas the activity increases in the order para > meta > ortho. Note that the molecular weight and molecular weight distribution are not very sensitive to details of the catalyst structures ( $M_w = 10.7\text{--}6.2 \times 10^4$ ; PDI = 2.1–2.5).<sup>50</sup> No mechanistic details regarding the differences in SI between the different xylene linkage patterns catalysts were reported by the authors.

In 2007, binuclear titanocenes linked by diether groups were reported by Xiao et al.<sup>52</sup> In ethylene homopolymerization in

presence of MAO cocatalyst, the catalytic properties of 17 (Chart 9) are highly dependent on the length of the flexible segment and the polymerization conditions. As the length of flexible linker is increased, catalytic activity increases, whereas the molecular weight of the polyethylene produced decreases. No explanation of these effects was proposed by the authors.

## 2.2. Linked Constrained Geometry Catalysts

Constrained geometry catalysts are well-known to produce polyolefins with high productivity and selectivity.<sup>24</sup> The open,

Scheme 7. Synthetic Route to Binuclear CGC Catalysts

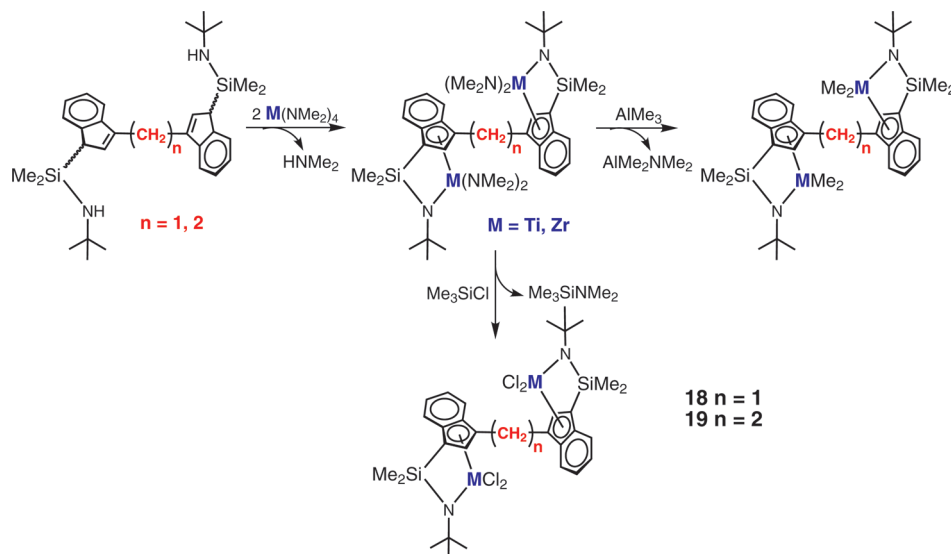
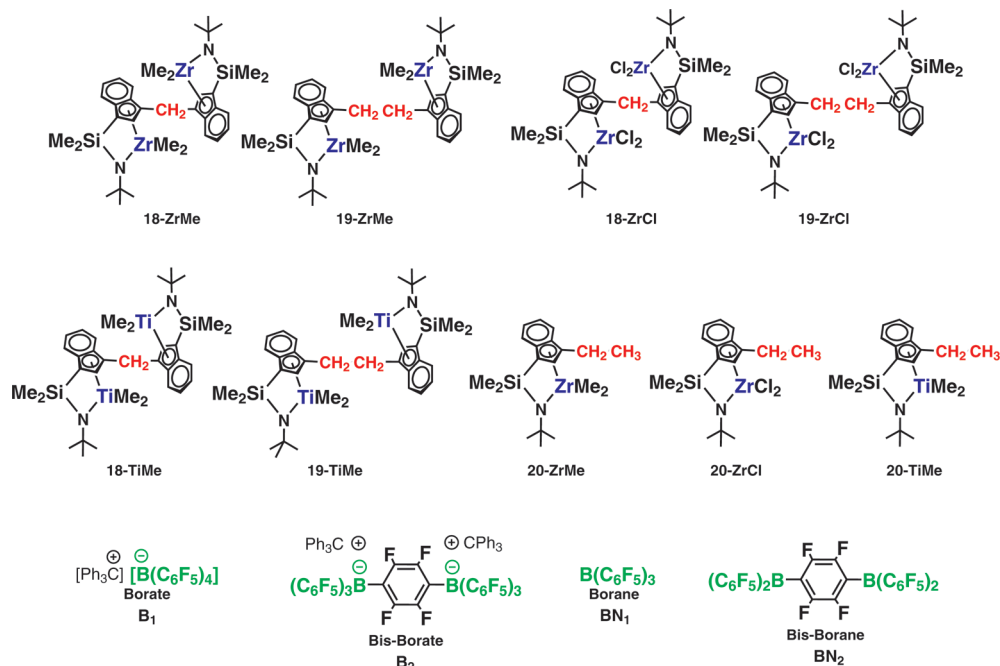
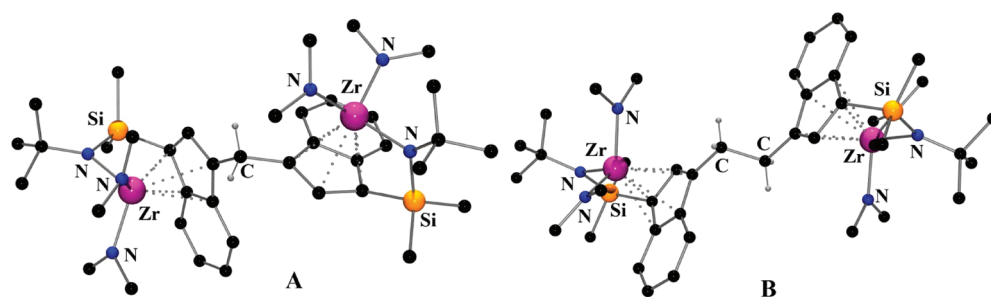


Chart 10. Structures of Binuclear and Mononuclear CGC-Type Catalysts and Borane/Borate Cocatalysts



coordinatively unsaturated nature of the active site allows, under optimum conditions, chain-transferred macromonomers that would normally diffuse away to undergo reinsertion into a proximate growing polymer chain to produce highly branched macromolecules (e.g., LDPE: density = 0.910–0.940 g/cm<sup>3</sup>; crystallinity = low;  $T_g$  = below  $-60$  °C;  $T_m$  = 80–115 °C). In addition, CGC systems permit rapid enchainment of sterically encumbered olefins into the polyethylene backbone. Notably, CGC catalysts exhibit increased thermal stability and produce higher molecular weight polymers than conventional metallocene catalysts. Li and Marks<sup>53</sup> reported the synthesis, characterization, and polymerization characteristics of a series of group 4 binuclear CGC complexes as well as analogous mono-

nuclear control catalysts. All compounds were synthesized via protodeamination of  $M(NMe_2)_4$  ( $M = Ti, Zr$ ) complexes by mono- and bifunctional CGCH<sub>2</sub> reagents, followed by reaction with excess  $AlMe_3$  to afford the corresponding tetramethyl complexes (Scheme 7). The corresponding chloride derivatives can be synthesized by reaction of  $Me_3SiCl$  with the binuclear CGC amido intermediate (Chart 10). In these complexes, the length of the bridge dramatically changes the catalyst conformation. Thus, the methylene-bridged binuclear catalysts (**18**)<sup>54</sup> have large computed rotational barriers ( $\sim 65$  kcal/mol) about the indenyl–CH<sub>2</sub>–indenyl bridging linkage, whereas the –CH<sub>2</sub>–CH<sub>2</sub>– bridged binuclear catalysts (**19**)<sup>55</sup> have a negligible computed rotational barrier (Figure 4). The shorter methylene



**Figure 4.** Molecular structures of (A) methylene-bridged MCGC–Zr<sub>2</sub>(NMe<sub>2</sub>)<sub>4</sub> [**18**-Zr<sub>2</sub>(NMe<sub>2</sub>)<sub>4</sub>] and (B) ethylene-bridged ECGC–Zr<sub>2</sub>(NMe<sub>2</sub>)<sub>4</sub> [**19**-Zr<sub>2</sub>(NMe<sub>2</sub>)<sub>4</sub>] complexes. Adapted from ref 54, copyright 2005 American Chemical Society, and ref 55, copyright 2002 American Chemical Society, respectively.

**Table 1.** Ethylene Polymerization Data for CGCZr Catalysts with Different Nuclearities and Cocatalysts<sup>a</sup>

entry	catalyst <sup>a</sup>	μmol cat.	reaction time (h)	polymer yield (g)	activity <sup>b</sup>	ethyl branches/1000 C	<i>n</i> -butyl branches/1000 C	<i>M<sub>n</sub></i> (× 10 <sup>2</sup> ) <sup>c</sup>	<i>M<sub>w</sub></i> / <i>M<sub>n</sub></i> <sup>c</sup>
1	<b>20</b> -ZrMe + B <sub>2</sub>	10	1.16	1.08	93	6.5	0.6	6.3	1.1
2	<b>18</b> -ZrMe + B <sub>2</sub>	5	1.50	0.19	13	1.6	~0	326	2.7
3	<b>19</b> -ZrMe + B <sub>2</sub>	5	1.50	0.94	63	12	1.0	11	1.2
4	<b>20</b> -ZrCl + MAO <sup>d</sup>	10	1.50	0.37	25	~0	~0	9.5	1.3
5	<b>18</b> -ZrCl + MAO <sup>d</sup>	5	1.50	0.38	25	~0	~0	2440	2.7
6	<b>19</b> -ZrCl + MAO <sup>d</sup>	5	1.50	0.35	23	~0	~0	2680	2.8
7	<b>20</b> -ZrMe + B <sub>2</sub> <sup>e</sup>	10	0.025	0.17	680	1.7	1.1	17	1.4
8	<b>18</b> -ZrMe + B <sub>2</sub> <sup>e</sup>	5	0.025	0.16	640	2.8	1.4	15	1.6
9	<b>19</b> -ZrMe + B <sub>2</sub> <sup>e</sup>	5	0.025	0.14	560	7.0	2.4	15	1.5

<sup>a</sup> Polymerizations carried out on a high-vacuum line at 24 °C in 100 mL of toluene under 1 atm of ethylene pressure. <sup>b</sup> kg of polyethylene (mol of Zr)<sup>−1</sup> atm<sup>−1</sup> h<sup>−1</sup>. <sup>c</sup> From GPC vs polystyrene standards. <sup>d</sup> Al/Zr = 1000:1. <sup>e</sup> Polymerizations carried out in chlorobenzene.

bridge constrains the two indenyl rings in a twisted conformation and brings the two Zr atoms to the same side of the molecule (Figure 4A), remarkably different from the orientation in complex **19**. Thus, the greater rigidity in **18** enforces a close Zr···Zr proximity (**18**, minimum Zr···Zr distance = 7.392(3) Å; **19**, minimum Zr···Zr distance = 8.671(3) Å) and thus favors conformations for binuclear metal–alkyl chain···metal–alkyl chain interactions (vide infra).

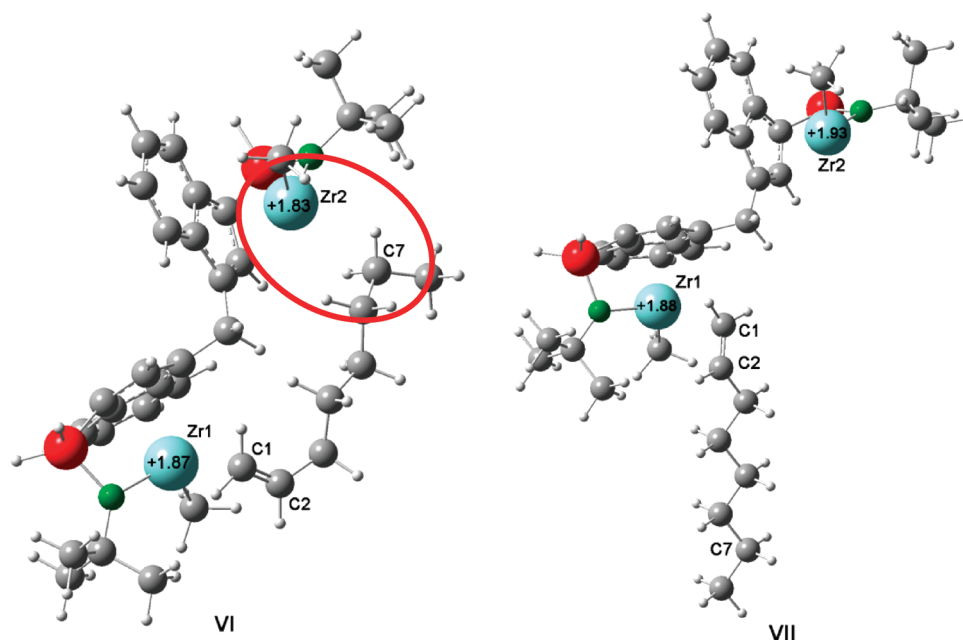
**2.2.1. Ethylene Polymerization Properties.** In ethylene polymerization, under identical reaction conditions, catalysts **18**-ZrMe and **19**-ZrMe show ~70× and ~130× increases, respectively, in product polymer molecular weight versus the monometallic analogue **20**. Both **18**-ZrMe and **19**-ZrMe (Table 1), in combination with bisborate cocatalyst B<sub>2</sub> (Chart 10), produce polyethylenes with substantial ethyl branching as characteristic microstructural features.<sup>56</sup> Moreover, the molecular weight of the polyethylene products is independent of ethylene pressure, implying that the dominant chain transfer is chain transfer to monomer.<sup>55</sup> The distinctive selectivity of the binuclear catalytic systems for introducing ethyl branching can be rationalized in terms of chain transfer to ethylene, yielding an oligomeric or polymeric vinyl macromonomer, followed by 1,2-intramolecular reinsertion at a proximate Zr–ethyl<sup>+</sup> or Zr–R<sup>+</sup> (Scheme 8), with ~8× greater ethyl branching per 1000 C atoms for **19**-ZrMe versus **18**-ZrMe, which correlates with the lower molecular weight of the polyethylene product produced by **19**-ZrMe.

DFT calculations on activated **18**-ZrMe + 1-octene<sup>57</sup> strongly suggest that the close proximity of the two Zr sites in such bimetallic catalysts promotes a non-negligible agostic interaction between an oligomeric π-bonded vinyl-terminated oligoethylene chain and the second metal site, a prerequisite for the proposed ethyl branch formation mechanism (Figure 5). The computational results indicate that the configuration with an agostically

bonded 1-octene is stabilized by ca. 3 kcal/mol versus that with no agostic interaction. Importantly, these agostic interactions adjacent to the chain propagation site modify the catalytic environment to increase the propagation/termination rate ratios, in turn favoring increased product molecular weight, as observed experimentally.<sup>54</sup>

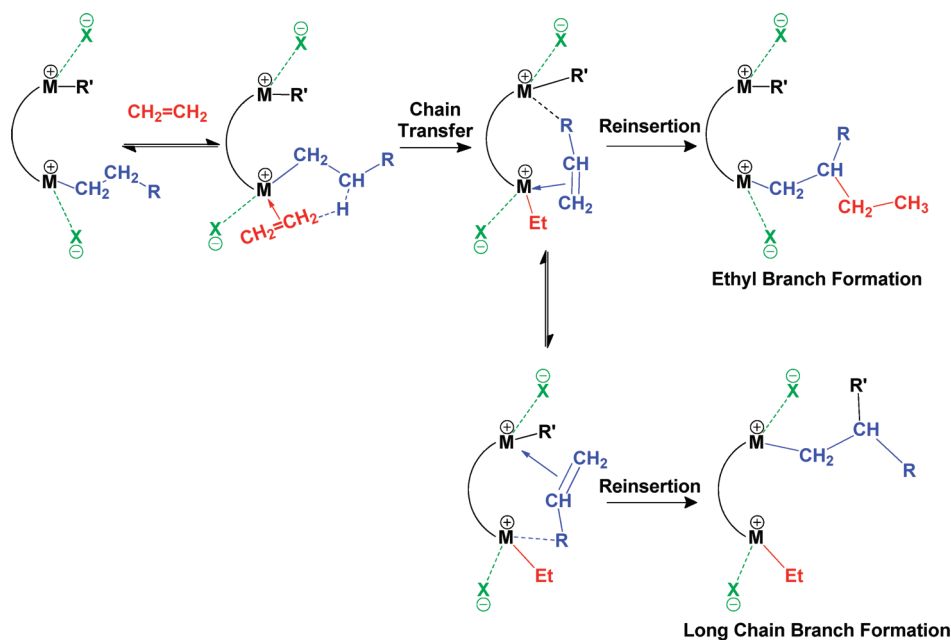
In ethylene homopolymerization using MAO as the cocatalyst, the binuclear precatalysts **18**-ZrCl and **19**-ZrCl afford very high and comparable molecular weight polyethylenes, with molecular weight increased up to ~600× versus mononuclear **20**-ZrCl, although the polymerization activities remain almost identical (Table 1). In contrast, **18**-ZrCl + MAO produces polyethylene with a higher molecular weight than **18**-ZrMe + B<sub>2</sub>, and with a negligible branch content, suggesting a scenario in which the relative chain termination rate is far slower in **18**-ZrCl + MAO than in **18**-ZrMe + B<sub>2</sub>. Note that Zr(μ-CH<sub>3</sub>)Zr species are detected by in situ NMR spectroscopy, for both binuclear compounds, which confirms that the two Zr centers can approach closely and that the bulky MAO cocatalyst/counterion stabilizes this intermediate (Chart 11).<sup>54,57</sup> These results support a pathway in which Zr···Zr cooperativity effects can dramatically depress chain transfer to monomer rates.

All of the experiments described above with binuclear CGC-type complexes were carried out in low dielectric constant solvents such as toluene or octane. When a polar solvent such as C<sub>6</sub>H<sub>5</sub>Cl (ε = 5.68) is used as the polymerization medium, a significant compression in the nuclearity-dependent dispersion of polymerization activities and molecular weights is observed versus polymerizations in toluene (ε = 2.38).<sup>54</sup> It appears that the polar solvent weakens the catalyst–cocatalyst ion pairing, enhancing the ion-pair flexibility and rendering the cation freer, as evidenced by the greater polymerization activity. However, polar



**Figure 5.** Two different  $\pi$ -complexes of 1-octene with the  $R,R$  diastereoisomer of the  $-\text{CH}_2-$  bridged **18-ZrMe** bimetallic dicationic CGC catalyst. The agostic interaction with octene is circled. Reprinted from ref 57. Copyright 2009 American Chemical Society.

#### Scheme 8. Ethyl Branch Formation Facilitated by Binuclear Macromonomer Binding



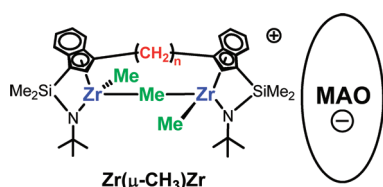
solvents can potentially compete for/coordinate with the electrophilic metal centers and could weaken/replace agostic interactions, thereby suppressing branch formation and propagation in competition with chain transfer. In control experiments, note that the binuclear CGCZr ethylene homopolymerization catalysts **18-ZrMe** and **19-ZrMe** activated with bisborate **B**<sub>2</sub>, and the mononuclear analogues activated with borate **B**<sub>1</sub>, exhibit the following phenomenology: rates are constant for more than 3 h, monomodal molecular weight distributions (PDI  $\sim$  2.0) are observed, product polyethylene molecular weights increase

with catalyst constituent nuclearity, and activities do not differ greatly. In addition, variable ethylene pressure experiments show invariant molecular weight, arguing that chain transfer to monomer is the predominant chain-transfer pathway. It is also found that the polymer microstructure does not change with catalyst concentration.

Noh et al.<sup>58</sup> investigated the comparative ethylene polymerization behaviors of binuclear CGC titanium catalysts having C<sub>6</sub>, C<sub>9</sub>, C<sub>12</sub> polymethylene bridges **21** (Chart 12) in the presence of a modified methylaluminoxane (MMAO) cocatalyst. Polymerization



Chart 11.  $\text{Zr}(\mu\text{-CH}_3)\text{Zr}$  Species Stabilized by the Bulky MAO Cocatalyst/Counteranion

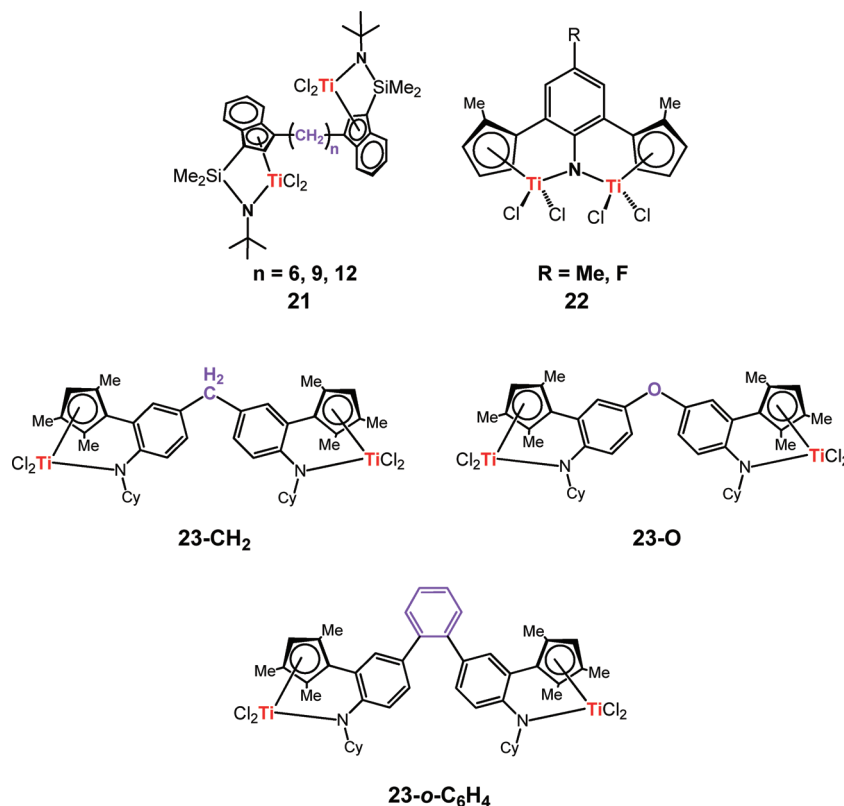


activities increase in the order  $\text{C}_6\text{-21} < \text{C}_9\text{-21} < \text{C}_{12}\text{-21}$ , which indicates that the presence of the longer bridge between active sites enhances the polymerization activities of these binuclear CGC catalysts. The same trend was observed by Marks and co-workers,<sup>53</sup> where ethylene-bridged catalyst **19-ZrMe** is more active than methylene-bridged catalyst **18-ZrMe**. However, the latter catalyst produces higher molecular weight polyethylene. No details concerning polyethylene branching or molecular weight or any other mechanistic observations were reported for complex **21**.

Binuclear titanium complexes, where the two metal centers share a central nitrogen fragment as in complex **22** (Chart 12), are not active for ethylene + 1-hexene copolymerization when activated with MAO.<sup>59</sup> However, a series of binuclear CGCTi complexes of structure **23** (Chart 12), in which the two metal centers are connected by a diphenylene bridge, are highly active for olefin polymerization when activated with MAO. The polymerization activities are greater than for the mononuclear analogue, as the molecular weights of the polymeric products.<sup>59</sup> Slightly greater long-chain branch contents are observed for the binuclear catalysts in the case of ethylene + 1-hexene copolymerization versus the mononuclear control.

**2.2.2. Ethylene +  $\alpha$ -Olefin and Ethylene + Encumbered Isoalkene Copolymerizations.** Notable binuclear effects are also observed in ethylene +  $\alpha$ -olefin copolymerizations using binuclear Ti and Zr CGC catalysts.<sup>15i,53–56,58,60</sup> Under identical copolymerization conditions with 1-hexene and 1-pentene comonomers, **18-ZrMe** + **B**<sub>2</sub> incorporates  $\sim 3\times$  more 1-hexene and  $\sim 4\times$  more 1-pentene than does **19-ZrMe** + **B**<sub>1</sub> (Table 2).<sup>52</sup> Although these binuclear catalysts operate with somewhat suppressed copolymerization activities, note that the product polymer molecular weight is  $\sim 60\times$  greater than for the mononuclear analogues. The closer achievable  $\text{Zr}\cdots\text{Zr}$  distance in the **18-ZrMe** + **B**<sub>2</sub> ion pair increases the selectivity for macromonomer binding and thus enhances the probability of reinsertion. Interestingly, the **18-ZrMe** + **B**<sub>2</sub>-derived copolymer contains similar quantities of ethyl branches as in the ethylene homopolymerizations, suggesting that a similar chain-transfer mechanism is operative in these ethylene homopolymerization experiments. With MAO as the cocatalyst and under identical polymerization conditions, the **18-ZrCl** and **19-ZrCl** catalysts incorporate  $\sim 4.2\times$  and  $\sim 3.5\times$  more 1-hexene, respectively, than does mononuclear **20-ZrCl** and with comparable polymerization activities. As seen in ethylene homopolymerization, the 1-hexene incorporation levels for both mononuclear and binuclear catalysts increase significantly in polar solvents (i.e.,  $\text{C}_6\text{H}_5\text{Cl}$ ) versus those in toluene, suggesting that “freer” cationic species with weaker ion pairing are now accessible (Table 2).<sup>54</sup> Both the ethylene + 1-hexene and ethylene + 1-pentene copolymerization data indicate that closer proximity between two Zr catalytic centers leads to significantly greater extents of comonomer enchainment, with the effects being substantially larger for less sterically encumbered  $\alpha$ -olefins. DFT calculations<sup>57</sup> argue that coordination of the  $\alpha$ -olefin to a cationic

Chart 12. Binuclear CGCTi Catalysts with Flexible or Rigid Bridges



**Table 2.** Ethylene + 1-Hexene (H) and Ethylene + 1-Pentene (P) Copolymerization Data for CGCZr Catalysts with Different Nuclearities and Cocatalysts<sup>a</sup>

entry	catalyst	monomer <sup>b</sup>	$\mu\text{mol cat.}$	reaction time (h)	polymer yield (g)	activity <sup>c</sup>	ethyl branches/ 1000 C	<i>n</i> -butyl branches/ 1000 C	$M_w$ ( $\times 10^3$ ) <sup>d</sup>	$M_w/M_n$ <sup>d</sup>
1	20-ZrMe + B <sub>2</sub>	E/H	10	0.75	1.00	133	6.0	3.2	8.0	1.1
2	18-ZrMe + B <sub>2</sub>	E/H	5.0	1.50	0.13	8.6	1.3	17.2	508	2.3
3	19-ZrMe + B <sub>2</sub>	E/H	5.0	1.25	1.09	87	10	5.5	13	1.2
4	20-ZrCl + MAO <sup>e</sup>	E/H	10	1.50	0.46	15	~0	5.4	4.4	1.3
5	18-ZrCl + MAO <sup>e</sup>	E/H	5.0	1.50	0.33	11	~0	22.8	3280	2.9
6	19-ZrCl + MAO <sup>e</sup>	E/H	5.0	3.00	0.27	9	~0	19.4	2530	2.9
7	20-ZrMe + B <sub>2</sub> <sup>f</sup>	E/H	10	0.033	0.28	848	1.7	35.1	3.8	1.4
8	18-ZrMe + B <sub>2</sub> <sup>f</sup>	E/H	5	0.033	0.19	575	2.2	48.3	3.8	1.8
9	19-ZrMe + B <sub>2</sub> <sup>f</sup>	E/H	5	0.033	0.26	787	5.6	44.9	2.5	1.5
10	20-ZrMe + B <sub>2</sub>	E/P	10	1.00	1.51	151	9.0	20 <sup>g</sup>	5.1	1.5
11	19-ZrMe + B <sub>2</sub>	E/P	5	1.50	1.59	106	10	43 <sup>g</sup>	9.5	1.5

<sup>a</sup> Polymerizations carried out on a high-vacuum line at 24 °C in 100 mL of toluene under 1 atm of ethylene pressure. <sup>b</sup> [Monomer] = 0.8 M. <sup>c</sup> kg of polyethylene (mol of Zr)<sup>-1</sup> h<sup>-1</sup> atm<sup>-1</sup>. <sup>d</sup> From GPC vs polystyrene standards. <sup>e</sup> Al/Zr = 1000:1. <sup>f</sup> Polymerizations carried out in chlorobenzene. <sup>g</sup> *n*-Propyl branches/1000 C.

metal center is stabilized by a secondary agostic interaction with the proximate cationic metal center, which facilitates/stabilizes  $\alpha$ -olefin capture/binding at the metal center and enhances the subsequent enchainment (Figure 5). On the other hand, the binding of the  $\alpha$ -olefin may partially block/compete for the ethylene activation site while not enchainment as rapidly (cf., Scheme 8), thereby affording reduced polymerization activity.

The binuclear CGC titanium catalysts (18-TiMe, 19-TiMe, and 20-TiMe) are also found to be very active when activated with bisborate B<sub>2</sub> or bisborane BN<sub>2</sub> cocatalysts (Chart 10), exhibiting an activity enhancement of ~100 $\times$  versus the binuclear CGC zirconium analogues in ethylene + 1-octene copolymerizations. Polymerization data (Table 3) indicate that, under identical reaction conditions, the 19-TiMe + B<sub>2</sub> ion-paired active system enchains ~11 $\times$  more 1-octene than that derived from mononuclear 20-TiMe.<sup>15i,59</sup>

Efficient ethylene + isoalkene coordinative copolymerizations present an exciting challenge from both academic and technological perspectives.<sup>62</sup> The 19-TiMe + BN<sub>2</sub> active system enchains sterically very hindered 1,1-disubstituted comonomers such as isobutene, methylene-cyclopentane, methylene-cyclohexane, and 1,1,2-trisubstituted 2-methyl-2-butene into the polyethylene backbone under mild conditions (Table 3).<sup>61</sup> The 19-TiMe + BN<sub>2</sub> ion-paired catalyst incorporates ~5 $\times$  more isobutene, ~2.5 $\times$  more methylenecyclopentane, ~2.5 $\times$  more methylenecyclohexane, and ~2.3 $\times$  more 2-methyl-2-butene than the analogous mononuclear catalysts, while product molecular weight and polymerization activities decline only moderately with increased catalyst/cocatalyst nuclearity (Chart 13).<sup>15i</sup> In addition, polar solvents are also found to weaken the catalyst–cocatalyst ion pairing, thus influencing the comonomer enchainment selectivity.

Mechanistic studies of bulky comonomer enchainment have identified two different copolymerization pathways: methylenecyclopentane and methylenecyclohexane are incorporated via a *ring-unopened* pathway (Scheme 9A),<sup>63</sup> whereas 2-methyl-2-butene is incorporated via a novel pathway involving comonomer isomerization to 2-methyl-1-butene, followed by a rapid enchainment into the copolymer backbone (Scheme 9B).

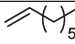
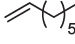
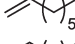
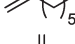
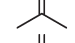
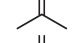
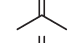
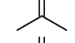
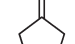

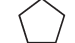
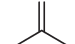
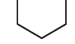
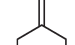
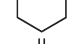
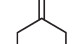
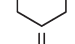
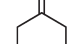
**2.2.3. Styrene Polymerization and Ethylene + Styrene Copolymerizations.** Mononuclear CGCTi catalysts exhibit negligible activity in styrene homopolymerization,<sup>64,65</sup> probably

due to catalyst deactivation via intramolecular arene interaction in the 2,1-insertion product (Chart 14, structure D). On the other hand, activated binuclear 19-TiMe not only exhibits greater activity for styrene homopolymerizations than does the mononuclear control, but installs unusual 1,2-insertion regiochemistry<sup>66</sup> (up to ~50%) in the propagation steps, and also affords broad-range controllable styrene incorporation in ethylene–styrene copolymerizations, arguing that multinuclear cooperative catalysis indeed mediates these unusual styrene polymerization patterns. The coordinated arene rings could in principle participate in several types of multimetallic/enchainment-altering interactions. As illustrated in Chart 14, structure E would formally favor 2,1-insertion, whereas structure F would formally favor 1,2-insertion.

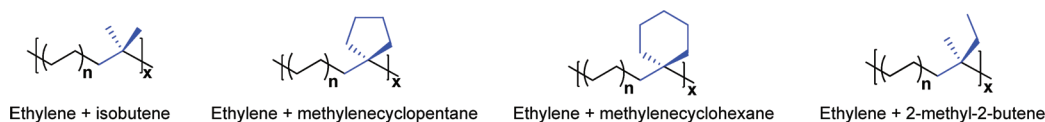
Under identical styrene homopolymerization conditions, 18-TiMe + B<sub>2</sub> and 19-TiMe + B<sub>2</sub> exhibit ~65 $\times$  and ~35 $\times$  greater polymerization activity, respectively, than does the monometallic catalyst 20-TiMe + B<sub>1</sub>. <sup>13</sup>C NMR analyses of the polystyrene produced with bimetallic catalysts show that 1,2-insertion competes with 2,1-insertion, arguing that this unusual insertion regiochemistry arises from the unique catalyst nuclearity (e.g., Scheme 10). In ethylene + styrene(s) copolymerization (Scheme 11), catalyst 19-TiMe enchains 15.4% more styrene, 28.9% more 4-methylstyrene, 31.0% more 4-bromostyrene, 41.2% more 4-chlorostyrene, and 45.4% more 4-fluorostyrene than does 20-TiMe + B<sub>1</sub>. These trends correlate with the <sup>13</sup>C NMR chemical shifts of the styrene C1 atoms and argue for the importance of the Ti<sup>+</sup>...styrene  $\pi$ -interaction.

Kinetic studies reveal that both the 19-TiMe + B<sub>2</sub>- and 20-TiMe + B<sub>1</sub>-mediated ethylene–styrene copolymerizations follow second-order Markov statistics and that the products tend to be alternating. In this regard, when styrene incorporation is >50%, at least three consecutive head-to-tail coupled styrene units are enchainment in addition to tail-to-tail coupled dyads.<sup>67</sup> Moreover, calculated reactivity ratios indicate that binuclear catalyst 19-TiMe + B<sub>2</sub> favors styrene insertion more than does catalyst 20-TiMe + B<sub>1</sub>. In addition, for ethylene–styrene copolymerization, polar solvents are found to increase copolymerization activities but also to coproduce atactic polystyrene impurities in addition to ethylene-*co*-styrene, without diminishing the comonomer incorporation selectivity.

**Table 3. Ethylene + 1-Octene and Ethylene + Isoalkene Copolymerization Results for 19-TiMe and 20-TiMe Catalysts with Cocatalysts B<sub>1</sub>, B<sub>2</sub>, BN<sub>1</sub>, BN<sub>2</sub><sup>a</sup>**

Entry	Cat.	Cocat.	Comonomer	Comonomer Conc. (M)	μmol cat.	Reaction Time (min)	Polymer yield (g)	Activity [x 10 <sup>3</sup> ] <sup>b</sup>	M <sub>w</sub> [x 10 <sup>3</sup> ] <sup>c</sup>	M <sub>w</sub> /M <sub>n</sub> <sup>c</sup>	% incorp. <sup>d</sup>
1	20-TiMe	B <sub>1</sub>		0.64	10	5	8.43	10.2	155	2.3	0.6
2	20-TiMe	B <sub>2</sub>		0.64	10	5	3.20	3.8	147	2.0	1.1
3	19-TiMe	B <sub>1</sub>		0.64	5	5	4.30	5.1	157	2.7	1.0
4	19-TiMe	B <sub>2</sub>		0.64	5	5	2.50	3.0	161	2.7	7.0
5	20-TiMe	BN <sub>1</sub>		1.20	10	5	0.80	0.96	577	2.1	3.1
6	20-TiMe	BN <sub>2</sub>		1.20	10	5	0.37	0.44	305	2.2	9.5
7	19-TiMe	BN <sub>1</sub>		1.20	5	10	0.61	0.36	490	2.4	7.3
8	19-TiMe	BN <sub>2</sub>		1.20	5	10	0.47	0.28	168	3.7	15.2
9	20-TiMe	BN <sub>1</sub>		1.60	10	5	0.67	0.80	503	2.4	8.3
10	19-TiMe	BN <sub>2</sub>		1.60	5	5	0.49	0.59	186	2.3	20.4
11	20-TiMe	BN <sub>1</sub>		1.40	10	4	0.87	1.3	475	1.8	3.3
12	19-TiMe	BN <sub>2</sub>		1.40	5	6	0.35	0.35	369	2.8	8.3
13	20-TiMe	BN <sub>1</sub>		Neat	10	8	0.64	0.48	320	2.2	6.8
14	19-TiMe	BN <sub>2</sub>		Neat	5	8	0.37	0.28	297	2.4	15.9
15	20-TiMe	BN <sub>1</sub>		2.70	10	5	0.61	0.73	769	2.9	1.1
16	19-TiMe	BN <sub>2</sub>		2.70	5	5	0.47	0.56	503	1.9	2.5
17	20-TiMe	BN <sub>1</sub>		Neat	10	10	0.73	0.44	486	2.1	3.2
18	19-TiMe	BN <sub>2</sub>		Neat	5	10	0.65	0.39	456	1.8	7.3

<sup>a</sup> Polymerizations carried out on a high-vacuum line at 24 °C in 100 mL of toluene under 1 atm of ethylene pressure. <sup>b</sup> kg of polyethylene (mol of Ti)<sup>-1</sup> h<sup>-1</sup> atm<sup>-1</sup>. <sup>c</sup> From GPC vs polystyrene standards. <sup>d</sup> Mole percentage calculated from <sup>13</sup>C NMR spectra (ref 61).

**Chart 13. Ethylene + Isoalkene Copolymers Obtained with the 19-TiMe + BN<sub>2</sub> Ion-Paired System**

**2.2.4. Alkenylsilane Chain Transfer.** Chain-transfer agents are defined as chemical reagents which both terminate and facilitate reinitiation of polymer chain growth and which can efficiently control molecular weight and concomitantly introduce chemical functionality into polymer chains. In the present context, func-

nalized polyolefins<sup>68</sup> offer many attractions versus nonfunctionalized polyolefins, including, but not limited to, increased adhesion, paintability, and compatibility with diverse, more polar materials.<sup>69</sup> Thus, the binuclear **19-TiMe** catalyst produces ethylene + alkenylsilane (allylsilane, 3-butenylsilane, 5-hexenylsilane, 7-octenylsilane)

Scheme 9. (A) Proposed Mechanism of Bulky Comonomer Enchainment with Binuclear CGC Catalysts via a *Ring-Unopened* Pathway; (B) Ethylene + 2-Methyl-2-butene Copolymerization via Comonomer Isomerization

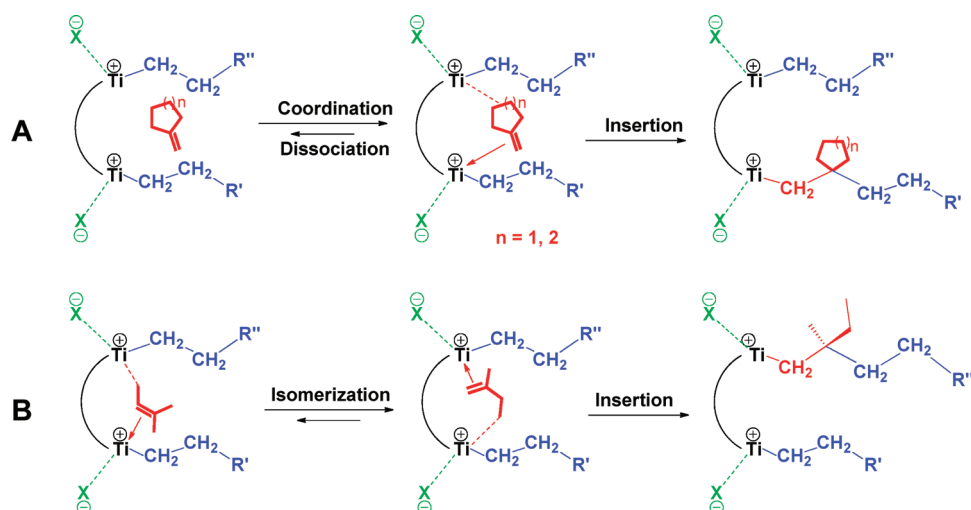
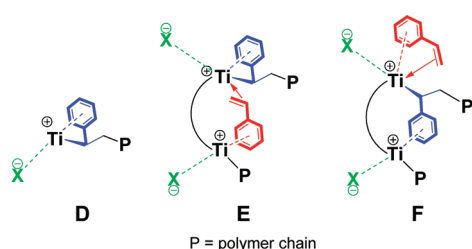


Chart 14. Possible Metal–Arene Interactions in Mononuclear and Binuclear Ti Catalyst Mediated Styrene Polymerization



copolymers with narrow polydispersity, higher levels of long-chain branching, and higher molecular weights versus the analogous mononuclear catalyst.<sup>70–72</sup> These results are attributable to cooperative enchainment/chain-transfer processes involving the two proximate active electrophilic centers, increasing the probability of macromonomer reinsertion and/or alkenylsilane branch chain transfer. These bimetallic cooperative effects, resulting in such reaction sequences (Scheme 12), thereby produce higher molecular weight polyolefin products having long-chain branches. These binuclear catalyst-mediated copolymerization + chain-transfer processes display a complex, nonlinear dependence of  $M_n$  on silane concentration, in contrast to mononuclear systems where the silane chain-transfer process is well-behaved, with a linear relationship of  $M_n$  to  $1/[\text{silane}]$ . For shorter C<sub>3</sub> and C<sub>4</sub> alkenylsilanes in the presence of the binuclear **19-TiMe** catalyst, the standard chain-transfer plot reveals that  $M_n$  falls sublinearly with increasing alkenylsilane concentration. One explanation for this nonlinear behavior is that interactions between proximate Ti centers and weakly basic, enchainment –SiH<sub>3</sub> groups may hinder olefin activation, thus depressing propagation rates. However, longer alkenylsilanes exhibit a linear relationship between product  $M_n$  and [alkenylsilane], which correlates with an increase in selectivity for long-chain branching in the corresponding copolymer microstructures. These observations demonstrate the flexibility and tunability of polyolefin micro-

structures by varying the alkenylsilane chain-transfer agent chain length and the catalyst nuclearity.

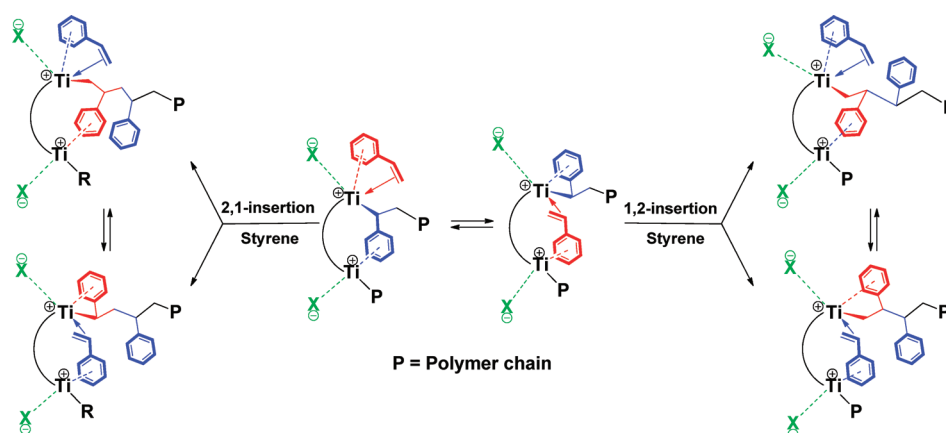
### 2.3. Linked Phenoxyiminato Catalysts

In the nonmetallocene area<sup>20,33,73</sup> of single-site polymerization catalysis, new families of group 4 bis-<sup>21,74</sup> and monophenoxyiminato<sup>75</sup> olefin polymerization catalysts (Chart 3) have been studied by several groups. Attractions of these catalysts include ease of preparation, activities competitive with those of group 4 metallocene catalysts, ability to support living polymerizations, and utility in producing unique polyolefin architectures.<sup>31,76</sup> A priori, the coordinatively open nature of monophenoxyiminato group 4 active sites would appear to be conducive to the enchainment of  $\alpha$ -olefin comonomers. However, monophenoxyiminato group 4 catalysts curiously exhibit limited productivity and comonomer incorporation selectivity in ethylene +  $\alpha$ -olefin copolymerizations.<sup>75</sup> Salata and Marks<sup>77,78</sup> reported the synthesis of rigid and planar naphthoxydiiminato zirconium (**24-Zr**) and titanium (**25-Ti**) olefin polymerization catalysts (Chart 15). The naphthalenic backbone prevents the metal centers from rotating away from each other during catalytic events in contrast to the situation for flexible polymethylene linkers. In addition to the imposed conformational rigidity, the M···M distance in the bis-phenoxyiminato system is estimated to be 5.4–5.9 Å and is thus shorter than in the crystal structures of group 4 bis(CGC) complexes (**18**, minimum Zr···Zr distance = 7.392(3) Å; **19**, minimum Zr···Zr distance = 8.671(3) Å) or in the optimized computed geometries of bis(CGC)/bisborate systems (**18**, Zr···Zr distance ~6.0 Å; **19**, Zr···Zr distance ~6.6 Å).<sup>78</sup>

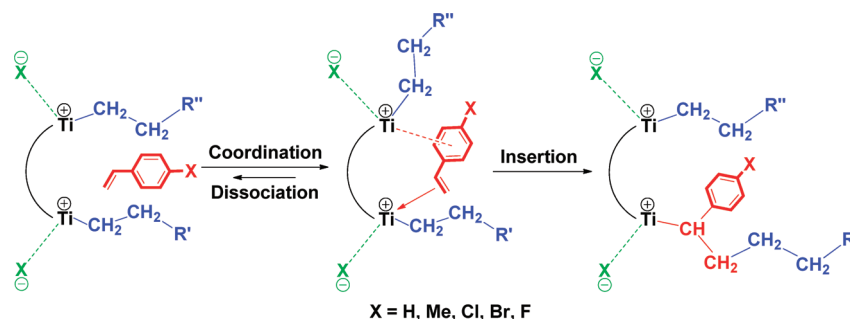
Ethylene homopolymerization using complex **24-Zr** activated with MAO affords high molecular weight linear polyethylene, with an activity ~8× that of mononuclear catalyst **26-Zr** (Table 4). The activities for **25-Ti** are modest and are slightly lower than those for **24-Zr**. At room temperature, the polyethylenes produced by both the mononuclear and binuclear catalysts are completely insoluble. However, at an elevated polymerization temperature (40 °C), product molecular weights are sufficiently depressed to obtain soluble polymers, although the polydispersities are somewhat greater than 2.0, indicating multiple active sites or conformations. Broadened polyethylene polydispersities



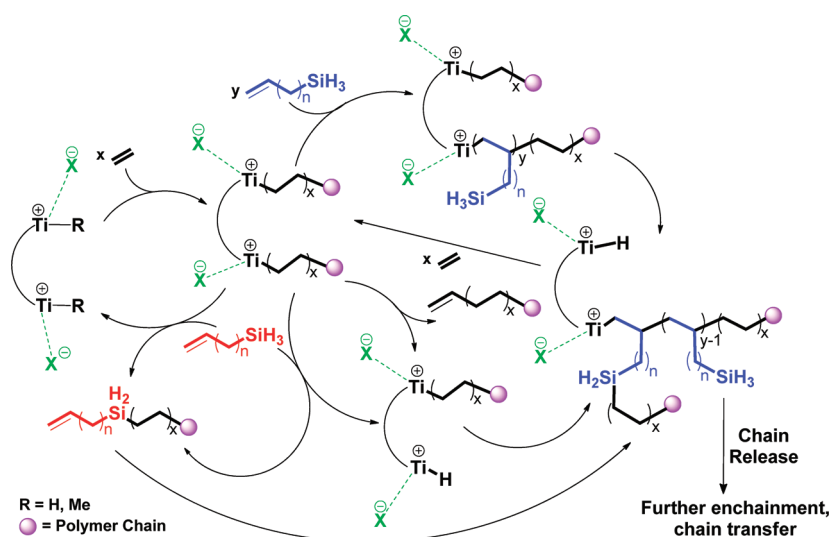
Scheme 10. Binuclear Polymerization Catalyst Enchainment-Altering Interactions with Styrene Monomers and Polystyrene Aryl Groups



Scheme 11. Proposed Pathways for Styrenic Comonomer Enchainment in Bimetallic Catalyst-Mediated Ethylene + Styrene Copolymerization



Scheme 12. Proposed Catalytic Cycle for Binuclear CGCTi-Mediated Ethylene + Alkenylsilane Copolymerization and Silanolytic Chain Transfer

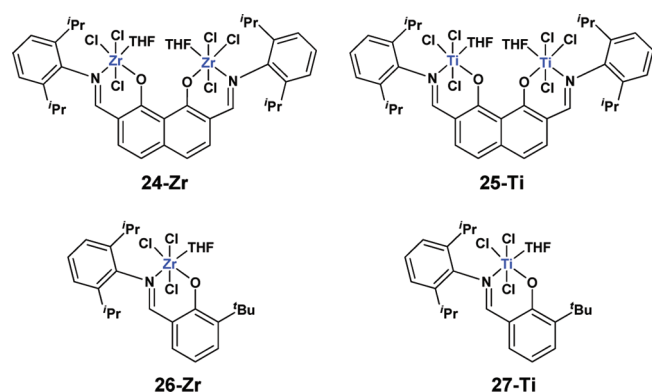


are commonly observed with phenoxyiminato catalysts, due to active site alteration via ligand rearrangement processes and/or

nucleophilic attack on the imine functionality, which can create additional catalytic species.<sup>79</sup> Both binuclear phenoxyiminato

catalysts **24-Zr** and **25-Ti** are active for ethylene + 1-hexene and ethylene + 1-octene copolymerization. The polymer characterization data indicate that the close enforced contact between the two catalytic centers leads to significantly greater extents of comonomer enchainment. The coordination/activation of the  $\alpha$ -olefin by one cationic metal center is likely stabilized by a secondary, presumably agostic interaction with the proximate cationic metal center, thus facilitating/stabilizing  $\alpha$ -olefin capture/binding at the metal center and enhancing the subsequent enchainment probability (Scheme 13). As discussed above, in the case of the binuclear versus mononuclear group 4 CGC catalysts, dramatically enhanced comonomer enchainment selectivity is observed along with substantial chain branching in ethylene homopolymerizations.<sup>53–56</sup> Note, however, that reduced overall polymerization activities are observed for the binuclear CGC catalysts versus the mononuclear CGC analogues. In contrast, for both binuclear **24-Zr** and **25-Ti** phenoxyiminato catalysts, an enhancement in activity versus the mononuclear catalysts is observed, albeit modest in some cases.

**Chart 15. Structures of Binuclear and Mononuclear Phenoxyiminato Group 4 Catalysts**



Binuclear phenoxyiminato catalysts **24-Zr** and **25-Ti** are also found to be active in the copolymerization of sterically encumbered olefins, such as methylenecyclopentane and methylenecyclohexane, or  $\alpha,\omega$ -dienes, such as 1,5-hexadiene and 1,4-pentadiene, with ethylene (Table 5). Catalysts **25-Ti** and **27-Ti** incorporate low levels of methylenecyclopentane with moderate polymerization activity. However, catalyst **25-Ti** is  $\sim 4.5\times$  more active and the copolymer molecular weight is  $\sim 2\times$  greater than that obtained using mononuclear control **27-Ti**. The low selectivity for comonomer incorporation of both titanium catalysts ( $<1\%$ ) indicates a substantial barrier for methylenecyclopentane insertion. This result is in marked contrast to the ethylene + methylenecyclohexane copolymerizations. Under identical reaction conditions, methylenecyclohexane is incorporated to a much greater extent for both the **27-Ti** (3.4%) and **25-Ti** (11.6%) catalyzed copolymerizations. Note also that **25-Ti** incorporates  $\sim 3.4\times$  more methylenecyclohexane than does **27-Ti**, and the product molecular weight is  $\sim 5\times$  greater for the **25-Ti**-derived copolymer than for the copolymer obtained with catalyst **27-Ti**. NMR studies of the copolymers indicate that both methylenecyclopentane and methylenecyclohexane are incorporated via *ring-unopened* pathways.<sup>63</sup> In marked contrast to these results, the Zr catalysts yield exclusively ethylene homopolymer. Tighter ion pairing between the Zr cation and the associated MAO anion may raise the barrier to coordination and insertion of the very bulky methylenecycloalkanes. For **25-Ti**, it appears that one electrophilic Ti center assists the proximate Ti center in enchainment of the bulky methylenecycloalkane comonomers (Scheme 14).

The copolymerizations of ethylene + 1,5-hexadiene and ethylene + 1,4-pentadiene follow essentially similar pathways to ethylene +  $\alpha$ -olefin copolymerizations with respect to the observed enhanced incorporation of comonomer (Table 5), along with increased copolymerization activities ( $\sim 15.3\times$  more for **24-Zr** in ethylene + 1,5-hexadiene and  $\sim 2.5\times$  more for **24-Zr** in ethylene + 1,4-pentadiene copolymerizations versus the mononuclear analogue **26**). In the case of the **24-Zr**- and **26-Zr**-catalyzed copolymerization of ethylene + 1,4-pentadiene,

**Table 4. Ethylene Homopolymerization and Ethylene +  $\alpha$ -Olefin Copolymerization Data for Phenoxyiminato Catalysts **24-Zr**, **25-Ti**, **26-Zr**, and **27-Ti**<sup>a</sup>**

entry	cat.	comonomer	temp °C	polymer yield (g)	activity ( $\times 10^3$ ) <sup>b</sup>	$M_w (\times 10^3)$ <sup>c</sup>	$M_w/M_n$ <sup>c</sup>	comonomer incorp (%) <sup>d</sup>
1	<b>26-Zr</b>	n/a	24	0.019	2.1	too insol	too insol	n/a
2	<b>24-Zr</b>	n/a	24	0.167	16	too insol	too insol	n/a
3	<b>26-Zr</b>	n/a	40	0.036	3.6	too insol	too insol	n/a
4	<b>24-Zr</b>	n/a	40	0.230	23	155	3.9	n/a
5	<b>27-Ti</b>	n/a	24	0.025	2.5	675	23.7	n/a
6	<b>25-Ti</b>	n/a	24	0.053	5.3	too insol	too insol	n/a
7	<b>27-Ti</b>	n/a	40	0.043	4.3	315	6.5	n/a
8	<b>25-Ti</b>	n/a	40	0.082	8.3	297	4.5	n/a
9	<b>26-Zr</b>	1-hexene	40	0.015	1.0	21	9.6	7.4
10	<b>24-Zr</b>	1-hexene	40	0.150	12	98	3.3	11.0
11	<b>27-Ti</b>	1-hexene	40	0.027	2.7	188	33.6	4.3
12	<b>25-Ti</b>	1-hexene	40	0.045	4.5	76	3.9	9.4
13	<b>26-Zr</b>	1-octene	40	0.022	2.2	22	11.9	4.1
14	<b>24-Zr</b>	1-octene	40	0.083	8.3	105	3.6	7.3
15	<b>27-Ti</b>	1-octene	40	0.022	2.2	96	5.4	8.4
16	<b>25-Ti</b>	1-octene	40	0.039	2.9	182	3.3	15.2

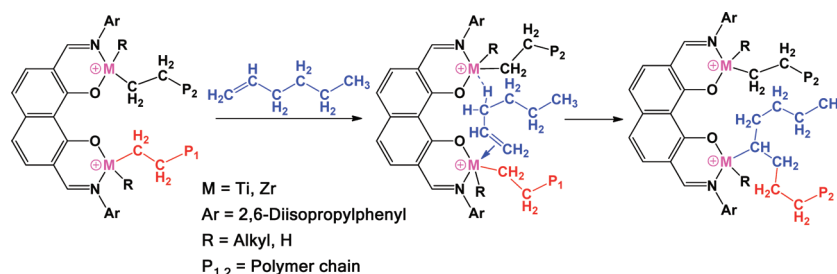
<sup>a</sup> Polymerizations and copolymerizations carried out on a high-vacuum line with 10  $\mu$ mol of Zr/Ti and MAO as cocatalyst (Al/M = 1000:1) in 50 mL of toluene under 1 atm of ethylene pressure for 60 or 90 min. Comonomer concentration = 0.72 M. <sup>b</sup> kg of polyethylene (mol of Zr/Ti)<sup>−1</sup> h<sup>−1</sup> atm<sup>−1</sup>.

<sup>c</sup> From GPC vs polystyrene standards. <sup>d</sup> Mole percentage calculated from <sup>13</sup>C NMR spectra (ref 61).

**Table 5.** Ethylene + Methylene cycloalkane and Ethylene +  $\alpha,\omega$ -Diene Copolymerization Results for Catalysts 24-Zr, 25-Ti, 26-Zr, and 27-Ti<sup>a</sup>

entry	cat.	comonomer	polymer yield (g)	activity ( $\times 10^3$ ) <sup>b</sup>	$M_w$ ( $\times 10^3$ ) <sup>c</sup>	$M_w/M_n$ <sup>c</sup>	comonomer incorp (%) <sup>d</sup>
1	27-Ti	MCP	0.025	3.4	58	20.2	0.4
2	25-Ti	MCP	0.115	15	121	4.0	0.7
3	26-Zr	MCP	0.042	3.3	n/a	n/a	PE
4	24-Zr	MCP	0.026	6.9	n/a	n/a	PE
5	27-Ti	MCH	0.080	8.1	20	13.1	3.4
6	25-Ti	MCH	0.096	9.7	104	3.5	11.6
7	26-Zr	MCH	0.031	2.6	n/a	n/a	PE
8	24-Zr	MCH	0.077	6.2	n/a	n/a	PE
9	27-Ti	1,5-HD	0.004	0.3	n/a	n/a	n/a
10	25-Ti	1,5-HD	0.003	0.2	n/a	n/a	n/a
11	26-Zr	1,5-HD	0.012	1.0	34	10.3	7.9
12	24-Zr	1,5-HD	0.151	15	78	3.2	10.3
13	27-Ti	1,4-PD	0.008	0.8	n/a	n/a	n/a
14	25-Ti	1,4-PD	0.007	0.7	n/a	n/a	n/a
15	26-Zr	1,4-PD	0.292	29	73	3.3	2.1
16	24-Zr	1,4-PD	0.742	74	75	4.8	5.4

<sup>a</sup> Copolymerizations carried out at room temperature on a high-vacuum line with 10  $\mu$ mol of Ti/Zr and MAO as cocatalyst (Al/M = 1000:1) under 1.0 atm of ethylene pressure for 45–75 min. <sup>b</sup> kg of polyethylene (mol of Zr/Ti)<sup>-1</sup> atm<sup>-1</sup> h<sup>-1</sup>. Comonomer concentration: MCP and MCH = neat; 1,5-HD and 1,4-PD = 0.3 M. <sup>c</sup> From GPC vs polystyrene standards. <sup>d</sup> Mol %, calculated from <sup>13</sup>C NMR spectra (ref 61). MCP = methylenecyclopentane; MCH = methylenecyclohexane; 1,5-HD = 1,5-hexadiene; 1,4-PD = 1,4-pentadiene; PE = polyethylene; n/a = not applicable.

**Scheme 13.** Proposed Scenario for Enhanced  $\alpha$ -Olefin Enchainment by Group 4 Bimetallic Phenoxyiminato Catalysts

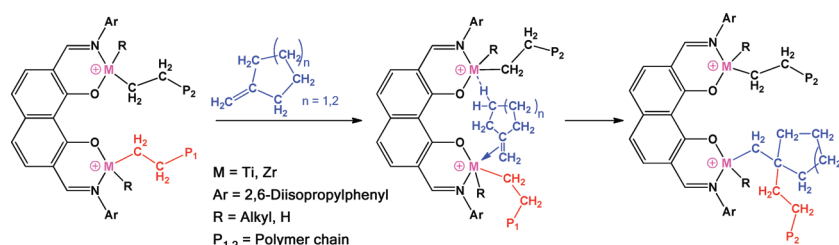
1,3-cyclopentyl units are incorporated affording polymer structure G (Scheme 15) with 82% *cis*- and 18% *trans*-1,3-cyclopentyl group selectivity. In the case 24-Zr- and 26-Zr-catalyzed copolymerization of ethylene + 1,5-hexadiene, 1,3-cyclohexyl units are enchainment to form polymer structure H (Scheme 15) with 69% *cis*- and 31% *trans*-1,3-cyclohexyl group selectivity. No detectable cross-linked structures are found in any of the product polymers. Interestingly, under identical reaction conditions, catalysts 25-Ti and 27-Ti yield only trace amounts of copolymer.

### 3. GROUP 10 BIMETALLIC CATALYSTS

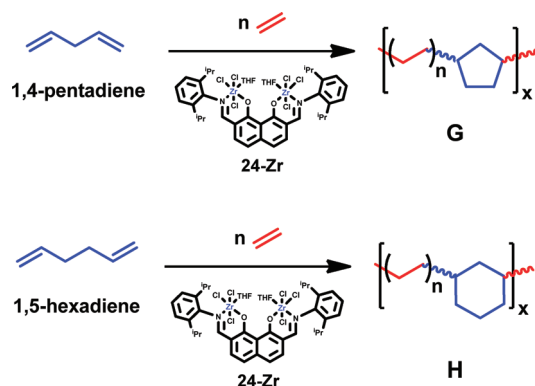
High olefin polymerization and copolymerization activities can be achieved with group 4 catalysts; however, the electrophilicity of these metal centers greatly depresses their activity in the presence of polar comonomers and/or solvents. Desirable properties arising from the incorporation of polar functionalities into polyolefins include control over polymer characteristics such as mechanical toughness, rheology, and surface properties,<sup>68c,80</sup> while the ability of the catalyst to withstand polar solvents bypasses the need for rigorous drying of the polymerization

solvent. In order to develop catalysts capable of achieving these properties, attention has turned from the oxophilic group 4 metals toward catalyst systems with more electron-rich transition metal centers, such as the group 10 metals. Cationic group 10 systems reported by Brookhart's group<sup>23</sup> demonstrated that coinorporation of polar monomers, such as acrylates, with olefins is indeed possible, yielding highly branched polyethylenes (>100 branches/1000 carbon atoms) or polypropylenes, with the enchainment acrylate units incorporated as caps on the branch ends. Contemporaneously, Grubbs and co-workers<sup>22</sup> demonstrated that a neutrally charged Ni catalytic system mediates ethylene copolymerization with functionalized norbornenes while producing very highly branched polymers. Also of note here is that these catalysts are active in the presence of polar solvent additives,<sup>22b</sup> with only minor reductions in activity, bypassing the need for hyperpurification of the polymerization medium. Although polar comonomers can be introduced into polyolefins via conventional radical and other polymerization methods, single-site catalysts offer the attraction of greater control over polymer microstructure, polydispersity, and tunability of comonomer content.<sup>68c,80</sup> The ability to perform these

**Scheme 14.** Proposed Scenario for Enhanced Methylene-Cycloalkane Enchainment by Bimetallic Group 4 Phenoxyiminato Catalysts



**Scheme 15.** Insertion Pathways for Ethylene + 1,4-PD and Ethylene + 1,5-HD Copolymerizations Mediated by Binuclear Catalyst 24-Zr



polymerizations via an insertive pathway instead of the conventional radical mechanism would also circumvent the need for expensive reactors and extremely high pressures. These catalyst systems are capable of introducing over 50 branches/1000 carbon atoms in the polyolefin chain, yielding homopolymers with lower melting points than those produced with their group 4 counterparts, although typically at much lower molecular weights and activities.

### 3.1. Nickel Catalysts

**3.1.1.  $\alpha$ -Diimine Catalysts.** In 1995, the pioneering work of Brookhart's group<sup>23</sup> on cationic  $\alpha$ -diimine Ni(II) catalysts for high molecular weight polyethylene revolutionized the area of late transition metal catalysts for polyolefin synthesis. In the field of binuclear polymerization catalysis, a large number of complexes bearing to  $\alpha$ -diimine ligands have been reported. Bridged bis(pyridinylamino) dinickel(II) complex **28** (Chart 16),<sup>81</sup> activated with MAO, shows good activity for ethylene oligomerization and polymerization, with relatively wide molecular weight distributions versus those obtained using mononuclear pyridinylimino Ni(II) catalysts. Similar ligands and catalysts were reported by Luo and Schumann.<sup>82</sup> The ligands were prepared by Schiff base condensation of 2,3-butanedione with 1 equiv of 2,6-diisopropylaniline, followed by 0.5 equiv of substituted bisaniline. Complexes **29** (Chart 16) are synthesized by reaction of (DME)NiCl<sub>2</sub> with variously substituted ligands in CH<sub>2</sub>Cl<sub>2</sub>. Catalytic studies show that catalysts **29** have high catalytic activity for ethylene polymerization. Compared to mononickel-centered catalysts, catalysts **29** exhibit much higher catalytic activity when the R substituents on the diphenyl framework

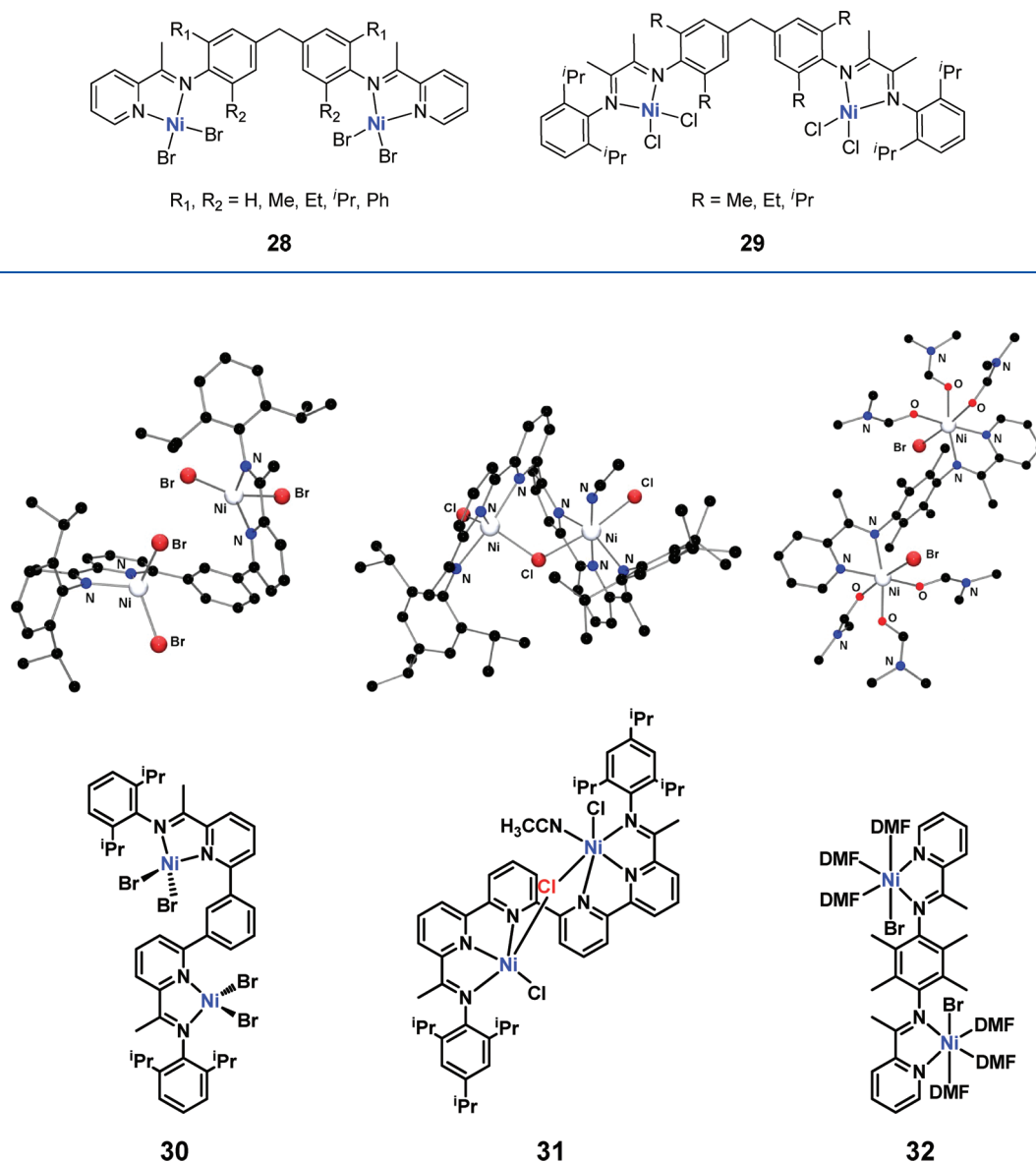
are either isopropyl or ethyl. In contrast, when the substituent is methyl, a drastic reduction in catalytic activity is observed versus the mononuclear control catalyst. Further mechanistic work would be required to interpret these results.

More rigid bridges between the two active centers have been introduced by several laboratories in order to have more conformational control and to minimize the Ni...Ni distance. Solan's group synthesized two bis(imino)pyridine late transition metal complexes as ethylene oligomerization catalysts. Thus, bidentate (N,N)<sup>83</sup> and tridentate (N,N,N)<sup>84</sup> ligands favor the formation of M<sub>2</sub>( $\mu$ -X)X<sub>2</sub>-type complexes in which the metal centers are in close proximity (complexes **30** and **31**, respectively; Figure 6). Both complexes are active in ethylene oligomerization, when activated with MAO. In addition, a tetramethylphenylene-linked iminopyridine Ni(II) complex (**32**) has been reported (Figure 6).<sup>85</sup> Activation with excess MAO generates an active ethylene polymerization catalyst, affording a mixture of waxes and low molecular weight solid polyethylene. No pronounced differences in the oligomeric product microstructures are apparent for the different bimetallic centers, although variations in productivity are noticeable. The exact mechanistic interplay between the two metal centers during oligomerization remains unclear at this point. Nevertheless, the capacity of these sterically bulky compartmentalized ligands to act as effective scaffolds for two oligomerization-active metal centers is clearly demonstrated.

**3.1.2. Phenoxyiminato Catalysts.** Beginning in 1998 when Grubbs reported the first neutrally charged mononuclear Ni(II) phenoxyiminato polymerization catalyst,<sup>22c</sup> a number of binuclear Ni(II) phenoxyiminato catalysts with different types of linkages have been reported. Single-component Ni(II) catalyst **33** (Chart 17),<sup>86</sup> based on a 3,3'-bis(acylaldimine) ligand, yields polyethylene with lower activity than the mononuclear Ni(II) Grubbs' catalyst, but under somewhat different reaction conditions [**33** = 9.4 kg of polyethylene (mol of Ni)<sup>-1</sup> atm<sup>-1</sup> h<sup>-1</sup> as a single-component; Grubbs' catalyst = 17.4 kg of polyethylene (mol of Ni)<sup>-1</sup> atm<sup>-1</sup> h<sup>-1</sup> using Ni(cod) as cocatalyst/phosphine scavenger]. Catalyst **33** produces high molecular weight polyethylene with a broad molecular weight distribution (PDI > 2.8) and a moderate degree of branching, ca. 10–15 methyl branches/1000 carbon atoms. Catalyst **33** activated with MMAO also displays higher activities in norbornene homopolymerization than does the mononuclear phenoxyiminato Ni(II) complex.<sup>87</sup> Variations in the skeletal backbone of catalyst **34** do not significantly influence the catalytic activity toward norbornene polymerization.



Chart 16. Structures of Bridged Bis(pyridinylamino) Dinickel(II) Complexes 28 and 29



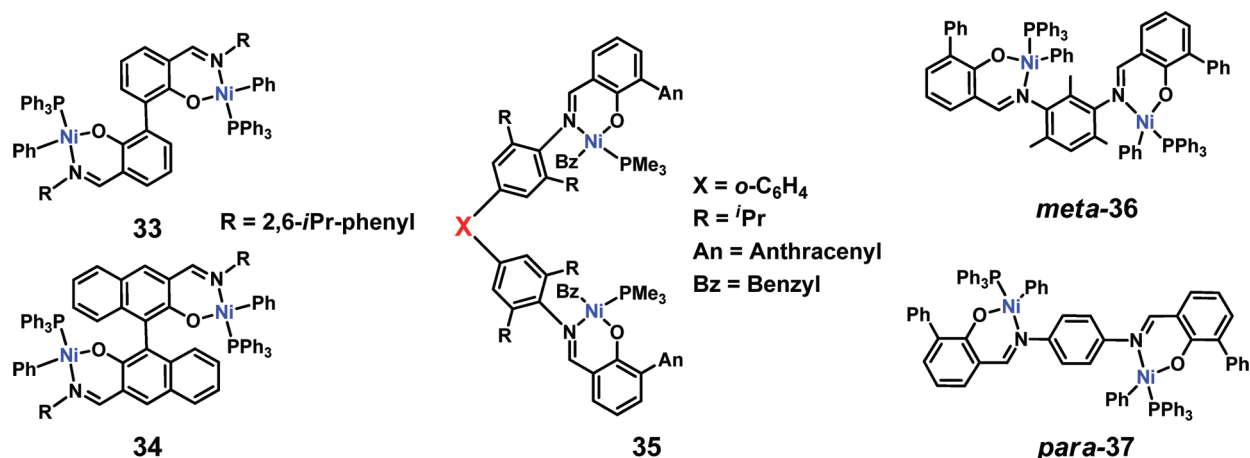
**Figure 6.** Molecular structures of binuclear Ni complexes **30**, **31**, and **32**. Adapted with permission from ref 83, copyright 2006 American Chemical Society, ref 84, copyright 2009 Royal Society of Chemistry, and ref 85, copyright 2008 Elsevier, respectively.

As mentioned above for group 4, binuclear complexes in a constrained conformation (active sites in close spatial proximity) are ideally suited for cooperation between the metal centers. In catalysts **35** (Chart 17),<sup>88</sup> the characteristic feature of these rigid bridging units is that any rotation around the phenylene bridge (X, Chart 17) is restricted. In ethylene homopolymerization, catalysts **35**, activated with  $\text{B}(\text{C}_6\text{F}_5)_3$  as the phosphine scavenger, exhibit higher activities than the mononuclear control complex and introduce higher levels of branching in the product polyolefin (16–51 branches/1000 carbon atoms), attributed to cooperative interactions between the two metal centers. Dramatic effects of the binuclearity are also observed in ethylene + polar-functionalized norbornene copolymerizations. Thus, binuclear complexes **35** show  $\sim 2\times$  higher activities and  $\sim 2\times$  higher comonomer incorporation levels than the mononuclear analogues, under the same conditions in ethylene + 2-(methoxycarbonyl)-norbornene

copolymerization. The same trend is observed for ethylene + 2-(acetoxymethyl)-norbornene copolymerization. Jin and co-workers reported two similar binuclear ethylene polymerization catalysts, changing only the position of the phenylene bridging: meta phenylene bridged (**36**, Chart 17)<sup>89</sup> and para phenylene bridged (**37**, Chart 17).<sup>90</sup> These two systems exhibit different catalytic properties, but accurate comparisons cannot be made due to different ethylene polymerization conditions.

The effect of ligand substituents on phenoxyiminato ethylene polymerization catalysts is significant.<sup>21</sup> Thus, electron-withdrawing groups on the ligand framework significantly enhances catalytic performance.<sup>41</sup> For example, introducing  $\text{X} = \text{NO}_2$  substituents in binuclear catalyst **38** (Chart 18)<sup>91</sup> significantly increases the polymerization activity. Highly branched polyethylenes (46–127 branches/1000 carbon atoms) with moderate

Chart 17. Structures of Binuclear Phenoxyiminato Ni(II) Polymerization Catalysts



molecular weights ( $M_n = (1.0-169) \times 10^4$ ) and narrow molecular weight distributions ( $M_w/M_n = 2.3-2.4$ ) are obtained by using catalysts **38** with or without a phosphine scavenger. In comparison to the corresponding mononuclear Ni catalysts, the binuclear Ni catalysts generally exhibit higher thermal stability, due to the increased steric congestion around the metal centers that reduces the probability of forming bis-ligating compounds, which are completely inactive (Chart 18).<sup>92</sup> In addition to the NO<sub>2</sub> electron-withdrawing group, Wehrmann and Mecking<sup>93</sup> introduced CF<sub>3</sub> electron-withdrawing groups on the ligand skeleton (**39**, Chart 18). In contrast to catalyst **38**, the two active sites in **39** are held together by a polymethylene bridge. The polymerization activity of binuclear complex **39** is higher than that of the mononuclear analogue. The greater polymerization activity of the binuclear complex, in comparison to the mononuclear analogue, appears to reflect an intrinsically higher rate of propagation rather than a more efficient activation of the catalyst precursor (pyridine dissociation). The nature of the bridge ( $n = 0$  or 1) does not have an obvious effect on the polymerization activity comparing the *i*Pr- and 3,5-(CF<sub>3</sub>)<sub>2</sub>C<sub>6</sub>H<sub>3</sub>-substituted complexes. Semicrystalline polyethylene with a low degree of chain branching (2–12 branches/1000 carbon atoms) is produced. In addition, binuclear Ni(II) compound **39** also yields high molecular weight linear polyethylene in aqueous emulsions,<sup>93</sup> and in supercritical CO<sub>2</sub> as the solvent,<sup>94</sup> both with a productivity lower than in toluene.

Macrocyclic binuclear Ni<sub>2</sub> phenoxyiminato catalysts **40** (Chart 18) were reported by Na et al.<sup>95</sup> Complex **40** is sparingly soluble in hydrocarbon solvents; however, ethylene polymerization with this catalyst activated with B(C<sub>6</sub>F<sub>5</sub>)<sub>3</sub> as a slurry in nonpolar solvents yields fairly good polymerization activity, considering the insoluble nature of the catalyst. Activities decrease with increasing temperature, and negligible activities are observed when the temperature is increased to 60 °C, indicating that the catalyst is thermally unstable.

Binuclear naphthloxydiiminato Ni(II) catalysts **41** (Chart 19), in which the rigid ligation ensures that the metal centers are bound in close proximity,<sup>96</sup> exhibit significant increases in ethylene homopolymerization activity versus the monometallic analogues **42** and **43**, as well as increased polyethylene branching and methyl branch selectivity, even in the absence of a Ni(cod)<sub>2</sub> cocatalyst. This enhanced activity is maintained in the presence

of polar solvents, while concurrently retaining the selectivity for large branch densities. Significant differences are observed versus **42** and **43** in the product polyethylene of the **41**-mediated ethylene polymerization, suggesting that the presence of the second metal center enhances chain walking but simultaneously suppresses ethyl branch formation compared to the mononuclear analogue. In fact, in low-temperature 1D and 2D NMR studies, a secondary agostic interaction is identified (Chart 20). This may be a “snapshot” of the species involved in the  $\beta$ -H elimination/readdition of the chain-walking process,<sup>97</sup> while increased propagation kinetics may reflect monomer binding to the neighboring Ni center, hence increased local substrate concentrations.

Binuclear catalysts **41** are also found to be active in the copolymerization of ethylene + polar-functionalized norbornenes and ethylene + acrylate esters. Thus, ethylene/norbornene polymerizations mediated by **41** proceed with  $\sim 4\times$  greater activity and with  $\sim 4\times$  greater selectivity for comonomer incorporation versus mononuclear catalysts **42** and **43**, with an incorporation mechanism plausibly similar to catalyst **24**-mediated copolymerization of ethylene + styrene (vide supra). The same trend is also observed for ethylene + acrylate ester copolymerizations, where binuclear catalysts **40** incorporate up to 11% acrylate comonomer into the polyethylene backbone versus minimal incorporation for the mononuclear analogues. It was proposed that mononuclear Ni(II) polymerization catalysts sluggishly incorporate acrylates due to formation of a six-membered chelating resting state involving the vacant Ni coordination site (**I**, Chart 21), otherwise used for further ethylene insertions. This is thought to poison/deactivate the catalyst (Chart 21).<sup>98</sup> However, it has been proposed that, in the binuclear systems, the second adjacent unsaturated catalytic site binds the deactivating carbonyl group (**J**), thereby opening a reactive coordination site for macromolecule propagation (Chart 21).

**3.1.3. Other Ligations.** It is well-known that nickel P–O chelate complexes are active catalysts for ethylene oligomerization to yield higher  $\alpha$ -alkenes.<sup>99</sup> They can be readily converted into catalysts for ethylene polymerization by introducing a phosphine scavenger.<sup>99</sup> In this regard, a series of binuclear Ni(II)-ylide complexes (**44**, Scheme 16),<sup>100</sup> based on various bis( $\alpha$ -ketoylide) ligands, exhibits far higher ethylene polymerization

Chart 18. Structures of Binuclear Phenoxyiminato Ni(II) Polymerization Catalysts

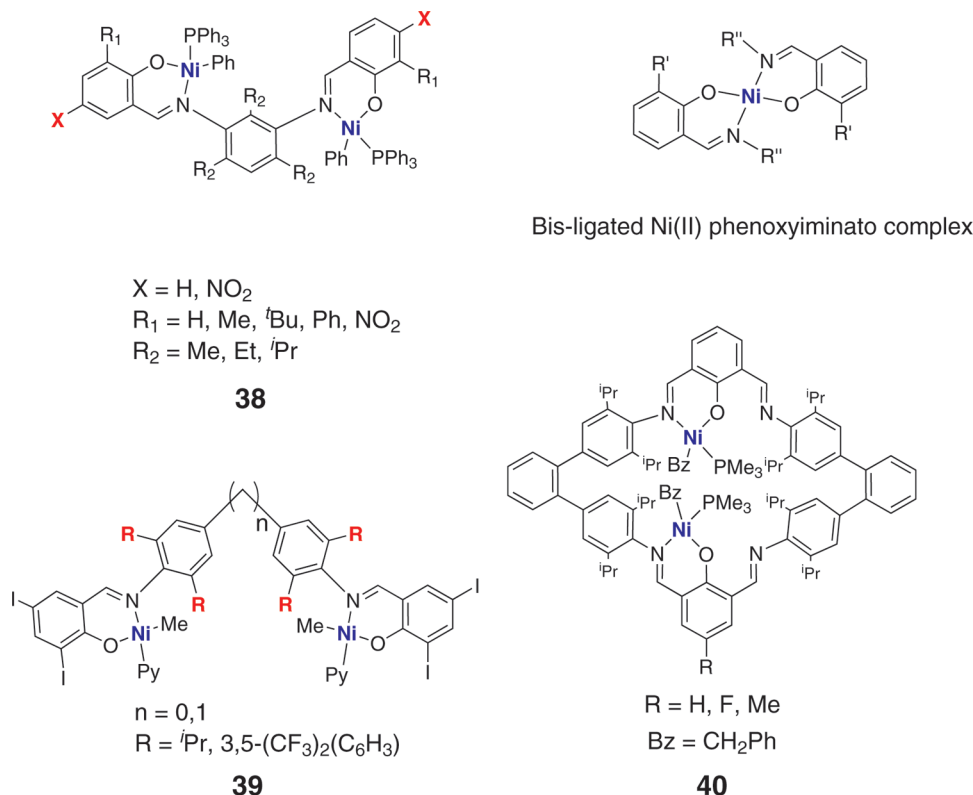


Chart 19. Structures of Binuclear Ni(II) Phenoxyiminato Catalyst 41 and Mononuclear Ni(II) Phenoxyiminato Catalysts 42 and 43

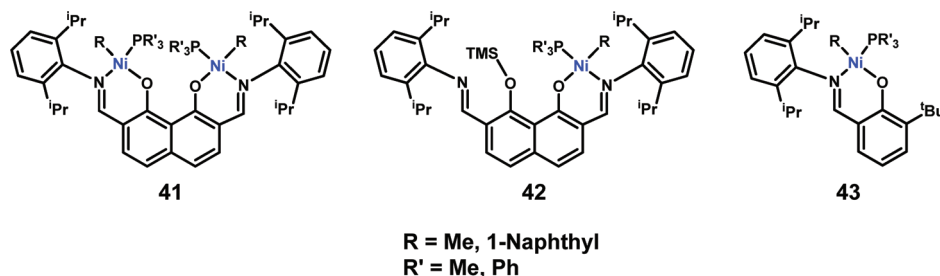
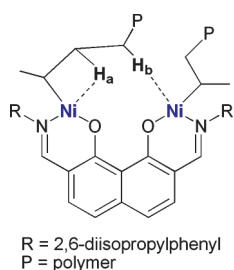


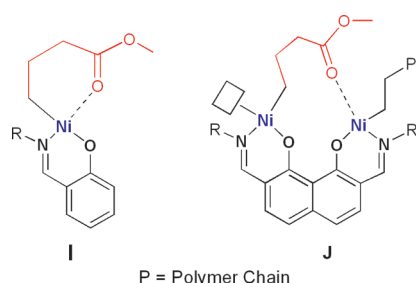
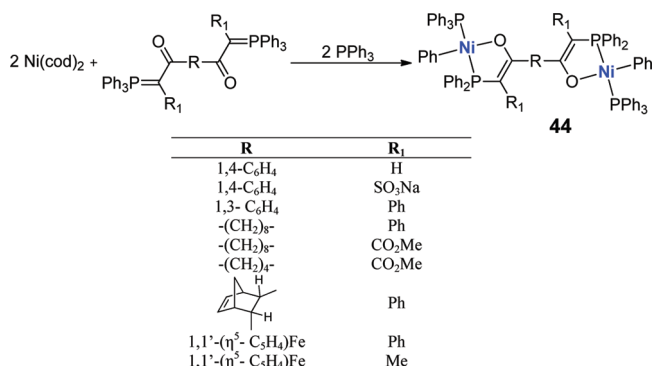
Chart 20. Binuclear Agostic Interactions in Ni Catalyst 41 Mediated Ethylene Polymerization as Detected by Low-Temperature NMR Spectroscopy



activity than the mononuclear analogues. The properties of the polyethylenes produced by catalysts **44** depend strongly on the moiety linking the active centers. Thus, when the bridge between

the active centers is 1,4- $\text{C}_6\text{H}_4$ , high molecular weight polyethylene is produced, with a very broad polydispersity ( $\text{PDI} = 30.1$ ). On the other hand, when the bridge is  $\text{-(CH}_2\text{)}_4\text{-}$ , low molecular weight polyethylene ( $M_w = 6200$ ) is produced with a narrow polydispersity ( $\text{PDI} = 2.0$ ). In addition, contracting the distance between the two metal centers leads to a significant increase in catalytic productivity, which is attributed to cooperative effects between active centers and indirect electronic interactions.<sup>100</sup> In this regard, it was found that the activity of binuclear catalyst **44** correlates with differences in the vibrational force constants of the ylide carbonyl groups in the bis( $\alpha$ -keto ylides) and that this correlation is a measure of the strength of ethylene coordination to the Ni centers, hence ethylene activation. The strength of the donor–acceptor interactions between ylide phosphorus and Ni depends on the substituent electron and steric properties in the chelate rings.

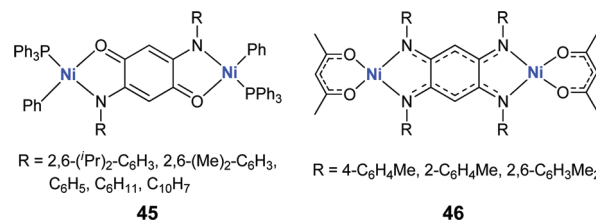
Cooperative effects in ethylene, norbornene, and methyl acrylate polymerizations, as well as in ethylene oligomerization, have also been

**Chart 21.** Proposed Resting States of Mono- and Binuclear Catalysts after Acrylate Insertion**Scheme 16.** Synthesis of Binuclear Catalyst Class 44

reported for binuclear Ni(II) catalysts containing 2,5-disubstituted amino-*p*-benzoquinone ligand (**45**, Chart 22)<sup>101</sup> or 2,5-diamino-1,4-benzoquinonediimines ligands (**46**, Chart 22).<sup>102,103</sup> Thus, single-component catalysts **46** show activities comparable to the mononuclear analogues in ethylene polymerization. However, relatively broad molecular weight distributions of 3.21–48.24 are observed, which are not consistent with those of well-defined single-site catalysts. These effects may be explained on the basis electronic communication and cooperative enchainment interactions between the two metal centers. Binuclear catalyst **46** activated with MAO exhibits high activity for norbornene addition polymerization and methyl methacrylate homopolymerization.<sup>103</sup> The PMMA obtained is syndiotactic-rich and exhibits a broad PDI. Catalyst **46**, upon activation with MAO or AlEtCl<sub>2</sub>, does not catalyze ethylene polymerization to yield high molecular weight polyethylene at atmospheric pressure or even under 7.0 atm of ethylene, but only yields oligomers in moderate activity.<sup>102</sup> Thus, catalysts **46** are highly selective for the formation of C<sub>4</sub> and C<sub>6</sub> olefins, but the oligomerization mechanism is not clear. Other binuclear Ni(II) ethylene oligomerization catalysts have been reported, and in many cases cooperative effects between active sites have been invoked to explain selectivity patterns.<sup>104–110</sup>

### 3.2. Palladium Catalysts

Mononuclear palladium(II) complexes with a broad range of ligands are active in olefin, norbornene, and acrylate polymerization and competent to effect alternating olefin + CO, styrene + CO, and norbornene + styrene copolymerizations.<sup>111</sup> However, few examples of Pd(II) binuclear catalysts have been reported compared to Ni(II) binuclear systems, even though Pd complexes are generally thought to

**Chart 22.** Structures of Binuclear Ni (II) Catalysts Based on 2,5-Disubstituted Amino-*p*-benzoquinone Ligand (**45**) and 2,5-Diamino-1,4-benzoquinonediimines Ligands (**46**)

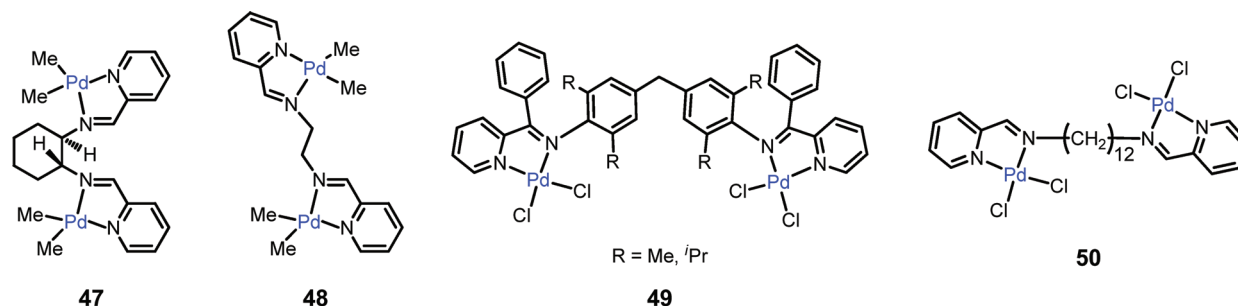
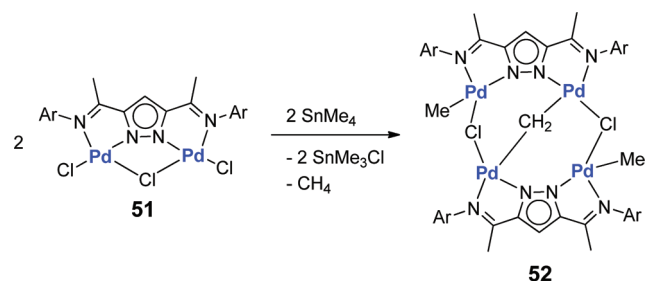
be less oxophilic than Ni complexes. Baar et al.<sup>112</sup> prepared two binuclear Pd(II) complexes **47** (chiral, Chart 23) and **48** (achiral, Chart 23) which are catalyst precursors for the copolymerization of styrene and 4-methylstyrene with CO, to give polyketones. In these compounds, the two Pd centers appear to act essentially independently and exhibit the same activity and stereoregulation as the mononuclear analogues. Vinyl addition polymerization of norbornene mediated by Pd-based bridged binuclear diimine complexes **49** activated with MAO (Chart 23) was reported by Mi et al.<sup>113</sup> Catalysts **49** exhibit higher activity than the corresponding mononuclear Ni(II) complex and the mononuclear Pd(II) analogue. Similar compounds, with longer spacers between the two pyridylimine palladium(II) centers **50** (Chart 23),<sup>114</sup> are active in ethylene polymerization and afford highly linear polyethylenes with high molecular weights. Binuclear catalyst **50** displays lower catalytic activity than the mononuclear analogue, and it has been proposed that this is due to differences in solubility of the two catalytic species in toluene.

Derivatives of pyrazol-based dinucleating ligands with appended imine functions were synthesized by Meyer and co-workers (Scheme 17).<sup>115,116</sup> These scaffolds have two adjacent coordination compartments to host metal ions in a highly preorganized environment. The series of binuclear Pd(II) complexes **51** are active in both ethylene and norbornene homopolymerizations, when activated with MAO. Overall, the product polymer properties are rather similar to those obtained under similar conditions with mononuclear Brookhart-type  $\alpha$ -diimine olefin polymerization catalysts. Interestingly, when complex **51** is reacted with SnMe<sub>4</sub>, a tetranuclear palladium complex is isolated in high yield (**52**, Scheme 17).<sup>117</sup> This Pd<sub>4</sub> complex reacts with ethylene to produce mainly propene and some butenes, along with the reformation of **51** and Pd(0), thus indicating gradual decomposition of the resulting organopalladium complexes. No details regarding mechanism of propene and butene formation from ethylene were reported.

Bis(phenoxyiminato) Pd(II) catalyst **53** (Chart 24)<sup>87</sup> with modified methylaluminoxane MMAO as the cocatalyst is capable of catalyzing the addition polymerization of norbornene with a higher activity than the mononuclear analogue. Bianchini et al.<sup>118</sup> also described rigid tetra(phosphine) Pd(II) complexes **54** (Chart 24) which, under standard ethylene + CO copolymerization conditions, are  $\sim 10\times$  more active than the analogous (diphenylphosphino)ethane-Pd(II) complex and comparable in activity to the catalyst used industrially, {Pd[(diphenylphosphino)propane](OCOME)<sub>2</sub>}.<sup>119,120</sup> To tune the proximity of the two metal centers and avoid excess rigidity, Casalino et al.<sup>121</sup> designed a binuclear complex employing a



Chart 23. Structures of Binuclear Pd(II) Olefin Polymerization Catalysts

Scheme 17. Synthesis of Pd<sub>4</sub> Complex 52

bis-chelating ligand based on [1,4]-dioxocino-[6,5-*b*:7,8-*b'*]-dipyridine moiety. Binuclear palladium catalyst **55** (Chart 24) is active for alternating styrene + CO copolymerization. The microstructure of the copolymer produced with **55** reveals a notable level of isotacticity, whereas the mononuclear analogue affords atactic copolymer. This observation suggests that cooperative effects between the two active sites influence enchainment selectivity during the copolymerization, perhaps in a manner similar to Scheme 18. The homopolymerization of methyl methacrylate mediated by binuclear palladium(II) imino-pyridyl complex **56** was reported by Bahuleyan et al. (Chart 24).<sup>122</sup> Under identical polymerization conditions, catalyst **56** in combination with MAO shows greater activity than the mononuclear analogues and gives rise to more syndio-rich PMMA (rr values ranged from 56% to 72%) with moderate molecular weights ( $1.3\text{--}3.9 \times 10^4 \text{ g mol}^{-1}$ ) and a slightly broadened PDI (1.29–3.63). It was proposed that the higher PDI values of the PMMAs obtained using the bimetallic complexes are probably due to the cooperative interactions of the two adjacent metal centers in the bimetallic catalyst. For bimetallic catalysts, a competition between monometallic and bimetallic propagation mechanisms can be expected since the two metal centers lie within moderate proximity (Scheme 18). Geometry optimization and molecular mechanics calculations show that the energy of the resting state of monometallic propagation (79.3 kJ/mol) is higher than that of bimetallic propagation (66.4 kJ/mol), arguing that bimetallic propagation is more favorable than monometallic propagation. In addition, bimetallic propagation may induce chain-transfer reactions which enhance the polymerization activity.

## 4. BIMETALLIC CATALYSTS WITH OTHER METALS

### 4.1. Iron and Cobalt Catalysts

In the late 1990s Bennet, Brookhart, and Gibson independently discovered the catalytic properties of mixtures of 2,6-bis(aryl-imino)pyridine–iron(II) halide/MAO and 2,6-bis(aryl-

imino)pyridine–cobalt(II) halide/MAO in ethylene polymerization.<sup>123</sup> These systems convert ethylene to either high-density polyethylene (HDPE) or to  $\alpha$ -olefins with very high turnover frequencies, through straightforward manipulation of the ligand framework. The advantages Fe(II) and Co(II) catalysts versus other types of single-site Ziegler–Natta catalysts for ethylene homopolymerization (metallocenes, CGCs) are, for example, the relative ease of preparation and handling (versus group 4) and the use of low-cost metals with negligible environmental impact (versus group 10).<sup>23,33</sup> Another intriguing feature of the bis(imino)pyridine Fe(II) and Co(II) precursors is provided by the facile tuning of their polymerization activity by simple modifications of the ligand architecture.<sup>23,33</sup>

Methylene-bridged binuclear bis(imino)pyridyl Fe(II) complexes **57** (Chart 25),<sup>124</sup> activated with  $\text{Al}(\text{i-Bu})_3$ , exhibit higher activity than the corresponding mononuclear iron catalysts, along with an enhanced molecular weight of the linear polyethylene produced. These marked differences in catalytic performance versus the mononuclear analogues are attributed to the combined electronic and steric effects although the Fe centers are quite distant. Symmetric bimetallic tridentate [N,N,N] Fe(II) (**58-Fe**, Chart 25) and Co(II) (**58-Co**, Chart 25) complexes with a rigid bridge were reported by Barbaro et al.<sup>125</sup> Effective catalysts for HDPE are generated by activating the bis(dichloride) precursors with MAO in toluene. Both complexes evidence very good productivity. In particular, **58-Co** is more active than any other Co(II) polymerization catalyst reported to date.

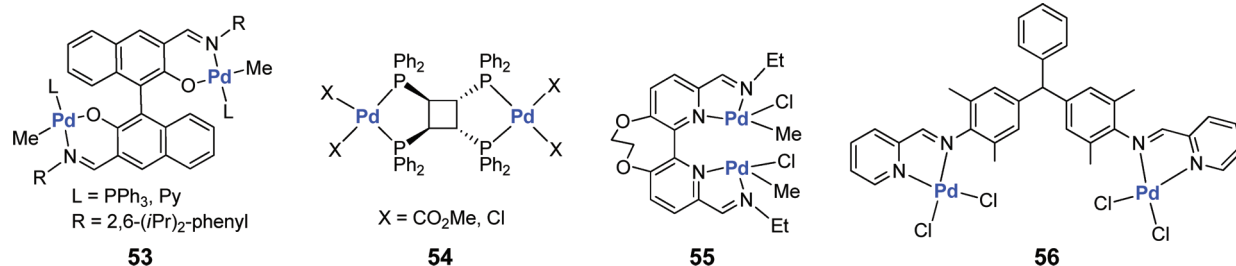
Asymmetric bimetallic Fe(II) and Co(II) systems **59**<sup>108,126</sup> and **60**<sup>109</sup> (Chart 26) were found to exhibit good activities for ethylene oligomerization and polymerization in the presence of MAO or MMAO. In the case of ethylene oligomerization, these catalysts afford  $\alpha$ -olefins in high selectivity, with the composition of these oligomers following a Schluz–Flory distribution.

### 4.2. Rare Earth Metal Catalysts

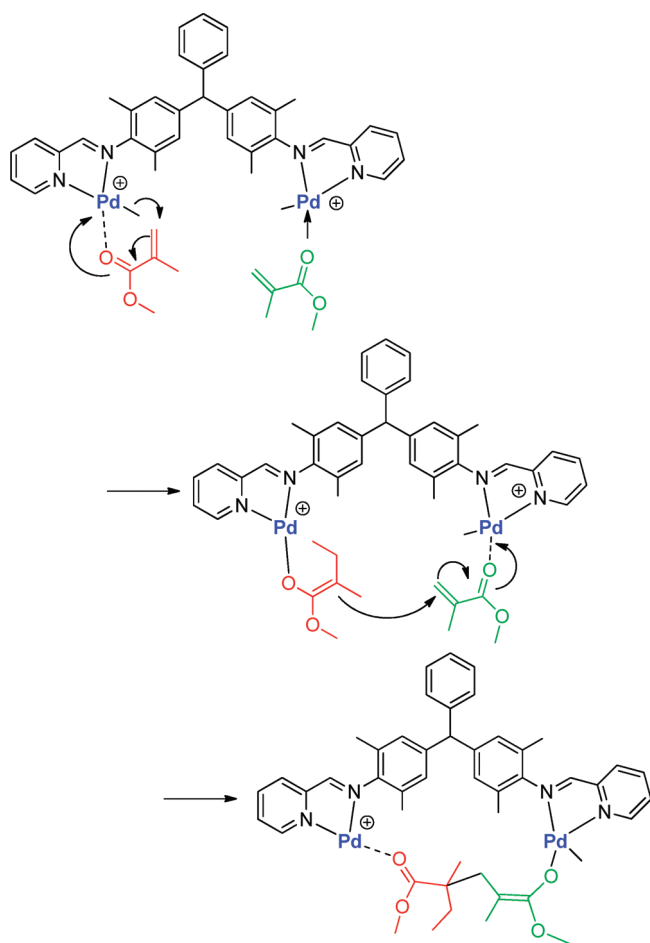
Binuclear samarocene hydride **61** (Figure 7),<sup>127</sup> obtained by hydrogenation of the corresponding monomeric samarocene alkyl, displays high catalytic activity for the polymerization of ethylene, leading to high molecular weight PE ( $M_n = 3\text{--}5 \times 10^4 \text{ g mol}^{-1}$ ) with a rather narrow molecular weight distribution (PDI = 1.63–1.68) and suggestive of a living polymerization (one chain/catalytic center). In contrast, the mononuclear samarocene alkyl is completely polymerization-inactive under the same conditions. Furthermore, in what is undoubtedly a living polymerization, binuclear samarocene **61** produces diblock copolymers of ethylene with polar monomers such as methyl methacrylate and  $\epsilon$ -caprolactone.



Chart 24. Structures of Binuclear Pd(II) Olefin Polymerization Catalysts



Scheme 18. Possible Mechanistic Pathway for Methylmethacrylate Homopolymerization Using Bimetallic Pd(II) Iminopyridyl Complex 56 Combined with MAO

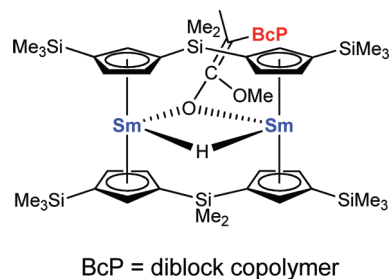


An intermediate is proposed in which cooperation between the active sites leads to formation of a block copolymer (Scheme 19).

## 5. HETEROBIMETALLIC CATALYSTS

Linear low-density polyethylene (LLDPE) is an important industrial polymeric material due to its excellent rheological and mechanical properties.<sup>128</sup> The C<sub>4</sub>–C<sub>6</sub> alkyl branching leads to excellent processability and high melt tensions suitable for film manufacture.<sup>129</sup> Typically, LLDPE branching is ob-

Scheme 19. Proposed Intermediate in the Formation of an Ethylene–Acrylate Block Copolymer with Catalyst 61



tained via copolymerization of ethylene with a linear  $\alpha$ -olefin comonomer. Single-site constrained geometry catalysts constitute another major advance in this field, since the polyethylene produced also contains long-chain branches arising from competing macromonomer re-enchainment processes. Homogeneous “tandem catalysis” has also received attention as an alternative approach to branched polyethylenes.<sup>130</sup> In this approach, one single-site catalytic center produces  $\alpha$ -olefin oligomers, which are subsequently incorporated into high molecular weight polyethylene by a proximate and different single-site catalytic center in the same reaction media, utilizing the same ethylene feed.<sup>130</sup> Since in conventional methodologies, this type of polymerization process requires intermolecular elimination + enchainment sequences at low catalyst concentrations, the attractive possibility of constraining two catalyst centers in close spatial proximity offers the potential for significantly enhanced efficiency. As an example, a covalently linked Zr/Ti catalyst for olefin polymerization, complex **62**, was synthesized by Marks' group.<sup>131</sup> In this catalytic system, two CGC moieties are linked via an ethylene bridge (**62**-(NMe<sub>2</sub>)<sub>4</sub>, Figure 8). Reaction of amido complex **62**-(NMe<sub>2</sub>)<sub>4</sub> with excess of AlMe<sub>3</sub> affords the tetramethyl heterobimetallic catalyst **62**-Me<sub>4</sub>.

The mononuclear CGCTi catalyst produces high molecular weight polyethylenes with high activity, whereas the mononuclear CGCZr catalyst yields low molecular weight polyethylenes having reactive vinylic end groups. Under identical conditions and upon activation with bisborate cocatalyst **B**<sub>2</sub> (Chart 10), heterobinuclear catalyst **62** produces exclusively homogeneous long-chain branched polyethylenes, in marked contrast to control experiments involving a mixture of mononuclear CGCZr and CGCTi catalysts which produces heterogeneous mixtures of high and low molecular weight polyolefins. This result argues that the covalently linked heterobimetallic structure of **62** spatially confines the Zr and Ti catalytic sites in such a way

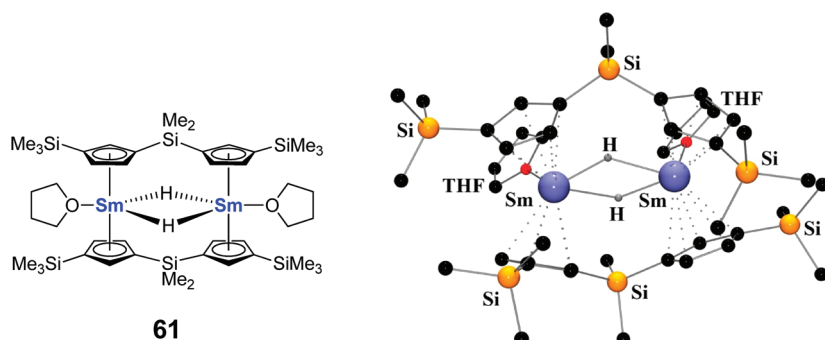


Figure 7. Crystal structure of bis(samarocene) polymerization catalyst precursor **61**. Adapted from ref 127. Copyright 2000 American Chemical Society.

Chart 25. Structures of Binuclear Bis(imino)pyridyl Fe(II) Complexes **57** and **58**

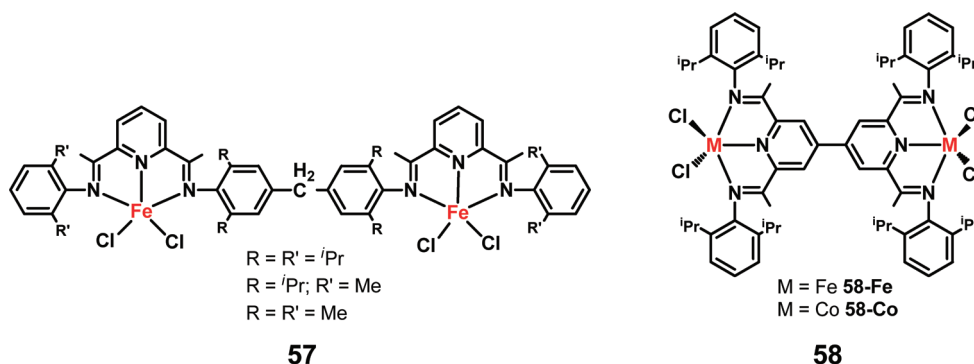
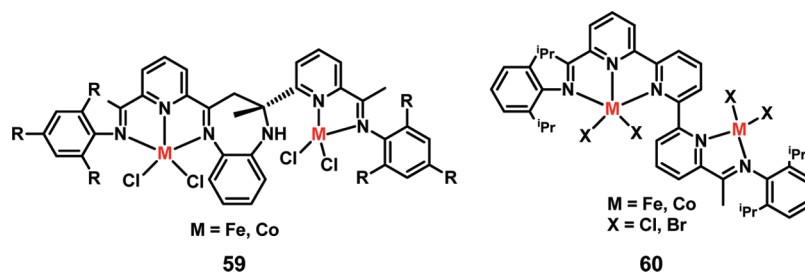


Chart 26. Structures of Asymmetric Bimetallic Fe(II) and Co(II) Ethylene Oligomerization and Polymerization Catalysts



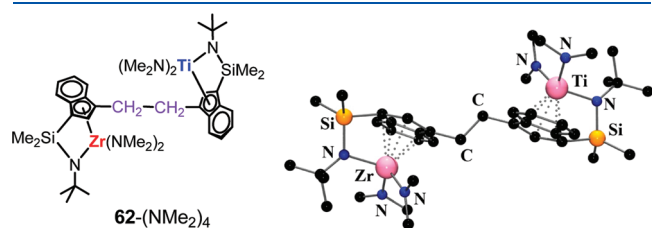
as to significantly increase the efficiency of intramolecular oligomer/macromonomer capture/enchainment, as proposed in Scheme 20.

Heterobimetallic metallocene complexes with silane bridges (**63**, Chart 27)<sup>132,133</sup> exhibit high activity for ethylene polymerization. Under similar experimental conditions, complexes **63** exhibit activities between those of  $\text{Cp}_2\text{TiCl}_2$  and  $\text{Cp}_2\text{ZrCl}_2$ , suggesting cooperation between the two active sites. The molecular weights of the polyethylenes produced with **63** ( $M_w = \sim 29\,000\text{--}124\,000$ ) are much greater than that produced with  $\text{Cp}_2\text{ZrCl}_2$  ( $M_w = \sim 25\,000$ ) and have a slightly broader molecular weight distribution (PDI  $\text{Cp}_2\text{ZrCl}_2 = 1.7$ ; PDI **63** = 2.0–3.0). Notably, for the catalyst exhibiting higher activity, molecular weight is lower due to higher relative rates of  $\beta$ -hydride elimination. It is proposed that this higher rate constant for  $\beta$ -hydride elimination is the result of the differing electronic environments of the catalytic sites. The authors proposed that the electron-withdrawing effects of one metal center reduce the electron density on the Cp ligand at the neighboring active site which in turn reduces electron

density at the other metal center, resulting in higher rates of  $\beta$ -hydride elimination. It is likely that steric effects also play a role.

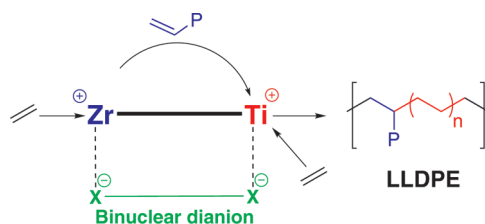
A series of ansa-heterobinuclear group 4 transition metal metallocenes **64**,<sup>39b</sup> **65**,<sup>134</sup> **66**,<sup>135</sup> **67**<sup>136</sup> (Chart 27) was prepared by Green and co-workers. In ethylene and propylene polymerization, heterobinuclear Zr/Hf catalyst **64** exhibits lower activity than the corresponding homobinuclear Zr catalyst and the mononuclear Zr analogue. Generally, hafnocenes exhibit lower activity, but give higher molecular weight polyethylenes, with this lower activity possibly associated with the metal–methyl bond enthalpy, which for the  $[\text{M}(\eta\text{-C}_5\text{Me}_5)_2\text{Me}_2]$  compounds is 306 kJ/mol for Hf and 284 kJ/mol for Zr.<sup>137</sup> In the early-late transition heterobinuclear olefin polymerization catalysts **67** (Chart 27), only the complex with the  $\text{CoCp}'$  fragment exhibits activity approaching that obtained for the mononuclear Zr compound. Kuwabara et al.<sup>138</sup> reported similar Zr(IV)–Co(III) heterobinuclear complexes **68** (Chart 27) with a bis(cyclopentadienyl) ligand. Cationic mononuclear cobaltocene complexes of general formula

$\{\text{Cp}'\text{Co}[\text{P}(\text{OMe}_3)]\text{R}\}^+\text{X}^-$ , where R = alkyl group, exhibit catalytic activity for the polymerization of olefins and polar vinyl monomers.<sup>139</sup> In any case, catalyst **68** displays lower catalytic activity than that of  $\text{Cp}_2\text{ZrCl}_2$ , yielding a broad molecular weight distribution. Note that late transition metal catalysts for olefin polymerization are very active when the metals are coordinated by  $\alpha$ -diimine ligands as discussed above. In this regard, selective cross-metathesis of a *ansa*-zirconocene having an allyl substituent with Co, Ni, and Pd (imino)pyridine complexes having an acrylate substituent affords, after recrystallization, the corresponding early late heterobinuclear catalyst **69** (Scheme 21 and Figure 9).<sup>140</sup> Although the mononuclear iminopyridine Co(II) complex produces a mixture of 1- and 2-butenes, the mononuclear *ansa*-zirconocene is competent to copolymerize ethylene + butenes, achieving polyethylenes with a range of ethyl branching, depending on the polymerization conditions (temperature, pressure). In contrast, at

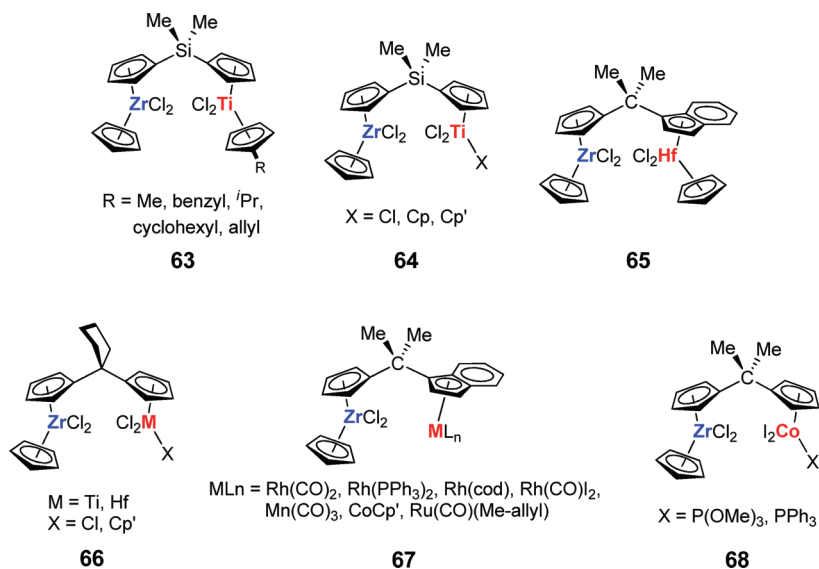


**Figure 8.** Crystal structure of heterobinuclear polymerization catalyst precursor **62**-(NMe<sub>2</sub>)<sub>4</sub>. Adapted from ref 131. Copyright 2004 American Chemical Society.

**Scheme 20. Proposed Scenario for Enhanced Polyolefin Chain Branching Mediated by a Covalently Joined Heterobinuclear Catalyst**



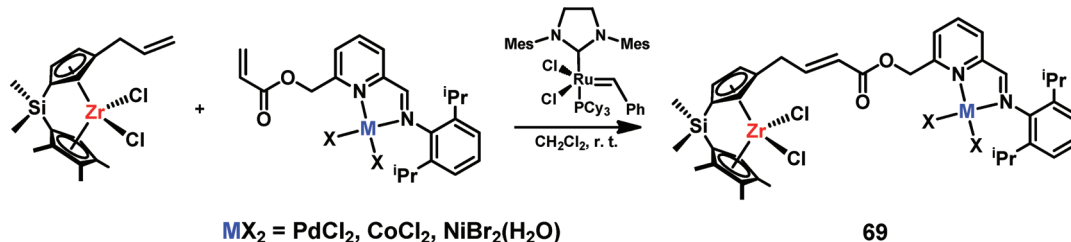
**Chart 27. Structures of Heterobimetallic Metallocene Olefin Polymerization Catalysts**



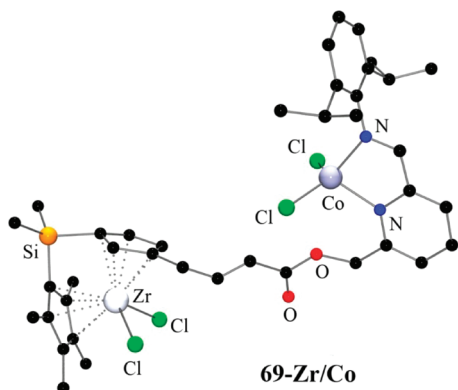
50 °C the covalently linked heterobinuclear **69**-Zr/Co catalyst activated with MMAO yields low molecular weight polyethylenes ( $M_n = 9400$ ; PDI = 2.5) having only ethyl branching (2.1 branches/1000 carbon atoms). It was proposed that a cooperative effect, due to the proximity of the Zr and Co active sites in **69**, enables the efficient incorporation of the oligomer into the polymer. The same scenario is also claimed for a **69**-Zr/Ni catalyst. The polymer produced with the **69**-Zr/Ni catalyst exhibits methyl, ethyl, and long-chain branches. These observations are explained by the formation of branched  $\alpha$ -olefins produced by the Ni center, which then undergo copolymerization with ethylene at the Zr center. The analogous **69**-Zr/Pd complex is not active for ethylene polymerization. Use of the heterobimetallic azanickelacycles **70** (Chart 28) as ethylene polymerization catalysts in the presence of MAO was investigated by Tanabiki et al.<sup>141</sup> In complex **70**, the azanickelacycle is thought to function as a source of ethylene oligomers and to enforce the planarity of the Brookhart-type  $\alpha$ -diimine ligand bonded to the second active site, with the function of the second metal center (Zn, Co, Fe, and Ni) being the copolymerization of the Ni-derived oligomer. The polymers obtained with the Ni/Co and Ni/Ni precatalysts exhibit monomodal molecular weight distributions, whereas the Ni/Fe precatalyst shows a bimodal distribution, due to independent ethylene polymerization by the two metal centers. Note that the heterobinuclear Ni/Co catalyst **71** exhibits a lower activity than that of a physical mixture of the corresponding mononuclear analogues, with a bimodal molecular weight distribution.<sup>142</sup> The low activity and broad molecular weight appear to reflect a different activation mechanism for the Ni and Co centers. Considering the large distance between the metal centers in catalyst **71**, more mechanistic information on these polymerization results would clearly be desirable.

## 6. MULTIMETALLIC CATALYSTS

The trinuclear Zr catalyst **72** (Chart 29), based on a combination of metallocene and phenoxyiminato structures, affords broad or bimodal molecular weight distributions in ethylene polymerizations, presumably due to the presence of differing catalytic centers.<sup>143</sup> In ethylene polymerization, trinuclear and tetranuclear titanocenes **73** (Chart 29) are slightly less active than the binuclear and mononuclear titanocene analogues, with a broad molecular

Scheme 21. Synthesis of Heterobinuclear Polymerization Catalyst 69<sup>a</sup>

<sup>a</sup> The pure heterobinuclear product is obtained after recrystallization.



**Figure 9.** Molecular structure of heterobinuclear Zr/Co polymerization catalyst precursor 69. Adapted with permission from ref 140. Copyright 2006 Royal Society of Chemistry.

weight distribution in the polyethylene produced.<sup>144</sup> The lower catalytic activity is attributed to steric crowding.

To organize multiple active olefin polymerization centers, dendrimeric structures have also been investigated. Tetra- and octanuclear half-titanocenes **74** (Chart 30), when activated with MAO, display high ethylene polymerization activities.<sup>145</sup> The polydispersity is consistent with a single-site catalyst, ruling out the significance of other types of polymerization processes. Thus, dendrimer catalyst **74** and the mononuclear analogue both afford high molecular weight HDPE ( $M_w = 10^6$ ) with melting point values in the range of 135–137 °C. The most noticeable feature is the greater polyethylene crystallinity percentage induced by dendrimer **74** catalyst (57%) compared to the monometallic derivative (39%). No further mechanistic studies were reported which would probe possible cooperative effects between the catalytic centers. A similar dendrimeric catalyst structure with eight binuclear pyridylimine Ni units (**75**; Chart 30) was reported by Benito et al.<sup>146</sup> Ni complex **75**

and the corresponding monometallic analogue activated with MAO are active in ethylene oligomerization and polymerization. Note that the monometallic compound is a superior catalyst yielding polyethylenes rather than oligomers, whereas the contrary is observed for polynuclear dendrimer **75**. The polyethylenes produced with dendrimer **75** show a lower degree of branching and lower molecular weight than those obtained with the monometallic control, along with a broad molecular weight distribution (PDI = 3–14). It was proposed that cooperative effects and steric encumbrance in catalyst **75** enhance chain-transfer processes, and promote the formation of oligomeric species, as supported by lowered Schulz–Flory chain length distributions and increased activity versus those of the monometallic analogue. In addition, the large molecular size also appears to congest the polymerization-active species, disfavoring catalytic chain-walking processes and leading to more linear polymers. Dendrimeric tetranuclear bis(phenoxyiminato) Ni catalyst **76** (Chart 31), when activated with MAO, displays higher activity toward norbornene polymerization than does the binuclear analogue.<sup>147</sup> The poly(propylene-imine)pyridylimine Pd(II) catalyst **77** (Chart 31) is also active in ethylene polymerization when activated with MAO.<sup>148</sup> This catalyst exhibits higher activity than the corresponding mononuclear Pd(II) diimine system. The higher activity may arise from the increased local concentrations of catalytic sites within multinuclear catalyst **77**. Linear high-density polyethylene is produced with a slightly broadened molecular weight distribution (PDI = 2.5–2.9).

A metallodendrimer containing eight bis(imino)pyridyl Fe(II) centers (**78**; Chart 31) was used as a catalyst precursor and activated with MMAO for ethylene polymerization.<sup>149</sup> In the case of low Al/Fe molar ratios, catalyst **78** exhibits much higher activity toward ethylene polymerization and produces much higher molecular weight polyethylene than does the corresponding mononuclear complex under the same reaction conditions. The reason for the higher activity may derive from steric crowding within catalyst **78** which weakens electrostatic pairing with the

**Chart 28.** Heterobinuclear Olefin Polymerization Catalysts **70** and **71**

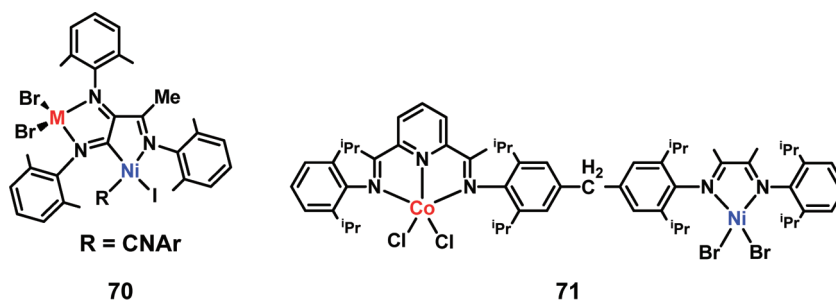


Chart 29. Structures of Multinuclear Olefin Polymerization Catalysts

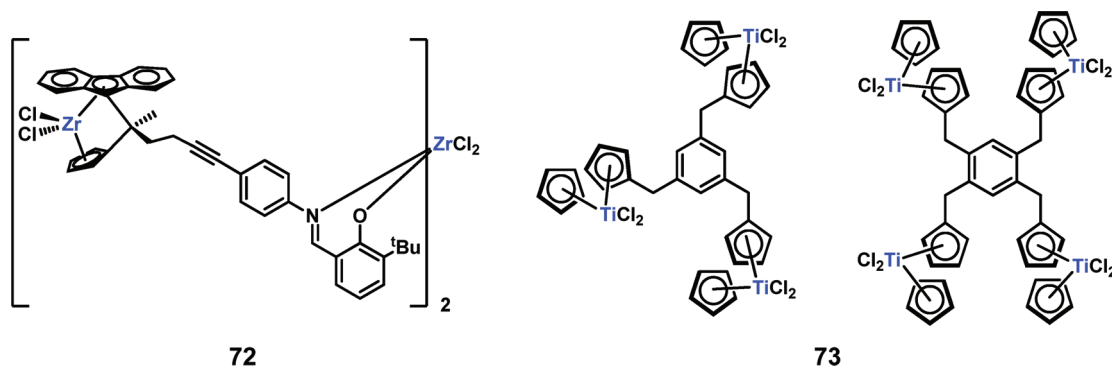
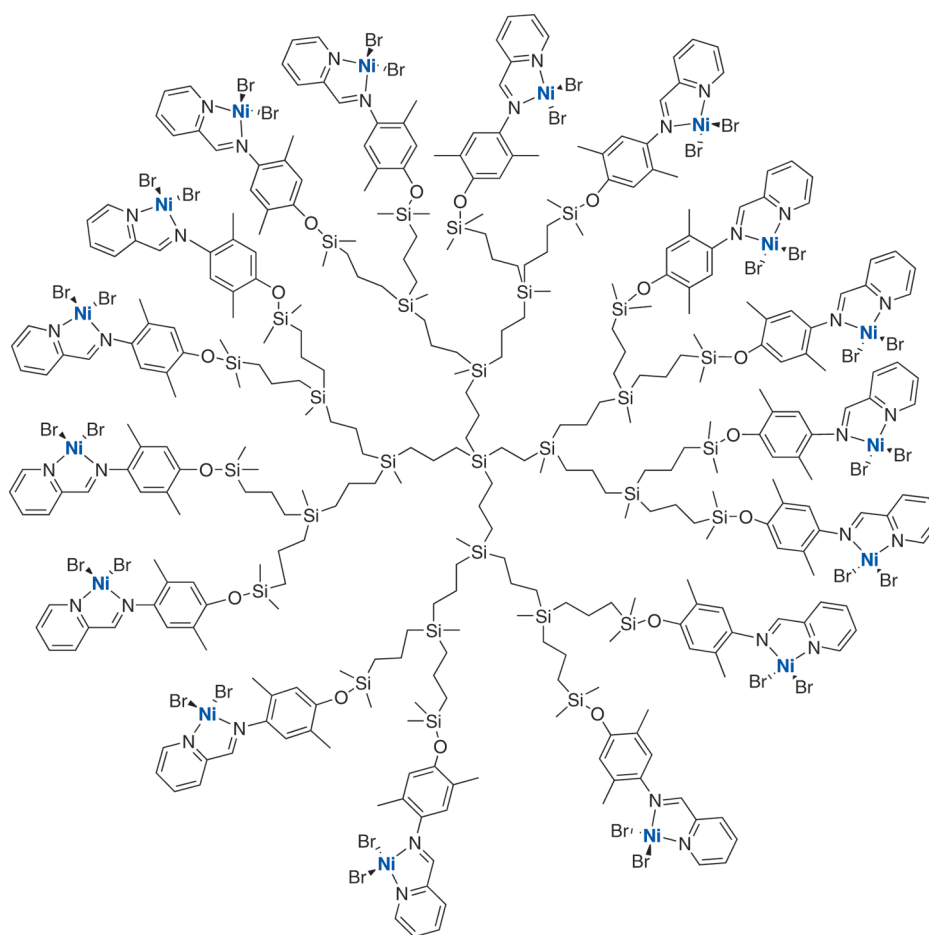


Chart 30. Dendrimeric Structures of Olefin Polymerization Catalysts 74 and 75



MMAO counteranions. In addition, the nonbonded repulsions may also enhance chain transfer during ethylene polymerization and protect the Fe active centers from deactivation.

Multinuclear oligomeric  $\alpha$ -diimine Ni catalyst **79** exhibits higher catalytic activity for ethylene polymerization than does the corresponding mononickel catalyst (Chart 32) when activated with MMAO.<sup>82</sup> It was shown that the bulk of the substituted aryl group is a key factor in reducing competing  $\beta$ -hydride elimination.<sup>150</sup> Trinuclear macrocyclic 2,6-bis(imino)-pyridyl iron catalyst **80** was reported by Liu et al. (Chart 32).<sup>151</sup>

Molecular simulation indicates that the iron atoms in complex **80** are located inside the macrocyclic cavity. Compared with its mononuclear analogue, precatalyst **80** exhibits higher activity and a longer lifetime for ethylene polymerization in the presence of MMAO as a cocatalyst and produces far higher molecular weight polyethylenes with higher melting temperatures. Furthermore, higher molecular weight polyethylenes with a unimodal molecular weight distribution can be obtained using  $\text{Al}(\text{iBu})_3$  as the cocatalyst. To explain the longer catalyst lifetime, it was proposed, based on molecular mechanics calculations, that the structure of catalyst **80**



Chart 31. Dendrimeric Structures of Olefin Polymerization Catalysts 76, 77, and 78

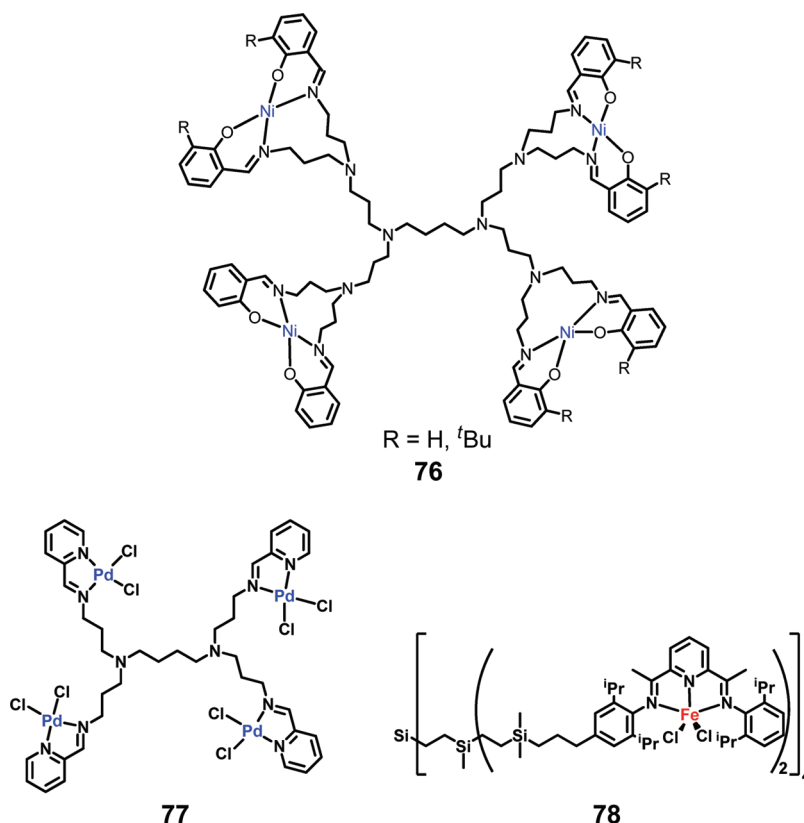
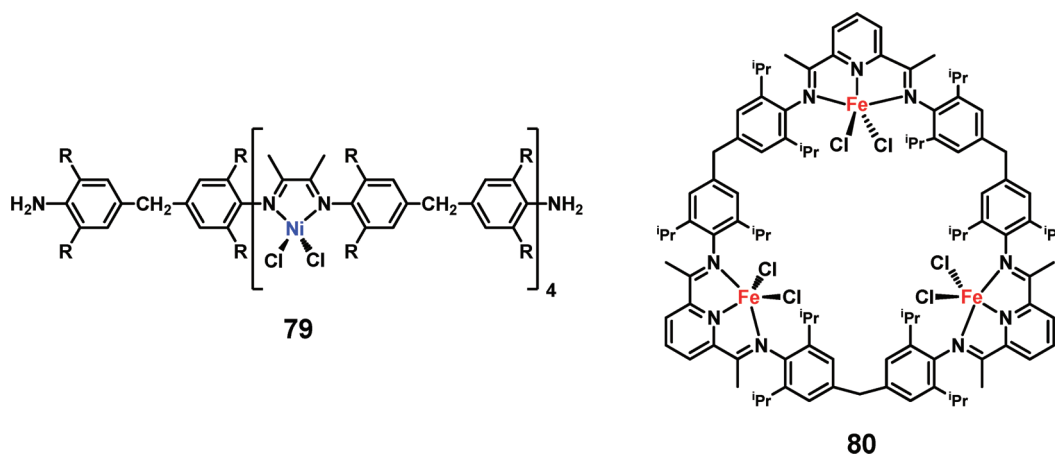


Chart 32. Structures of Multinuclear Olefin Polymerization Catalysts 79 and 80



restrains the active iron center from deactivation and effectively controls chain-transfer reactions, such as  $\beta$ -hydride transfer to the metal or to the monomer.

## 7. CONCLUSIONS AND OUTLOOK

From the results presented in this review it is evident that properly designed binuclear or multinuclear olefin polymerization catalysts can afford unique polymerization activities and polyolefin microstructures, not achievable via the mononuclear analogues. In general, such multinuclear olefin polymerization catalysts have the following distinctive features:

- (1) in most cases, greater polymerization activity per metal center than the mononuclear analogues;
- (2) high levels of product polyolefin branching;
- (3) enhanced enchainment selectivity of comonomers, such as linear  $\alpha$ -olefins, encumbered  $\alpha$ -olefins, and polar monomers (polar substituted norbornenes, acrylates);
- (4) enhanced tacticity and molecular weight in the product polyolefins;
- (5) unusual 1,2-insertion regiochemistry in styrene enchainment;
- (6) modified chain-transfer kinetics, such as in  $\beta$ -hydride transfer to the metal or to the monomer;

- (7) linear low-density polyethylene (LLDPE) formation using a single catalyst and ethylene only.

Nevertheless, the design and synthesis of bimetallic olefin polymerization catalysts is not necessarily straightforward, and structures which optimize cooperative effects between catalytic centers require both rational design and empiricism. Notably, these studies have provided a far better understanding of how mononuclear active sites work alone and cooperatively in polymerization processes. All prospects are that progress in this area will lead to new kinds of polymerization processes as well as completely new, instructive, and useful polymeric materials.

## AUTHOR INFORMATION

### Corresponding Author

\*Phone: (+1) 847 491 5658. Fax: (+1) 847 491 2990. E-mail: t-marks@northwestern.edu.

## BIOGRAPHIES



Massimiliano Delferro was born in 1981 in Parma, Italy. He received his B.S. degree in inorganic chemistry with honor and completed his Ph.D. in Chemical Sciences from the University of Parma under the supervision of Professor Antonio Tiripicchio and Professor Daniele A. Cauzzi. He carried out postdoctoral research at Northwestern University with Professor Tobin J. Marks. In 2009, he joined Northwestern University where he is currently a Research Assistant Professor. Dr. Delferro's research interests include polyolefin synthesis and structure–activity/reactivity relationships in homobimetallic and heterobimetallic single-site homogeneous polymerization catalysts, preparation and application of zwitterionic metallates, metal clusters, and inorganic–organic materials via sol–gel.



Tobin Marks was born in Washington, DC. He is currently Ipatieff Professor of Chemistry and Professor of Materials Science and Engineering at Northwestern University. He received a B.S. degree from the University of Maryland (1966) and Ph.D. from MIT (1971) in Chemistry. He is a member of the U. S. National Academy of Sciences (1993), a Fellow, American Academy of Arts and Sciences (1993), a Member, German National Academy of Sciences (2005), and a Fellow of the Royal Society of Chemistry (2005). Among other recognitions, he received the U.S. National Medal of Science in 2007, the Spanish Principe de Asturias Prize for Scientific Research in 2008, and the Von Hippel Award of the Materials Research Society in 2009.

## ACKNOWLEDGMENT

Financial support by the DOE (Grant 86ER13511) and NSF (CHE-0809589) is gratefully acknowledged. We thank Mr. M. P. Weberski, Jr., Mr. S. D. Wobser, and Ms. J. P. McInnis for helpful discussions and Mr. B. M. Savoie for the cover art.

## GLOSSARY

PE	polyethylene
PS	polystyrene
HDPE	high-density polyethylene
LDPE	low-density polyethylene
LLDPE	linear low-density polyethylene
iPP	isotactic polypropylene
aPP	atactic polypropylene
MAO	methylaluminoxane
MMAO	modified methylaluminoxane
CGC	constrained geometry complexes
MCGC	methylene-bridged CGC
ECGC	ethylene-bridged CGC
$T_g$	glass transition temperature
$T_m$	melting temperature
Me	methyl
Et	ethyl
$i$ Pr	isopropyl
$i$ Bu	isobutyl
$t$ Bu	<i>tert</i> -butyl
Ph	phenyl
Cp	cyclopentadienyl ligand
Cp'	pentamethyl-Cp ligand
$M_w$	weight-average molecular weight
$M_n$	number-average molecular weight
PDI	polydispersity index
DFT	density functional theory
MM	molecular mechanics
MCP	methylenecyclopentane
MCH	methylenecyclohexane
1,5-HD	1,5-hexadiene
1,4-PD	1,4-pentadiene

## REFERENCES

- (1) Representative metalloenzymes with multinuclear active sites: (a) Gahan, L. R.; Smith, S. J.; Neves, A.; Schenk, G. *Eur. J. Inorg. Chem.* **2009**, 2745 and references therein. (b) Superoxide dismutase: Cao, X.; Antonyuk, S. V.; Seetharaman, S. V.; Whitson, L. J.; Taylor, A. B.; Holloway, S. P.; Strange, R. W.; Doucette, P. A.; Valentine, J. S.; Tiwari, A.; Hayward, L. J.; Padua, S.; Cohlberg, J. A.; Hasnain, S. S.; Hart, P. J. *J. Biol. Chem.* **2008**, 283, 16169. (c) Mitić, N.; Smith, S. J.; Neves, A.; Guddat, L. W.; Gahan, L. R.; Schenk, G. *Chem. Rev.* **2006**, 106, 3338 and references therein. (d) Belle, C.; Pierre, J.-L.

- Eur. J. Inorg. Chem.* **2003**, 4137 and references therein. (e) Alkaline phosphatases: Jedrzejewski, M. J.; Setlow, P. *Chem. Rev.* **2001**, *101*, 607. (f) Bruice, T. C.; Benkovic, S. J. *S. Biochemistry* **2000**, *39*, 6267 and references therein. (g) Yachandra, V. K.; Sauer, K.; Klein, M. P. *Chem. Rev.* **1996**, *96*, 2927. (h) Urease: Jabri, E.; Carr, M. B.; Hausinger, R. P.; Karplus, P. A. *Science* **1995**, *268*, 998. (i) Page, M. L., Ed. *The Chemistry of Enzyme Action*; Elsevier: New York, 1984; p 1.
- (2) (a) Bauer-Siebenlist, B.; Decher, S.; Meyer, F. *Chem.—Eur. J.* **2005**, *11*, 5343. (b) Collman, J. P.; Boulatov, R.; Sunderland, C. J.; Fu, L. *Chem. Rev.* **2004**, *104*, 561. (c) Krishnan, R.; Voo, J. K.; Riordan, C. G.; Zahkarov, L.; Rheingold, A. L. *J. Am. Chem. Soc.* **2003**, *125*, 4422. (d) Bruce, T. C. *Acc. Chem. Res.* **2002**, *35*, 139. (e) O'Brien, D. P.; Entress, R. M. N.; Matthew, A. C.; O'Brien, S. W.; Hopkinson, A.; Williams, D. H. *J. Am. Chem. Soc.* **1999**, *121*, 5259. (f) Carazo-Salas, R. E.; Guarguaglini, G.; Gruss, O. J.; Segref, A.; Karsenti, E.; Mattaj, L. W. *Nature* **1999**, *400*, 178. (g) Menger, F. M. *Acc. Chem. Res.* **1993**, *26*, 206 and references therein.
- (3) (a) Steinhagen, H.; Helmchen, G. *Angew. Chem., Int. Ed. Engl.* **1996**, *35*, 2339. (b) Wilcox, D. E. *Chem. Rev.* **1996**, *96*, 2435. (c) Sträter, N.; Lipscomb, W. N.; Klabunde, T.; Krebs, B. *Angew. Chem., Int. Ed. Engl.* **1996**, *35*, 2024.
- (4) Yamatsugu, K.; Yin, L.; Kamijo, S.; Kimura, Y.; Kanai, M.; Shibasaki, M. *Angew. Chem., Int. Ed.* **2009**, *48*, 1070.
- (5) Kato, N.; Mita, T.; Kanai, M.; Therrien, B.; Kawano, M.; Yamaguchi, K.; Danjo, H.; Sei, Y.; Sato, A.; Furusho, S.; Shibasaki, M. *J. Am. Chem. Soc.* **2006**, *128*, 6768.
- (6) For recent review of cooperative multimetallic catalysts using metallosalen, see: Haak, R. H.; Wezenberg, S. J.; Kleij, A. W. *Chem. Commun.* **2010**, *46*, 2713.
- (7) Paull, D. H.; Abraham, C. J.; Scerba, M. T.; Alden-Danforth, E.; Lectka, T. *Acc. Chem. Res.* **2008**, *41*, 655.
- (8) Sone, T.; Yamaguchi, A.; Matsunaga, S.; Shibasaki, M. *J. Am. Chem. Soc.* **2008**, *130*, 10078.
- (9) (a) Shibasaki, M.; Kanai, M.; Matsunaga, S.; Kumagai, N. *Acc. Chem. Res.* **2009**, *42*, 1117. (b) Matsunaga, S.; Shibasaki, M. *Bull. Chem. Soc. Jpn.* **2008**, *81*, 60. (c) Ma, J.-A.; Cahard, D. *Angew. Chem., Int. Ed.* **2004**, *43*, 4566. (d) Shibasaki, M.; Kanai, M.; Funabashi, K. *Chem. Commun.* **2002**, 1989. (e) Jacobsen, E. N. *Acc. Chem. Res.* **2000**, *33*, 421. (f) Tokunaga, M.; Larrow, J. F.; Kakiuchi, F.; Jacobsen, E. N. *Science* **1997**, *277*, 936.
- (10) (a) Esswein, A. J.; Veige, A. S.; Piccoli, P. M. B.; Schultz, A. J.; Nocera, D. G. *Organometallics* **2008**, *27*, 1073. (b) Li, C.; Chen, L.; Garland, M. J. *Am. Chem. Soc.* **2007**, *129*, 13327. (c) Weng, Z.; Teo, S.; Liu, Z.; Hor, T. S. A. *Organometallics* **2007**, *26*, 2950. (d) Zuend, S. J.; Jacobsen, E. N. *J. Am. Chem. Soc.* **2007**, *129*, 15872. (e) Lalonde, M. P.; Chen, Y.; Jacobsen, E. N. *Angew. Chem., Int. Ed.* **2006**, *45*, 6366. (f) Feng, G.; Natale, D.; Prabakaran, R.; Mareque-Rivas, J. C.; Williams, N. H. *Angew. Chem., Int. Ed.* **2006**, *45*, 7056. (g) Martin, M.; Sola, E.; Tejero, S.; Lopez, J. A.; Oro, L. A. *Chem.—Eur. J.* **2006**, *12*, 4057. (h) Trost, B. M.; Jaratjaroonphong, J.; Reutrakul, V. J. *Am. Chem. Soc.* **2006**, *128*, 2778. (i) Sammis, G. M.; Danjo, H.; Jacobsen, E. N. *J. Am. Chem. Soc.* **2004**, *126*, 9928. (j) Collman, J. P.; Boulatov, R.; Sunderland, C. J.; Fu, L. *Chem. Rev.* **2004**, *104*, 561. (k) Moore, D. R.; Cheng, M.; Lobkovsky, E. B.; Coates, G. W. *J. Am. Chem. Soc.* **2003**, *125*, 11911. (l) Trost, B. M.; Mino, T. J. *Am. Chem. Soc.* **2003**, *125*, 2410. (m) Iranzo, O.; Kovalevsky, A. Y.; Morrow, J. R.; Richard, J. P. *J. Am. Chem. Soc.* **2003**, *125*, 1988. (n) Trost, B. M.; Mino, T. J. *Am. Chem. Soc.* **2003**, *125*, 2410. (o) Molenveld, P.; Engbersen, J. F. J.; Reinhoudt, D. N. *Chem. Soc. Rev.* **2000**, *29*, 75. (p) Konsler, R. G.; Karl, J.; Jacobsen, E. N. *J. Am. Chem. Soc.* **1998**, *120*, 10780. (q) Molenveld, P.; Kapsabelis, S.; Engbersen, J. F. J.; Reinhoudt, D. N. *J. Am. Chem. Soc.* **1997**, *119*, 2948. (r) Mathews, R. C.; Howell, D. H.; Peng, W.-J.; Train, S. G.; Treleaven, W. D.; Stanley, G. G. *Angew. Chem., Int. Ed. Engl.* **1996**, *35*, 2253. (s) Sawamura, M.; Sudoh, M.; Ito, Y. *J. Am. Chem. Soc.* **1996**, *118*, 3309.
- (11) Nobel Prize Home Page. [http://nobelprize.org/nobel\\_prizes/chemistry/laureates/1963/](http://nobelprize.org/nobel_prizes/chemistry/laureates/1963/) (accessed 2/3/2011).
- (12) Galli, P.; Vecellio, G. *Prog. Polym. Sci.* **2001**, *26*, 1287.
- (13) (a) Kaminsky, W.; Funck, A.; Hähnsen, H. *Dalton Trans.* **2009**, 8803. (b) Sinn, H.; Kaminsky, W.; Vollmer, H. J.; Woldt, R. *Angew. Chem., Int. Ed. Engl.* **1980**, *19*, 390.
- (14) (a) Möhring, P. C.; Coville, N. J. *Coord. Chem. Rev.* **2006**, *250*, 18. (b) Razavi, A.; Thewalt, U. *Coord. Chem. Rev.* **2006**, *250*, 155.
- (15) (a) Bochmann, M. *Organometallics* **2010**, *29*, 4711 and references therein. (b) Bryliakov, K. P.; Talsi, E. P.; Voskoboynikov, A. Z.; Lancaster, S. J.; Bochmann, M. *Organometallics* **2008**, *27*, 6333. (c) Roberts, J. A. S.; Chen, M.-C.; Seyam, A. M.; Li, L.; Zuccaccia, C.; Stahl, N. G.; Marks, T. J. *J. Am. Chem. Soc.* **2007**, *129*, 12713. (d) Alonso-Moreno, C.; Lancaster, S. J.; Zuccaccia, C.; Macchioni, A.; Bochmann, M. *J. Am. Chem. Soc.* **2007**, *129*, 9282. (e) Song, F.; Lancaster, S. J.; Cannon, R. D.; Schormann, M.; Humphrey, S. M.; Zuccaccia, C.; Macchioni, A.; Bochmann, M. *Organometallics* **2005**, *24*, 1315. (f) Chen, M.-C.; Roberts, J. A.; Marks, T. J. *Organometallics* **2004**, *5*, 932. (g) Zuccaccia, C.; Stahl, N. G.; Macchioni, A.; Chen, M.-C.; Roberts, J. A.; Marks, T. J. *J. Am. Chem. Soc.* **2004**, *126*, 1448. (h) Chen, M.-C.; Roberts, J. A.; Marks, T. J. *J. Am. Chem. Soc.* **2004**, *126*, 4605. (i) Li, H.; Li, L.; Marks, T. J.; Liable-Sands, L.; Rheingold, A. L. *J. Am. Chem. Soc.* **2003**, *125*, 10788. (j) Stahl, N. G.; Zuccaccia, C.; Jensen, T. R.; Marks, T. J. *J. Am. Chem. Soc.* **2003**, *125*, 5256. (k) Lanza, G.; Fragala, I. L.; Marks, T. J. *Organometallics* **2002**, *21*, 5594. (l) Metz, M. V.; Sun, Y.; Stern, C. L.; Marks, T. J. *Organometallics* **2002**, *21*, 3691. (m) Metz, M. V.; Schwartz, D. J.; Stern, C. L.; Marks, T. J. *Organometallics* **2002**, *21*, 4159. (n) Schaper, F.; Geyer, A.; Brintzinger, H. H. *Organometallics* **2002**, *21*, 473. (o) Chen, M.-C.; Marks, T. J. *J. Am. Chem. Soc.* **2001**, *123*, 11803. (p) Beck, S.; Lieber, S.; Schaper, F.; Geyer, A.; Brintzinger, H.-H. *J. Am. Chem. Soc.* **2001**, *123*, 1483. (q) Zhou, J.; Lancaster, S. J.; Walker, D. A.; Beck, S.; Thornton-Pett, M.; Bochmann, M. *J. Am. Chem. Soc.* **2000**, *123*, 223. (r) Lanza, G.; Fragala, I.; Marks, T. J. *J. Am. Chem. Soc.* **2000**, *122*, 12764. (s) Li, L.; Stern, C. L.; Marks, T. J. *Organometallics* **2000**, *19*, 3332. (t) Beswick, C. L.; Marks, T. J. *J. Am. Chem. Soc.* **2000**, *122*, 10358. (u) Chen, E. Y.-X.; Marks, T. J. *Chem. Rev.* **2000**, *100*, 1391 and references therein. (v) Beck, S.; Geyer, A.; Brintzinger, H.-H. *Chem. Commun.* **1999**, 2477. (w) Bochmann, M. *J. Chem. Soc., Dalton Trans.* **1996**, 255. (x) Brintzinger, H.-H.; Fischer, D.; Müllhaupt, R.; Rieger, B.; Waymouth, R. M. *Angew. Chem., Int. Ed.* **1995**, *34*, 1143.
- (16) (a) Ciancaleoni, G.; Fraldi, N.; Budzelaar, P. H. M.; Busico, V.; Macchioni, A. *Dalton Trans.* **2009**, 8824. (b) Stahl, N. G.; Salata, M. R.; Marks, T. J. *J. Am. Chem. Soc.* **2005**, *127*, 10898. (c) Sillars, D. R.; Landis, C. R. *J. Am. Chem. Soc.* **2003**, *125*, 9894. (d) Landis, C. R.; Rosaen, K. A.; Uddin, J. *J. Am. Chem. Soc.* **2002**, *124*, 12062. (e) Liu, Z. X.; Somsook, E.; White, C. B.; Rosaen, K. A.; Landis, C. R. *J. Am. Chem. Soc.* **2001**, *123*, 11193. (f) Beswick, C. L.; Marks, T. J. *Organometallics* **1999**, *18*, 2410. (g) Deck, P. A.; Beswick, C. L.; Marks, T. J. *J. Am. Chem. Soc.* **1998**, *120*, 1772.
- (17) (a) Kaminsky, W., Ed. *Macromol. Symp.* **2006**, *236*, 1, special issue on Olefin Polymerization. (b) Alt, H. G., Ed. *Coord. Chem. Rev.* **2006**, *250*, 1.
- (18) (a) Vanka, K.; Xu, Z. T.; Ziegler, T. *Organometallics* **2004**, *23*, 2900. (b) Xu, Z. T.; Vanka, K.; Firman, T.; Michalak, A.; Zurek, E.; Zhu, C. B.; Ziegler, T. *Organometallics* **2002**, *21*, 2444. (c) Vanka, K.; Ziegler, T. *Organometallics* **2001**, *20*, 905. (d) Lanza, G.; Fragala, I.; Marks, T. J. *Organometallics* **2001**, *20*, 4006. (e) Chan, M. S. W.; Ziegler, T. *Organometallics* **2000**, *19*, 5182. (f) Vanka, K.; Chan, M. S. W.; Pye, C. C.; Ziegler, T. *Organometallics* **2000**, *19*, 1841. (g) Chan, M. S. W.; Vanka, K.; Pye, C. C.; Ziegler, T. *Organometallics* **1999**, *18*, 4624. (h) Lanza, G.; Fragala, I. L.; Marks, T. J. *J. Am. Chem. Soc.* **1998**, *120*, 8257.
- (19) (a) Schwardtfefer, E. D.; Miller, S. A. *Macromolecules* **2007**, *40*, 5662. (b) Tomasi, S.; Razavi, A.; Ziegler, T. *Organometallics* **2007**, *26*, 2024. (c) Alfano, F.; Boone, H. W.; Busico, V.; Cipullo, R.; Stevens, J. C. *Macromolecules* **2007**, *40*, 7736. (d) Miller, S. A.; Bercaw, J. E. *Organometallics* **2006**, *25*, 3576. (e) Chirik, P. J.; Bercaw, J. E. *Organometallics* **2005**, *24*, 5407. (f) Fan, W.; Leclerc, M. K.; Waymouth, R. M. *J. Am. Chem. Soc.* **2001**, *123*, 9555. (g) Leino, R.; Gomez, F. J.; Cole, A. P.; Waymouth, R. M. *Macromolecules* **2001**, *34*, 2072. (h) Veghini, D.; Henling, L. M.; Burkhardt, T. J.; Bercaw, J. E. *J. Am. Chem. Soc.* **1999**, *121*, 564. (i) Ewen, J. A.; Jones, R. L.; Razavi, A.; Ferrara, J. D. *J. Am. Chem. Soc.* **1988**, *110*, 6255.
- (20) Gibson, V. C.; Spitzmesser, S. K. *Chem. Rev.* **2003**, *103*, 283.
- (21) Makio, H.; Fujita, T. *Acc. Chem. Res.* **2009**, *42*, 1532.



- (22) (a) Connor, E. F.; Younkin, T. R.; Henderson, J. I.; Hwang, S.; Grubbs, R. H.; Roberts, W. P.; Litzau, J. J. *J. Polym. Sci., Part A: Polym. Chem.* **2002**, *40*, 2842. (b) Younkin, T. R.; Connor, E. F.; Henderson, J. I.; Friedrich, S. K.; Grubbs, R. H.; Bansleben, D. A. *Science* **2000**, *287*, 460. (c) Wang, C.; Friedrich, S. K.; Younkin, T. R.; Li, R. T.; Grubbs, R. H.; Bansleben, D. A.; Day, M. W. *Organometallics* **1998**, *17*, 3149.
- (23) (a) Ittel, S. D.; Johnson, L. K.; Brookhart, M. *Chem. Rev.* **2000**, *100*, 1169. (b) Johnson, L. K.; Bennett, A. M. A.; Ittel, S. D.; Wang, L.; Parthasarathy, A.; Hauptman, E.; Simpson, R. D.; Feldman, J.; Coughlin, E. B. Patent WO 98/30609, 1998.
- (24) Braunschweig, H.; Breitling, F. M. *Coord. Chem. Rev.* **2006**, *250*, 2691.
- (25) For reviews of single-site olefin polymerization, see: (a) Amin, S. B.; Marks, T. J. *Angew. Chem., Int. Ed.* **2008**, *47*, 2006. (b) Vanka, K.; Xu, Z.; Seth, M.; Ziegler, T. *Top. Catal.* **2005**, *34*, 143. (c) Kaminsky, W. *J. Polym. Sci., Part A: Polym. Chem.* **2004**, *42*, 3911. (d) Bochmann, M. *J. Organomet. Chem.* **2004**, *689*, 3982. (e) Gibson, V. C.; Spitzmesser, S. K. *Chem. Rev.* **2003**, *103*, 283. (f) Wang, W.; Wang, L. *J. Polym. Mater.* **2003**, *20*, 1. (g) Kaminsky, W.; Arndt-Rosenau, M. *Applied Homogeneous Catalysis with Organometallic Compounds*, 2nd ed.; Wiley-VCH: Weinheim, Germany, 2002. (h) Lin, S.; Waymouth, R. M. *Acc. Chem. Res.* **2002**, *35*, 765. (i) Schweizer, G.; Brintzinger, H.-H. *Macromol. Symp.* **2001**, *173*, 89. (j) Pedetour, J.-N.; Radhakrishnan, K.; Cramail, H.; Defieux, A. *Macromol. Rapid Commun.* **2001**, *22*, 1095. (k) Gladysz, J. A. *Chem. Rev.* **2000**, *100*, 1 ff, special issue on "Frontiers in Metal-Catalyzed Polymerization". (l) Marks, T. J.; Stevens, C. J. *Top. Catal.* **1999**, *7*, 1 ff, special volume on Advances in Polymerization Catalysis, Catalysts and Processes. (m) Kaminsky, W.; Arndt, M. *Adv. Polym. Sci.* **1997**, *127*, 144. (n) *Catalyst Design for Tailor-Made Polyolefins*; Soga, K., Terano, M., Eds.; Elsevier: Tokyo, 1994. (o) Marks, T. J. *Acc. Chem. Res.* **1992**, *25*, 57.
- (26) (a) Marks, T. J. *Proc. Natl. Acad. Sci. U.S.A.* **2006**, *103*, 1 ff, special feature on polymerization. (b) Severn, J. R.; Chadwick, J. C.; Duchateau, R.; Friederichs, N. *Chem. Rev.* **2005**, *105*, 4073. (c) Suzuki, N. *Top. Organomet. Chem.* **2005**, *8*, 177. (d) Alt, H. G. *Dalton Trans.* **2005**, No. 20, 3271. (e) Arndt, S.; Okuda, J. *Chem. Rev.* **2002**, *102*, 1953. (f) Chum, P. S.; Kruper, W. J.; Guest, M. J. *Adv. Mater.* **2000**, *12*, 1759. (g) McKnight, A. L.; Waymouth, R. M. *Chem. Rev.* **1998**, *98*, 2587. (h) Harrison, D.; Coulter, I. M.; Wang, S. T.; Nistala, S.; Kuntz, B. A.; Pigeon, M.; Tian, J.; Collins, S. J. *Mol. Catal. A: Chem.* **1998**, *128*, 65. (i) Soga, K.; Shiono, T. *Prog. Polym. Sci.* **1997**, *22*, 1503. (j) Soga, K.; Uozumi, T.; Nakamura, S.; Toneri, T.; Teranishi, T.; Sano, T.; Arai, T.; Shiono, T. *Macromol. Chem. Phys.* **1996**, *197*, 4237. (k) Devore, D. D.; Timmers, F. J.; Hasha, D. L.; Rosen, R. K.; Marks, T. J.; Deck, P. A.; Stern, C. L. *Organometallics* **1995**, *14*, 3132.
- (27) Abramo, G. P.; Li, L.; Marks, T. J. *J. Am. Chem. Soc.* **2002**, *124*, 13966.
- (28) (a) Takeuchi, D. *Dalton Trans.* **2010**, *39*, 311. (b) Hustad, P. H. *Science* **2009**, *325*, 704 and references therein.
- (29) Coates, G. W. *Chem. Rev.* **2000**, *100*, 1223.
- (30) (a) Nakamura, A.; Ito, S.; Nozaki, K. *Chem. Rev.* **2009**, *109*, 5215. (b) Chen, E. Y.-X. *Chem. Rev.* **2009**, *109*, 5157.
- (31) (a) Arriola, D.; Carnahan, E.; Hustad, P.; Kuhlman, R.; Wenzel, T. *Science* **2006**, *312*, 714. (b) Gibson, V. *Science* **2006**, *312*, 703.
- (32) Chum, P. S.; Swogger, K. W. *Prog. Polym. Sci.* **2008**, *33*, 797 and references therein.
- (33) Britovsek, G. J. P.; Gibson, V. C.; Wass, D. F. *Angew. Chem., Int. Ed.* **1999**, *38*, 429.
- (34) Jüngling, S.; Mülhaupt, R. *J. Organomet. Chem.* **1993**, *460*, 191.
- (35) Lee, M. H.; Kim, S. K.; Do, Y. *Organometallics* **2005**, *24*, 3618.
- (36) Soga, K.; Ban, H. T.; Uozumi, T. *J. Mol. Catal. A: Chem.* **1998**, *128*, 273.
- (37) (a) Noh, S. K.; Byun, G. G.; Lee, C. S.; Lee, D.; Yoon, K. B.; Kang, K. S. *J. Organomet. Chem.* **1996**, *518*, 1. (b) Lee, D. H.; Yoon, K. B.; Lee, E. H.; Noh, S. K.; Byun, G. G.; Lee, C. S. *Macromol. Rapid Commun.* **1995**, *16*, 265.
- (38) (a) Xu, S.; Dai, X.; Wu, T.; Wang, B.; Zhou, X.; Weng, L. *J. Organomet. Chem.* **2002**, *645*, 212. (b) Jung, J.; Noh, A. K.; Lee, D.; Park, S. K.; Kim, H. *J. Organomet. Chem.* **2000**, *595*, 147.
- (39) (a) Tian, G.; Wang, B.; Xu, S.; Zhou, X.; Liang, B.; Zhao, L.; Zou, F.; Li, Y. *Macromol. Chem. Phys.* **2002**, *203*, 31. (b) Ushioda, T.; Green, M. L. H.; Haggitt, J.; Yan, X. *J. Organomet. Chem.* **1996**, *518*, 155.
- (40) Noh, S. K.; Kim, S.; Kim, D. H.; Lee, D. H.; Yoon, K. B.; Lee, H. B.; Lee, S. W.; Huh, W. S. *J. Polym. Sci., Part A: Polym. Chem.* **1997**, *35*, 3717.
- (41) Delferro, M.; McInnis, J. P.; Marks, T. J. *Organometallics* **2010**, *29*, 5040 and references therein.
- (42) (a) Xu, S.; Feng, Z. F.; Huang, J. L. *J. Mol. Catal. A: Chem.* **2006**, *250*, 35. (b) Lang, H.; Blau, S.; Muth, A.; Weiss, K.; Neugebauer, U. *J. Organomet. Chem.* **1995**, *490*, C32.
- (43) Deckers, P. J. W.; Hessen, B.; Teuben, J. H. *Organometallics* **2002**, *21*, 5122.
- (44) (a) Lee, H. W.; Ahn, A. H.; Park, Y. H. *J. Mol. Catal. A: Chem.* **2003**, *194*, 19. (b) Lee, H. W.; Park, Y. H. *Catal. Today* **2002**, *74*, 309. (c) Noh, S. K.; Kim, J.; Jung, J.; Ra, C. S.; Lee, D. H.; Lee, H. B.; Lee, S. W.; Huh, W. S. *J. Organomet. Chem.* **1999**, *580*, 90.
- (45) Noh, S. K.; Kim, S.; Yang, Y.; Lyoo, W. S.; Lee, D. H. *Eur. Polym. J.* **2004**, *40*, 227.
- (46) Spaleck, W.; Küber, F.; Bachmann, B.; Fritze, C.; Winter, A. *J. Mol. Catal. A: Chem.* **1998**, *128*, 279.
- (47) Sierra, J. C.; Hüerländer, D.; Hill, M.; Kehr, G.; Erker, G.; Fröhlich, R. *Chem.—Eur. J.* **2003**, *9*, 3618.
- (48) Kuwabara, J.; Takeuchi, D.; Osakada, K. *Organometallics* **2005**, *24*, 2705.
- (49) Trnka, T. M.; Grubbs, R. H. *Acc. Chem. Res.* **2001**, *34*, 18.
- (50) (a) Linh, N. T. B.; Huyen, N. T. D.; Noh, S. K.; Lyoo, W. S.; Lee, D. H.; Kim, Y. *J. Organomet. Chem.* **2009**, *694*, 3438. (b) Noh, S. K.; Jung, W.; Oh, H.; Lee, Y. R.; Lyoo, W. S. *J. Organomet. Chem.* **2006**, *691*, 5000.
- (51) Liu, X.; Sun, J.; Zhang, H.; Xiao, X.; Lin, F. *Eur. Polym. J.* **2005**, *41*, 1519.
- (52) Xiao, X.; Sun, J.; Li, X.; Li, H.; Wang, Y. *J. Mol. Catal. A: Chem.* **2007**, *267*, 86.
- (53) Li, H.; Marks, T. J. *Proc. Natl. Acad. Sci. U.S.A.* **2006**, *103*, 15295.
- (54) Li, H.; Stern, C. L.; Marks, T. J. *Macromolecules* **2005**, *38*, 9015.
- (55) Li, L.; Metz, M. V.; Li, H.; Chen, M.-C.; Marks, T. J.; Liable-Sands, L.; Rheingold, A. L. *J. Am. Chem. Soc.* **2002**, *124*, 12725.
- (56) Li, H.; Li, L.; Marks, T. J. *Angew. Chem., Int. Ed.* **2004**, *43*, 4937.
- (57) Motta, A.; Fragalà, I. L.; Marks, T. J. *J. Am. Chem. Soc.* **2009**, *131*, 3974.
- (58) Noh, S. K.; Lee, J.; Lee, D. H. *J. Organomet. Chem.* **2003**, *667*, 53.
- (59) Lee, S. H.; Wu, C. J.; Joung, U. B.; Lee, B. Y.; Park, J. *Dalton Trans.* **2007**, 4608.
- (60) Li, H.; Li, L.; Schwartz, D. J.; Metz, M. V.; Marks, T. J.; Liable-Sands, L.; Rheingold, A. L. *J. Am. Chem. Soc.* **2005**, *127*, 14756.
- (61) NMR assay: (a) Liu, W.; Ray, D. G., III; Rinaldi, P. L. *Macromolecules* **1999**, *32*, 3817. (b) Breitmaier, E.; Voelter, W. *Carbon-13 NMR Spectroscopy*; VCH Publishers: Weinheim, Germany, 1987. (c) Spectral Database for Organic Compounds, SDBS. (d) The assignment is based on relative intensity changes of these peaks at different incorporation levels.
- (62) (a) Pino, P.; Giannini, U.; Porri, L. In *Encyclopedia of Polymer Science and Engineering*, 2nd ed.; Mark, H. F., Bikales, N. M., Overberger, C. C., Menges, G., Eds.; Wiley-Interscience: New York, 1987; Vol. 8, p 175. (b) Kaminsky, W.; Bark, A.; Spiehl, R.; Möller-Linderhof, N.; Niedoba, S. In *Transition Metals and Organometallics as Catalysts for Olefin Polymerization*; Kaminsky, W., Sinn, H., Eds.; Springer-Verlag: Berlin, 1988; pp 291 f.
- (63) Jia, L.; Yang, X. M.; Seyam, A. M.; Albert, I. D. L.; Fu, P. F.; Yang, S. T.; Marks, T. J. *J. Am. Chem. Soc.* **1996**, *118*, 7900.
- (64) Guo, N.; Li, L.; Marks, T. J. *J. Am. Chem. Soc.* **2004**, *126*, 6542.
- (65) Sernetz, F. G.; Mülhaupt, R.; Waymouth, R. M. *Macromol. Chem. Phys.* **1996**, *197*, 1071.
- (66) For studies of styrene insertion regiochemistry, see: (a) Theaker, G. W.; Morton, C.; Scott, P. *Dalton Trans.* **2008**, 6883. (b) Capacchione, C.; Proto, A.; Ebeling, H.; Mülhaupt, R.; Möller, K.; Spaniol, T. P.; Okuda, J. *J. Am. Chem. Soc.* **2003**, *125*, 4964. (c) Izzo,

- L.; Napoli, M.; Oliva, L. *Macromolecules* **2003**, *36*, 9340. (d) Caporaso, L.; Izzo, L.; Zappile, S.; Oliva, L. *Macromolecules* **2000**, *33*, 7275. (e) Pellecchia, C.; Pappalardo, D.; Oliva, L.; Zambelli, A. *J. Am. Chem. Soc.* **1995**, *117*, 6593. (f) Zambelli, A.; Longo, P.; Pellecchia, C.; Grassi, A. *Macromolecules* **1987**, *20*, 2035. (g) Pellecchia, C.; Longo, P.; Grassi, A.; Ammendola, P.; Zambelli, A. *Makromol. Chem., Rapid Commun.* **1987**, *8*, 277.
- (67) (a) Nomura, K.; Okumura, H.; Komatsu, T.; Naga, N. *Macromolecules* **2002**, *35*, 5388. (b) Xu, G.; Lin, S. *Macromolecules* **1997**, *30*, 685.
- (68) Reviews on functionalization of polyolefins, see: (a) Dong, J.-Y.; Hu, Y. *Coord. Chem. Rev.* **2006**, *250*, 47. (b) Coates, G. W.; Hustad, P. D.; Reinartz, S. *Angew. Chem., Int. Ed.* **2002**, *41*, 2236. (c) Yanjarappa, M. J.; Sivaram, S. *Prog. Polym. Sci.* **2002**, *27*, 1347 and references therein. (d) Chung, T. C. *Prog. Polym. Sci.* **2002**, *27*, 39. (e) Koo, K.; Marks, T. J. *CHEMTECH* **1999**, *29* (10), 13. (f) Chung, T. C. *J. Mol. Catal.* **1992**, *76*, 15.
- (69) Effects of functional groups and branching on polyolefin properties: (a) Imuta, J.-I.; Kashiwa, N.; Toda, Y. *J. Am. Chem. Soc.* **2002**, *124*, 1176. (b) Dong, J. Y.; Wang, Z.; Hong, H.; Chung, T. C. *Macromolecules* **2002**, *35*, 9352. (c) Chung, T. C. *Polym. Mater. Sci. Eng.* **2001**, *84*, 33. (d) Chum, P. S.; Kruper, W. J.; Guest, M. J. *Adv. Mater.* **2000**, *12*, 1759. (e) Alt, H. G.; Föttinger, K.; Milius, W. J. *Organomet. Chem.* **1999**, *572*, 21. (f) Harrison, D.; Coulter, I. M.; Wang, S. T.; Nistala, S.; Kuntz, B. A.; Pigeon, M.; Tian, J.; Collins, S. J. *Mol. Catal. A: Chem.* **1998**, *128*, 65. (g) Nesarikar, A. R.; Carr, S. H.; Khait, K.; Mirabella, F. M. *J. Appl. Polym. Sci.* **1997**, *63*, 1179.
- (70) Amin, S. B.; Marks, T. J. *Angew. Chem., Int. Ed.* **2008**, *47*, 2006.
- (71) Amin, S. B.; Marks, T. J. *J. Am. Chem. Soc.* **2007**, *129*, 2938.
- (72) Amin, S. B.; Marks, T. J. *Organometallics* **2007**, *26*, 2960.
- (73) Suzuki, Y.; Terao, H.; Fujita, T. *Bull. Chem. Soc. Jpn.* **2003**, *76*, 1493.
- (74) (a) Makio, H.; Kashiwa, N.; Fujita, T. *Adv. Synth. Catal.* **2002**, *344*, 477. (b) Tian, J.; Hustad, P. D.; Coates, G. W. *J. Am. Chem. Soc.* **2001**, *123*, 5134.
- (75) (a) Pennington, D. A.; Clegg, W.; Coles, S. J.; Harrington, R. W.; Hursthouse, M. B.; Hughes, D. L.; Light, M. E.; Schormann, M.; Bochmann, M.; Lancaster, S. J. *Dalton Trans.* **2005**, No. 3, 561. (b) Pennington, D. A.; Hughes, D. L.; Bochmann, M.; Lancaster, S. J. *Dalton Trans.* **2003**, No. 18, 3480. (c) Owiny, D.; Parkin, S.; Ladipo, F. T. *J. Organomet. Chem.* **2003**, *678*, 134. (d) Goyal, M.; Mishra, S.; Singh, A. *Synth. React. Inorg. Met.-Org. Chem.* **2001**, *31*, 1705.
- (76) Mitani, M.; Saito, J.; Ishii, S.; Nakayama, Y.; Makio, H.; Matsukawa, N.; Matsui, S.; Mohri, J.; Furuyama, R.; Terao, H.; Bando, H.; Tanaka, H.; Fujita, T. *Chem. Rec.* **2004**, *4*, 137.
- (77) Salata, M. R.; Marks, T. J. *J. Am. Chem. Soc.* **2008**, *130*, 12.
- (78) Salata, M. R.; Marks, T. J. *Macromolecules* **2009**, *42*, 1920.
- (79) (a) Bott, R. K. J.; Hughes, D. L.; Schormann, M.; Bochmann, M.; Lancaster, S. J. *J. Organomet. Chem.* **2003**, *665*, 135. (b) Tohi, Y.; Makio, H.; Matsui, S.; Onda, M.; Fujita, T. *Macromolecules* **2003**, *36*, 523. (c) Woodman, P. R.; Alcock, N. W.; Munslow, I. J.; Sanders, C. J.; Scott, P. J. *Chem. Soc., Dalton Trans.* **2000**, No. 19, 3340.
- (80) Boffa, L. S.; Novak, B. M. *Chem. Rev.* **2000**, *100*, 1479 and references therein.
- (81) Jie, S.; Zhang, D.; Zhang, T.; Sun, W. H.; Chen, J.; Ren, Q.; Liu, D.; Zheng, G.; Chen, W. *J. Organomet. Chem.* **2005**, *690*, 1739.
- (82) Luo, H. K.; Schumann, H. *J. Mol. Catal. A: Chem.* **2005**, *227*, 153.
- (83) Champouret, Y. D. M.; Fawcett, J.; Nodes, W. J.; Singh, K.; Solan, G. A. *Inorg. Chem.* **2006**, *45*, 9890.
- (84) Khamker, Q.; Champouret, Y. D. M.; Singh, K.; Solan, G. A. *Dalton Trans.* **2009**, 8935.
- (85) Pelletier, J. D. A.; Fawcett, J.; Singh, K.; Solan, G. A. *J. Organomet. Chem.* **2008**, *693*, 2731.
- (86) Hu, T.; Tang, L. M.; Li, X. F.; Li, Y. S.; Hu, N. H. *Organometallics* **2005**, *24*, 2628.
- (87) Hu, T.; Li, Y. G.; Li, Y. S.; Hu, N. H. *J. Mol. Catal. A: Chem.* **2006**, *253*, 155.
- (88) Sujith, S.; Joe, D. J.; Na, S. J.; Park, Y. W.; Chow, C. H.; Lee, B. Y. *Macromolecules* **2005**, *38*, 10027.
- (89) Zhang, D.; Jin, G. X. *Inorg. Chem. Commun.* **2006**, *9*, 1322.
- (90) Wang, W. H.; Jin, G. X. *Inorg. Chem. Commun.* **2006**, *9*, 548.
- (91) Chen, Q.; Yu, J.; Huang, J. *Organometallics* **2007**, *26*, 617.
- (92) Berkefeld, A.; Mecking, S. *J. Am. Chem. Soc.* **2009**, *131*, 1565 and references therein.
- (93) Wehrmann, P.; Mecking, S. *Organometallics* **2008**, *27*, 1399.
- (94) Guironnet, D.; Friedberger, T.; Mecking, S. *Dalton Trans.* **2009**, No. 41, 8929.
- (95) Na, S. J.; Joe, D. J.; Sujith, S.; Han, W. S.; Kang, S. O.; Lee, B. Y. *J. Organomet. Chem.* **2006**, *691*, 611.
- (96) Rodriguez, B. A.; Delferro, M.; Marks, T. J. *Organometallics* **2008**, *27*, 2166.
- (97) Rodriguez, B. A.; Delferro, M.; Marks, T. J. *J. Am. Chem. Soc.* **2009**, *131*, 5902.
- (98) Mecking, S.; Johnson, L. K.; Wang, L.; Brookhart, M. J. *Am. Chem. Soc.* **1998**, *120*, 888 and references therein.
- (99) (a) Kuhn, P.; Semeril, D.; Matt, D.; Chetcuti, M. J.; Lutz, P. *Dalton Trans.* **2007**, 515. (b) Speiser, F.; Braunstein, P.; Saussine, W. *Acc. Chem. Res.* **2005**, *38*, 784.
- (100) (a) Tomov, A.; Kurtev, K. *J. Mol. Catal. A: Chem.* **1995**, *103*, 95. (b) Kurtev, K.; Tomov, A. *J. Mol. Catal.* **1994**, *88*, 141.
- (101) Zhang, D.; Jin, G. X. *Organometallics* **2003**, *22*, 2851.
- (102) Taquet, J. P.; Siri, O.; Braunstein, P. *Inorg. Chem.* **2006**, *45*, 4668.
- (103) Huang, Y. B.; Tang, G. R.; Jin, G. Y.; Jin, G. X. *Organometallics* **2008**, *27*, 259.
- (104) Döhler, T.; Görls, H.; Walther, D. *Chem. Commun.* **2000**, 945.
- (105) Walther, D.; Döhler, T.; Theysen, N.; Görls, H. *Eur. J. Inorg. Chem.* **2001**, 2049.
- (106) Bianchini, C.; Gonsalvi, L.; Oberhauser, W.; Semeril, D.; Brüggeller, P.; Gutmann, R. *Dalton Trans.* **2003**, 3869.
- (107) Weng, Z.; Teo, S.; Liu, Z. P.; Hor, T. S. A. *Organometallics* **2007**, *26*, 2950.
- (108) Zhang, S.; Sun, W. H.; Kuang, X.; Vystorop, I.; Yi, J. *J. Organomet. Chem.* **2007**, *692*, 5307.
- (109) Armitage, A. P.; Champouret, Y. D. M.; Grigoli, H.; Pelletier, J. D. A.; Singh, K.; Solan, G. A. *Eur. J. Inorg. Chem.* **2008**, 4597.
- (110) Bahuleyan, B. K.; Lee, U.; Ha, C. S.; Kim, I. *Appl. Catal., A* **2008**, *351*, 36.
- (111) For reviews on Pd(II) catalysts for copolymerizations of olefins and different substrates, see: (a) Ma, R.; Hou, Y.; Gao, J.; Bao, F. *Polym. Rev.* **2009**, *49*, 249. (b) Anselment, T. M. J.; Vagin, S. I.; Rieger, B. *Dalton Trans.* **2008**, 4537. (c) Nozaki, K.; Hiyama, T. *J. Organomet. Chem.* **1999**, *576*, 248. (d) Drent, E.; Budzelaar, P. H. M. *Chem. Rev.* **1996**, *96*, 663. (e) Sen, A. *Acc. Chem. Res.* **1993**, *26*, 303.
- (112) Baar, C. R.; Jennings, M. C.; Puddephatt, R. J. *Organometallics* **2001**, *20*, 3459.
- (113) Mi, X.; Ma, Z.; Wang, L.; Ke, Y.; Hu, Y. *Macromol. Chem. Phys.* **2003**, *204*, 868.
- (114) Chen, R.; Mapolie, S. F. *J. Mol. Catal. A: Chem.* **2003**, *193*, 33.
- (115) Noel, G.; Roder, J. C.; Dechert, S.; Pritzkow, H.; Bolk, L.; Mecking, S.; Meyer, F. *Adv. Synth. Catal.* **2006**, *348*, 887.
- (116) Sachse, A.; Demeshko, S.; Dechert, S.; Daebel, V.; Lange, A.; Meyer, F. *Dalton Trans.* **2010**, 39, 3903.
- (117) Sachse, A.; John, M.; Meyer, F. *Angew. Chem., Int. Ed.* **2010**, *49*, 1986.
- (118) Bianchini, C.; Lee, H. M.; Meli, A.; Oberhauser, W.; Vizza, F.; Brüggeller, P.; Rainer, H. B.; Langes, C. *Chem. Commun.* **2000**, 777.
- (119) Drent, E. Patent EP-A 121965, 1984; Drent, E. Patent EP-A 181014, 1986; van Broekhoven, J. A. M.; Drent, E.; Klei, E. Patent EP-A 213671, 1987; van Broekhoven, J. A. M.; Drent, E.; Klei, E. Patent EP-A 235865, 1987.
- (120) Drent, E.; Vanbroekhoven, J. A. M.; Doyle, M. J. *J. Organomet. Chem.* **1991**, *417*, 235.
- (121) Casalino, M.; De Felice, V.; Fraldi, N.; Panunzi, A.; Ruffo, F. *Inorg. Chem.* **2009**, *48*, 5913.
- (122) Bahuleyan, B. K.; Kim, J. H.; Seo, H. S.; Oh, J. M.; Ahn, I. Y.; Ha, C. S.; Park, D. W.; Kim, I. *Catal. Lett.* **2008**, *126*, 371.



- (123) Gibson, V. C.; Solan, G. A. *Top. Organomet. Chem.* **2009**, 1 and references therein. (b) Bennett, A. M. A. (DuPont). Patent WO 98/27124, 1998.
- (124) Wang, L. C.; Sun, J. Q. *Inorg. Chim. Acta* **2008**, 361, 1843.
- (125) Barbaro, P.; Bianchini, C.; Giambastiani, G.; Rios, I. G.; Meli, A.; Oberhauser, W.; Segarra, A. M.; Sorace, L.; Toti, A. *Organometallics* **2007**, 26, 4639.
- (126) Zhang, S.; Vystorop, I.; Tang, Z.; Sun, W. H. *Organometallics* **2007**, 26, 2456.
- (127) Desurmont, G.; Li, Y.; Yasuda, H.; Maruo, T.; Kanehisa, N.; Kai, Y. *Organometallics* **2000**, 19, 1811.
- (128) James, D. E. In *Encyclopedia of Polymer Science and Engineering*; Mark, H. F., Bikales, N. M., Overberger, C. G., Menges, G., Eds.; Wiley-Interscience: New York, 1985; Vol. 6, p 429.
- (129) (a) Jin, H.-J.; Kim, S.; Yoon, J.-S. *J. Appl. Polym. Sci.* **2002**, 84, 1566. (b) Starck, P.; Malmberg, A.; Lofgren, B. *J. Appl. Polym. Sci.* **2002**, 83, 1140. (c) Kulshrestha, A. K.; Talapatra, S. In *Handbook of Polyolefins*; Vasile, C., Ed.; Marcel Dekker: New York, 2000; p 1. (d) Quijada, R.; Narvaez, A.; Rojas, R.; Rabagliati, F. M.; Galland, G. B.; Maules, R. S.; Benabente, R.; Perez, E.; Perena, J.; Bello, A. *Macromol. Chem. Phys.* **1999**, 200, 1306. (e) Galland, G. B.; Seferin, M.; Mauler, R. S.; Dos, S.; Joao, H. Z. *Polym. Int.* **1999**, 48, 660. (f) Quijada, R.; Scipioni, R.; Mauler, R.; Galland, G.; Miranda, M. S. *Polym. Bull.* **1995**, 35, 299. (g) Quijada, R.; Dupont, J.; Lacerda, M.; Scipione, R.; Galland, G. *Macromol. Chem. Phys.* **1995**, 196, 3991.
- (130) (a) Komon, Z. J. A.; Diamond, G. M.; Leclerc, M. K.; Murphy, V.; Okazaki, M.; Bazan, G. C. *J. Am. Chem. Soc.* **2002**, 124, 15280. (b) Quijada, R.; Rojas, R.; Bazan, G. C.; Komon, Z. J. A.; Mauler, R. S.; Galland, G. B. *Macromolecules* **2001**, 34, 2411. (c) Alt, H. G.; Köppl, A. *Chem. Rev.* **2000**, 100, 1205. (d) Komon, Z. J. A.; Bu, X.-H.; Bazan, G. C. *J. Am. Chem. Soc.* **2000**, 122, 12379. (e) Komon, Z. J. A.; Bu, X.-H.; Bazan, G. C. *J. Am. Chem. Soc.* **2000**, 122, 1830. (f) Chen, E.-Y.; Metz, M. V.; Li, L.; Stern, C. L.; Marks, T. J. *J. Am. Chem. Soc.* **1998**, 120, 6287.
- (131) Wang, J. X.; Li, H. B.; Guo, N.; Li, L. T.; Stern, C. L.; Marks, T. J. *Organometallics* **2004**, 23, 5112.
- (132) Mitani, M.; Oouchi, K.; Hayakawa, M.; Yamada, T.; Mukaiyama, T. *Polym. Bull.* **1995**, 35, 677.
- (133) Huang, J.; Feng, Z.; Wang, H.; Qian, Y.; Sun, J.; Xu, Y.; Chen, W.; Zheng, G. *J. Mol. Catal. A: Chem.* **2002**, 189, 187.
- (134) Diamond, G. M.; Chernega, A. N.; Mountford, P.; Green, M. L. H. *J. Chem. Soc., Dalton Trans.* **1996**, 921.
- (135) Yan, X. F.; Chernega, A.; Green, M. L. H.; Sanders, J.; Souter, J.; Ushioda, T. *J. Mol. Catal. A: Chem.* **1998**, 128, 119.
- (136) Green, M. L. H.; Popham, N. H. *J. Chem. Soc., Dalton Trans.* **1999**, 1049.
- (137) (a) Simoes, J. A. M.; Beauchamp, J. L. *Chem. Rev.* **1990**, 90, 629. (b) Schock, L. E.; Marks, T. J. *J. Am. Chem. Soc.* **1988**, 110, 7701.
- (138) Kuwabara, J.; Takeuchi, D.; Osakada, K. *J. Organomet. Chem.* **2005**, 690, 269.
- (139) (a) Tanner, M. J.; Brookhart, M.; DeSimone, J. M. *J. Am. Chem. Soc.* **1997**, 119, 7617. (b) Brookhart, M.; DeSimone, J. M.; Grant, B. E.; Tanner, M. J. *Macromolecules* **1995**, 28, 5378.
- (140) Kuwabara, J.; Takeuchi, D.; Osakada, K. *Chem. Commun.* **2006**, 3815.
- (141) Tanabiki, M.; Tsuchiya, K.; Motoyama, Y.; Nagashima, H. *Chem. Commun.* **2005**, 3409.
- (142) Sun, T. X.; Wang, Q.; Fan, Z. Q. *Polymer* **2010**, 51, 3091.
- (143) Görl, C.; Alt, H. G. *J. Organomet. Chem.* **2007**, 692, 5727.
- (144) Xiao, X. H.; Sun, J. Q.; Li, X.; Wang, Y. G.; Schumann, H. *Eur. Polym. J.* **2007**, 43, 164.
- (145) Arevalo, S.; de Jesus, E.; de la Mata, F. J.; Flores, J. C.; Gomez, R.; Rodrigo, M. M.; Vigo, S. J. *Organomet. Chem.* **2005**, 690, 4620.
- (146) Benito, J. M.; de Jesus, E.; de la Mata, F. J.; Flores, J. C.; Gomez, R. *Chem. Commun.* **2005**, 5217.
- (147) Malgas-Enus, R.; Mapolie, S. F.; Smith, G. S. *J. Organomet. Chem.* **2008**, 693, 2279.
- (148) Smith, G.; Chen, R.; Mapolie, S. J. *Organomet. Chem.* **2003**, 673, 111.
- (149) Zheng, Z. J.; Chen, J.; Li, Y. S. *J. Organomet. Chem.* **2004**, 689, 3040.
- (150) Johnson, L. K.; Killian, C. M.; Brookhart, M. J. *Am. Chem. Soc.* **1995**, 117, 6414.
- (151) Liu, J. Y.; Li, Y. S.; Liu, J. Y.; Li, Z. S. *Macromolecules* **2005**, 38, 2559.